THE UNIVERSITY OF CHICAGO

EXPRESSION OF A CHIMERIC CORECEPTOR ENHANCES THE ANTITUMOR IMMUNITY OF CD22-TARGETED CAR-T CELLS

A DISSERTATION SUBMITTED TO

THE FACULTY OF THE PRITZKER SCHOOL OF MOLECULAR ENGINEERING

IN CANDIDACY FOR THE DEGREE OF

DOCTOR OF PHILOSOPHY

BY

NICHOLAS WILLIAM ASBY

CHICAGO, ILLINOIS

AUGUST 2024

To my friend and father-in-law Christopher Neal McGowan, taken too soon.

TABLE OF CONTENTS

LIST OF FIGURES

LIST OF TABLES

ACKNOWLEDGEMENTS

I'd like to first acknowledge my wife Heather, who I deeply love and admire. She's strong, caring, and wise and has supported me well over the last six years. There is no path in which I could have completed this degree without her partnership. I thank my parents - Mary and John Asby - for their love and guidance. I thank my parents-in-law - Chris and Paula McGowan - for accepting me with open arms and always having my back. I thank my sisters and brothers - Luke, Sarah, Taylor, Taylor, Blake, and Valerie - for their friendship and support. I thank my nieces and nephews – Blake, Olivia, Beverley, and Avery – for their joy and love. I thank my paternal grandparents – Bill (Papa) and Joyce (Grandma), for teaching me gentleness and kindness. I thank my maternal grandparents – Jim (Grandpa) and Mary (Grandma) - for always encouraging my curiosity and learning. Lastly, I'd like to thank my friends - Naomi, Renan, Grant, Carly, and Ruth – for their love, the memories we have made together, and for greatly enriching my life.

Many members of the Huang Lab have come and gone over the years and I'd like to thank a selected few that have played a particularly big role in getting me to this point. I'd like to thank Guoshuai (Daniel) Cao and Jill Rosenberg for their mentorship and guidance early on in my graduate career. I'd like to thank Yifei Hu, a dear colleague and collaborator, for his wisdom, friendship, and joy. I'd also like to thank Erting Tang, Laura Pulido, Tony Pan, Sara Woessner, Thuc Nguyen, Xiaolei Cao, Min Chen, and Nick Ankenbruck. Many smiles, laughs, tears, and frustrations have been shared and I thank you all for building such a supportive environment. Lastly, I'd like to thank my undergraduate mentees – Leandra Wilson-Patrick, Annie Mitchell, Etty Soto, and Jordan Poon. Thank you for your patience, curiosity, and enthusiasm. It's been an honor being a part of your respective scientific journeys.

The University of Chicago has introduced me to many people who have supported this work and my development as a scientist. I'd like to thank Briana Konnick and Abby Stayart, to whom I attribute the majority of my professional development. I'd like to thank Xiufen Chen, Steven Wolf, Ani Solanki, Richard Koya, David Leclerc, Mandel Davis, Mike Olson, Bert Ladd, and Laura Johnston for their technical guidance and mentorship. I'd like to thank Emiliano Medellin and Kristen Shema for their friendship and support. Lastly, I'd like to thank a few collaborators not yet mentioned - Nada Aboelella, Haley Dugan, Chris Stamper, Lei Li, Patrick Wilson, and Augusta Broughton. I've learned much from working with you all.

I've been fortunate to receive mentorship and guidance from those at other institutions and would like to acknowledge a few of those people. I'd like to thank Jenny Munson and Mete Civelek who collectively gave me my start in research and encouraged me even as an immature and fledgling scientist. I am forever grateful for the opportunities yall provided me. I'd also like to thank Robbie Majzner and Sneha Ramakrishna, both brilliant scientists who have provided me with advice and guidance at pivotal stages of this project.

For their guidance and support, I'd like to thank my committee – Jeff Hubbell, Barbara Kee, Yun Fang, and Justin Kline. Collectively you have taught me what it means to do quality research and have supported me well over the last six years, keeping me on track and always pushing me to improve. I'd like to especially thank Barbara for her guidance at the earliest stages of my graduate career and for setting me on a path to mature and grow. Lastly, I'd like to thank my advisor, Jun Huang. You provided me with a space where I could learn, nurtured my curiosity, and helped me grow as an independent scientist. You have been kind and understanding in moments of personal hardship and I am honored to call you both a mentor and friend. If I were to start over tomorrow, I would surely do it again with you as my mentor.

ABSTRACT

Chimeric antigen receptor (CAR) T cells are T cells genetically engineered to express an antigen binding domain, such as a single-chain variable fragment (scFv), fused to intracellular signaling domains, so to induce activation upon binding to the target epitope. Many clinically-used CAR designs are limited by up to 1,000-fold reduced sensitivity for antigen relative to T-cell receptors (TCRs), in part due to poor recruitment of downstream signaling molecules such as LCK to facilitate T-cell signaling. This inefficient signaling combined with observed downregulation of targeted antigens contribute to many patients relapsing even after exhibiting a complete response. Hence, more sensitive CAR designs are needed in the clinic to reduce instances of relapse. In this body of work, I first provide a brief history of CAR design, clinical use, and inefficiencies compared to the TCR (Chapter 1). Afterwards, I describe the iterative design process in which we engineered and evaluated a novel chimeric coreceptor (CoCAR), capable of improving antitumor functionality and increasing the sensitivity of a second-generation anti-CD22 CAR anywhere from five- to seven-fold (Chapter 3). In order to gain a better understanding of the underlying mechanisms behind the CoCAR we then modified or mutated selected features of the system (Chapter 4). Lastly, we successfully display a degree of modularity by re-engineering the CoCAR system to target BCMA (Chapter 5). I conclude with a brief review of strategies undertaken by others to combat CAR-T relapse, putting this study in perspective to the greater field (Chapter 6). Collectively, these findings describe a novel approach to increase the antitumor functionality of CAR-T cells with relatively minor modifications to existing CAR constructs. I hope that the further evaluation and eventual adoption of the CoCAR to clinically-approved constructs translate to more durable responses to CAR-T therapy.

1. INTRODUCTION

1.1 Antigen recognition by the T cell

Immune cells can be divided into innate and adaptive groups based on how they recognize threats to the host. Generally, innate cells recognize conserved features of pathogen classes while adaptive cells recognize peptides or epitopes unique to individual pathogens. An immune response is triggered by danger signals, which alert innate and adaptive cells to appropriately polarize the response and generate adaptive memory against the pathogen in case of later reemergence in the host's life. While redundancies and functional overlap exists, each immune cell type has its own specialized role to play in the recognition and removal of pathogens or pathogen-infected cells [1, 2].

One of such players is the T cell, an adaptive cell capable of cell-mediated cytotoxicity and polarizing the immune response towards specific pathogens through cytokine secretion. All T cells recognize peptides presented on major histocompatibility complexes (MHC) of other cells through the T cell receptor (TCR) and can be broadly broken up into two subtypes, dependent on expression of the CD4 or CD8 TCR coreceptor. While exceptions exist, such as with cross-presentation, $CD8^+$ T cells recognize MHCI-presented peptides originating from the cytoplasm which while $CD4^+$ T cells recognize MHCII-presented peptides of extracellular origin. It is the cooperation between $CD8^+$ and $CD4^+$ T cells that provide comprehensive immunosurveillance of the host for both intercellular and extracellular threats [3-10]. Each TCR contains variable regions, endowing each T cell with the ability to recognize a unique collection of potentially dangerous peptides [11, 12]. Mechanisms of central tolerance during T cell development and peripheral tolerance afterwards ensure that the mature T cell pool express

functional TCRs with inconsequential self-reactivity [13-16]. In total, it is estimated that an individual's T cell repertoire includes $1e^6$ to $1e^7$ unique TCR clonotypes [17, 18].

Upon recognition of peptide-MHC (pMHC) complexes through the TCR, conformational changes induce calcium flux and initial phosphorylation of immunoreceptor tyrosine-based activation motifs (ITAMs) found in cytoplasmic domains of the TCR complex, such as CD3ζ [19, 20]. This initial signaling is further amplified by either CD4- or CD8-associated LCK, which further phosphorylates ITAMs and the tyrosine kinase ZAP-70. ZAP-70 then phosphorylates LAT, a transmembrane-bound protein which acts as a scaffold for other signaling molecules to bind, effectively translating phosphorylation induced by pMHC binding to specialized biological pathways [21-24]. Three key adaptor proteins that bind to LAT are PLCγ1, GRB2, and GADS. PLCγ1 primarily functions by increasing calcium flux, subsequently moving NFAT into the nucleus, and by promoting NF-κB activation via PKCθ [25-28]. GRB2 binds SOS which activates RAS signaling [29-31]. Lastly, GADS binds the SLP76 which induces cytoskeletal remodeling through the Rho family of GTPases [32-34]. Altogether, these distinct pathways cooperate to greatly alter metabolism, adhesion, and transcriptional expression to support proliferation, migration, and effector functions. In order to prevent activation-induced cell death or anergy, a second signal is required through binding of costimulatory receptors such as CD28 or 4-1BB to their respective ligands on antigen-presenting cells (APCs). Together, signaling through the TCR and costimulatory receptor allow for a durable T cell response to a particular peptide [35-39].

Blocking either coreceptor impairs TCR-mediated activation by decreasing ITAM phosphorylation and subsequent calcium flux, proliferation, expression of activation markers, and cytokine production [40-44]. While the TCR complex is capable of effectively recognizing a

single pMHC, blocking the coreceptor decreases sensitivity between 10 to 100 times [45-47]. Mechanistically both CD4 and CD8 primarily function by colocalizing with and delivering LCK to the TCR, not by increasing TCR-pMHC complex stability, adhesion to target cells, or avidity [44, 48-52].

1.2 Early chimeric T cell receptors and the rise of the chimeric antigen receptor

Despite the high sensitivity and diversity of the TCR repertoire, pathogenic cells harboring altered or non-self peptides can avoid T cell immunosurveillance. Downregulation of pMHC or costimulatory ligands are but a few examples of defense mechanisms many cancers employ to avoid recognition through the TCR [53-59].

Although primarily interested in the structural differences found in the variable regions of the B cell receptor and TCR, Kuwana *et al.* 1987 provided the first published data that would inspire future chimeric receptors for therapeutic uses [60]. The authors replaced TCR V_α and V_β

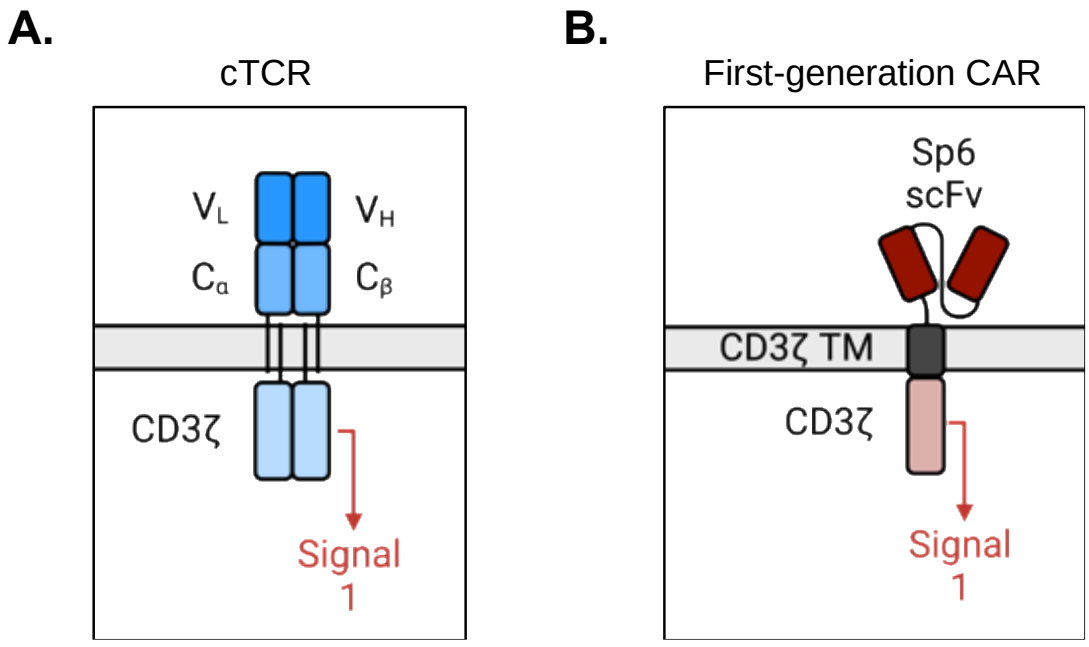

Figure 1.1 Design of the first chimeric T cell and chimeric antigen receptors
Schematics of **A.** a simplified cTCR complex showing V_L-C_α and V_H-C_β molecules complexed with endogenous CD3ζ. **B.** a first-generation CAR containing the Sp6 scFv, CD3ζ transmembrane (TM) domain, and cytoplasmic CD3ζ domain.

chains with V_L and V_H chains from an anti-phosphorylcholine (PC) antibody, forming a chimeric molecule theoretically capable of providing TCR-like activation with antibody-like specificity (Figure 1.1.A). Two plasmids - one encoding the V_L-C_α chain and another the V_H-C_β chain - were transfected into the EL4 mouse T cell line and the first chimeric T cell receptor (cTCR) was expressed. These chimeric receptors were functional and induced antigen-specific calcium flux after coculturing transfected-EL4 cells with PC^+ bacteria. While the authors hypothesized that their chimeric receptors would be able to induce T cell effector functions such as cytokine secretion and cytotoxicity, it would take another two years for another group to confirm their hypothesis. In 1989, Gross *et al.* generated their own cTCRs, replacing TCR V_α and V_β chains with V_L and V_H chains from an anti-trinitrophenyl (TNP) antibody [61]. After expressing the cTCRs in the MD.45 murine cytotoxic T cell hybridoma line and coculturing transfected cells with TNP^+ A.20 cells, they observed antigen-specific IL-2 secretion and lysis of target cells.

While cTCRs were functional, transfection of two plasmids was inefficient. Since bicistronic expression elements such as the IRES and 2A peptides had not been well established, this limitation was addressed by simplifying the cTCR structure into a single-chain chimeric receptor. In 1993, the first chimeric antigen receptor (CAR) was generated by fusing an anti-TNP single-chain variable fragment (scFv) to the full CD3ζ chain derived from the TCR complex (Figure 1.1.B) [62]. Structurally simple, the CAR's main strength over the cTCR was that it was a significantly smaller gene and therefore capable of being expressed via a single plasmid. The anti-TNP CAR was transfected into MD.45 cells and after coculture with TNP^+ A.20 cells, CAR-expressing hybridomas produced IL-2 and specifically lysed $A20^+$ targets. Best expressed by the authors, the "chimeric protein endowed the CTL hybridomas with MHC-nonrestricted specificity." Collectively, these three studies laid the groundwork for the CAR field, providing

evidence that cTCRs and CARs were functional TCR-like molecules with MHC-independent and epitope-specific recognition.

1.3 Second-generation chimeric antigen receptors

While first-generation CAR-T cells were capable of antigen-specific activation, they did not persist long *in vitro* due to lack of costimulation. One of the clearest examples of this phenomena was provided by Brentjens *et al.* 2003, where *in vitro* expansion of CAR-T cells only occurred when target cells expressed CD80, providing costimulation through the endogenous CD28 receptor [63]. It became apparent that the first-generation of CARs would need to be improved upon or clinical efficacy would prove unsatisfactory in diseases with downregulation of costimulatory ligands CD80 or CD86, such as in B cell acute lymphoblastic lymphomas (B-

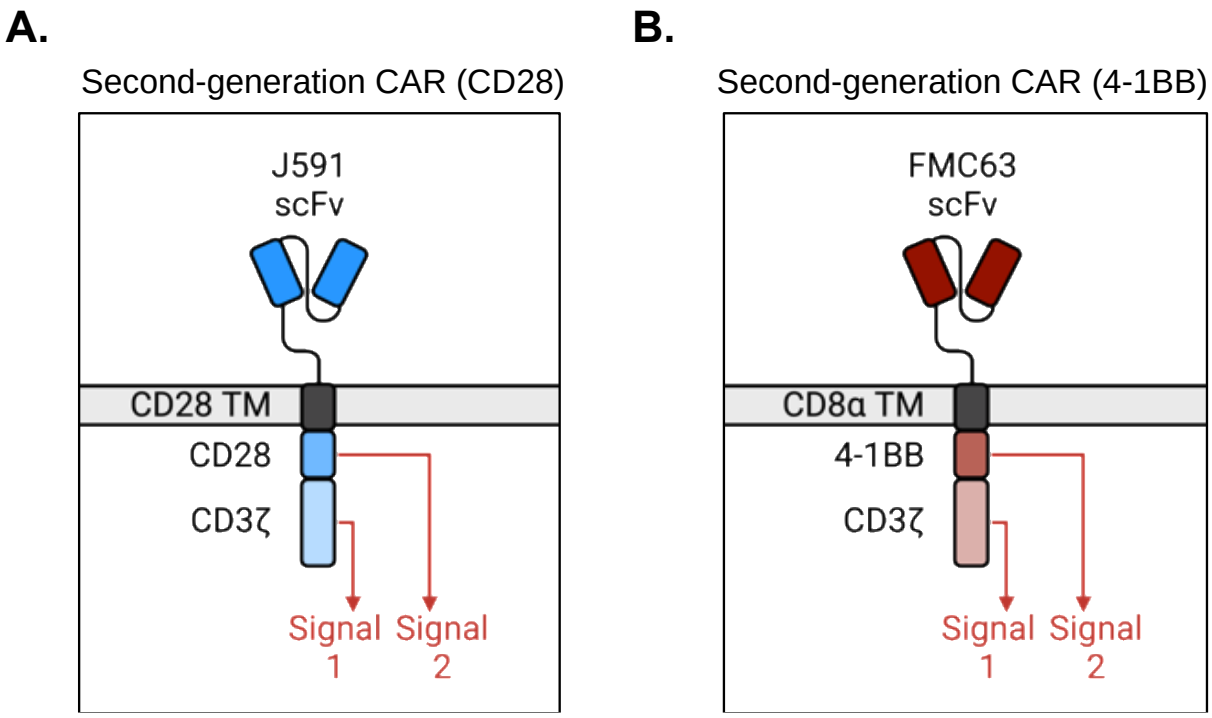

Figure 1.2 Design of second-generation chimeric antigen receptors
Schematics of **A.** a second-generation CAR with CD28 costimulation containing the J591 scFv, CD28 transmembrane (TM) domain, CD28 cytoplasmic domain, and CD3ζ cytoplasmic domain. **B.** a second-generation CAR with 4-1BB costimulation containing the FMC63 scFv, CD8α TM domain, 4-1BB cytoplasmic domain, and CD3ζ cytoplasmic domain.

ALL), B cell lymphomas, and lung adenocarcinomas [53-55]. Clinical trials using first-generation CAR-T cells supported *in vitro* observations that while functional, *in vivo* persistence was low [64, 65].

The second generation of CAR design incorporated an additional costimulatory domain derived from either CD28 or 4-1BB to increase persistence. CD28 costimulation was first used in 2002, in a CAR design consisting of an anti-prostate specific membrane antigen (PSMA) scFv fused to hinge and transmembrane domains from CD28, and the intracellular domains from CD28 and CD3ζ (Figure 1.2.A) [66]. As a state-of-the-art control, a first-generation CAR with omission of the CD28 intracellular domain was also constructed. While primary human T cells transduced with either CAR design produced IL-2 and elicited cytotoxicity against $PSMA^+$ target cells, only cells those expressing both CD28 and CD3ζ intracellular domains persisted and expanded *in vitro* after two rounds of stimulation. 4-1BB-based costimulation was similarly shown to improve *in vitro* expansion of CAR-T cells, first shown in 2004 with a construct consisting of an anti-CD19 scFv (FMC63), hinge and transmembrane domains from CD8α, and intracellular domains from 4-1BB and CD3ζ (Figure 1.2.B) [53]. Primary human T cells expressing the novel CAR showed increased functionality and *in vitro* survival compared to first-generation CARs devoid of the 4-1BB domain. In 2009, Milone *et al.* would provide a comprehensive study assessing the persistence of CAR-T cells containing 4-1BB or CD28 costimulatory domains in a murine model of B-ALL [67]. Human PBMCs were lentivirally-transduced with CARs consisting of an anti-CD19 scFv (FMC63), hinge and transmembrane domains from CD8α, costimulatory domains from 4-1BB or CD28, and the intracellular domain of CD3ζ. CAR-T cells with both 4-1BB and CD3ζ domains provided superior *in vitro* proliferation and clearance of primary human B-ALL tumors in NOD.Cg-*Prkdc*^{scid} *Il2rg*^{tm1Wjl}/SzJ

(NSG) mice. Importantly, these 4-1BB-containing CAR-T cells were detected in the blood of mice even at 6 months post-injection, showing potential for persistence and long-term immunosurveillance in humans.

1.4 Use of chimeric antigen receptors in pre-B cell acute lymphoblastic leukemia

Leukemias are a collection of cancers arising from cells of the bone marrow and blood. They are the most common cancer in children and adolescents, making up 31% of total cases of patients under 14 years old, with an incidence of approximately 5.3 cases per 100,000 [68]. Acute lymphoblastic leukemia (ALL) is a subset of leukemias arising from immature B or T cells, with B-ALL being the most common and comprising about 85% of ALL cases in children. The peak incidence of ALL in children is within those between 1 to 4 years old at 7.0 cases per 100,000. Fortunately, ALL death rates within this age group are low at only 0.2 per 100,000. While less common in adults, risk of developing leukemia increases greatly after 50 years of age with peak prevalence in those between 70 to 80 years old. Across all age groups, deaths rates due to leukemia have steadily dropped from 7.7 per 100,000 in 2000 to 5.7 per 100,000 in 2022, partially due to the introduction of better therapies such as CAR-T cells capable of delivering more durable responses in subtypes like B-ALL [69].

There are currently six FDA-approved CAR-T therapies for treating immature B cell cancers such as B-ALL, mature B cell cancers such as diffuse large B cell lymphoma (DLBCL) and follicular lymphoma (FL), and the plasma cell-derived multiple myeloma (MM). All FDA-approved constructs are second-generation CARs, containing an antigen binding domain, hinge, transmembrane domain, a costimulatory domain from either CD28 or 4-1BB, and a CD3ζ stimulatory domain. Four of the six therapies target CD19, a common B cell surface marker expressed in 100% of B-ALL and 99% of mature B cell cancers, and two target BCMA, a

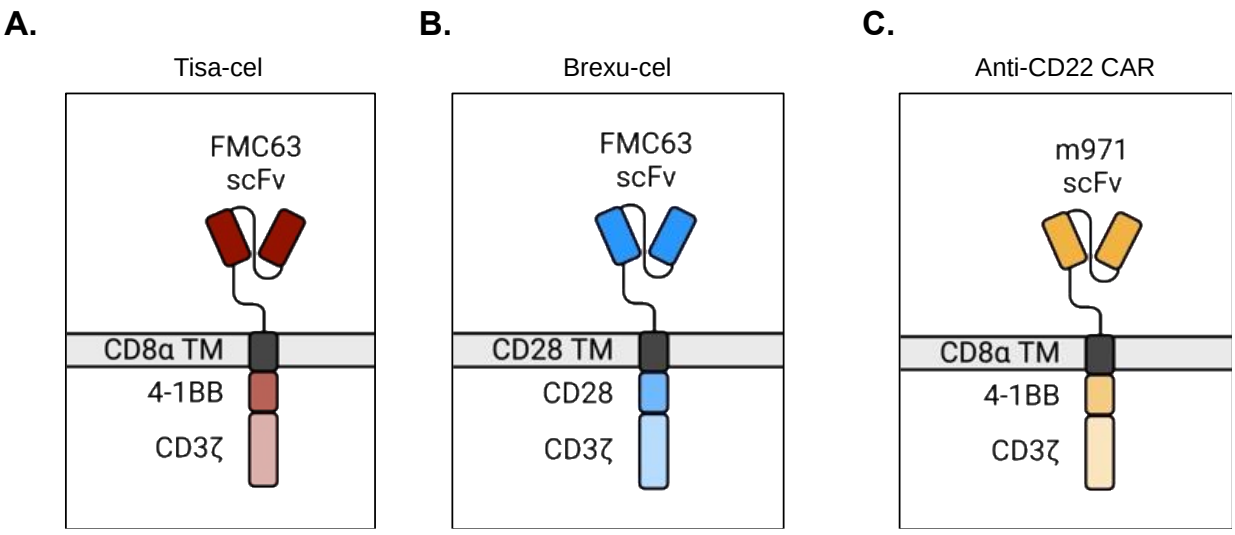

Figure 1.3 Design of chimeric antigen receptors used for treatment of B cell acute lymphoblastic leukemia
Schematics of **A.** Tisa-cel, consisting of the FMC63 scFv, CD8α transmembrane (TM) domain, 4-1BB cytoplasmic domain, and CD3ζ cytoplasmic domain. B. Brexu-cel, consisting of the FMC63 scFv, CD28 TM domain, CD28 cytoplasmic domain, and CD3ζ cytoplasmic domain. **C.** a clinically-used anti-CD22 CAR consisting of the m971 scFv, CD8α TM domain, 4-1BB cytoplasmic domain, and CD3ζ cytoplasmic domain.

common surface marker of plasma cells expressed in nearly 100% of MM cases [70, 71]. Only two of the six therapies are approved for B-ALL: tisagenlecleucel (tisa-cel) and brexucabtagene autoleucel (brexu-cel). Both tisa-cel and brexu-cel are autologous, CD19-targeted CAR products generated from the patient's own peripheral blood T cells [72]. Tisa-cel contains the anti-CD19 scFv FMC63, hinge and transmembrane domains from CD8α, the 4-1BB costimulatory domain, and CD3ζ stimulatory domain (Figure 1.3.A). Complete responses have been reported to range from roughly 80% to 90%. Despite these impressive initial responses, long term remission is not achieved for all patients, with relapse-free survival (RFS) five years after treatment only achieved in 44% of complete responders. Relapse after tisa-cel administration has been observed in responders at earlier timepoints, with one study showing an 80% RFS at 6 months which drops to 59% RFS at 12 months [73-75]. Brexu-cel contains the anti-CD19 scFv FMC63, hinge and transmembrane domains from CD28, the CD28 costimulatory domain, and CD3ζ stimulatory

domain (Figure 1.3.B). Clinical efficacy of brexu-cel is comparable to tisa-cel, with complete responses ranging from 75% to 90%. Unfortunately, durable long-term responses are not achieved in all patients with one study reporting only 50% RFS at 6 months [76-78]. Median overall survival between the two therapies is similar, ranging from 15.6 to 19.1 months.

Although not FDA-approved, CAR-T cells targeting antigen other than CD19 have experienced clinical successes in treating B-ALL. A well-evaluated alternative antigen is CD22, expressed in about 94% of B-ALL cases [70]. The first anti-CD22 CARs were reported in 2013 and one of the constructs, containing an anti-CD22 scFv m971, hinge and transmembrane domains from CD8α, the 4-1BB costimulatory domain, and CD3ζ stimulatory domain, has made it into clinical trials (Figure 1.3.C) [79, 80]. Initial clinical responses are strong, with complete responses reported at approximately 70%. However, this particular therapy is greatly limited in that 75% of responding patients relapse. One mechanism behind this high percentage of relapse is downregulation of CD22 expression on B-ALL cells during treatment, on average between 3- to 5-fold. Mean antibody binding capacities (ABCs) post-relapse are reported at only 1,100 to 1,300 molecules of CD22 per cell [81, 82]. A dominant factor behind failure in CD22-targeted CAR-T therapies, antigen downregulation or loss has also been observed after administration of CD19- and BCMA-directed CAR-T therapies [83-89].

1.5 Contrasting chimeric antigen receptor and T cell receptor signaling

While antigen downregulation certainly plays a role in relapse to CAR-T therapy there are also contributing CAR-intrinsic factors, such as deviations from the synaptic structure and signaling dynamics of the TCR. Davenport *et al.* provided early examples of differences between the TCR and CAR synapse, highlighted by the lack of the canonical bullseye structure formed by concentric cSMAC and pSMAC domains [90, 91]. While the CAR synapse contained a cSMAC-

like domain, LCK was recruited at lower levels and highly dispersed. Additionally, they observed that the CAR synapse was devoid of a proper pSMAC domain, indicating that the LFA-1-containing ring is not necessary for CAR adhesion. The highly disorganized nature of the CAR synapse causes shifts in signaling timing and duration. CAR signaling was shown to both peak and fade quicker than the TCR, with distal pERK levels dropping 30 minutes after CAR engagement. Altered timing of ITAM phosphorylation has also been observed. While phosphorylation of CD3ζ ITAMs 1, 2, and 3 peaked at 10 minutes after CAR engagement, phosphorylation of the same domains was still rising 90 minutes after TCR stimulation [92].

The differences in CAR and TCR structure not only lead to changes in signaling dynamics, but also strength. While CARs and TCRs have been both shown to engage their target molecules efficiently, synaptic calcium flux, phosphorylation of CD3ζ ITAMs 1, 2, 3, ZAP-70, and LCK were lower in CAR-stimulated cells across a range of antigen densities [93]. An independent study validated these findings, showing that synaptic calcium flux and overall levels of phosphorylated CD3δ, CD3ε, CD3γ, LAT, and ZAP-70 were lower after CAR-based activation compared to the TCR [92]. Lastly, PKCθ, important for cell-mediated cytotoxicity, secretion, and membrane trafficking as well as pJNK, a driver of cell proliferation and survival, have been reported lower in CAR-stimulated cells [90]. While CAR signaling employs TCR signaling pathways, changes in structure and insufficient recruitment of key signaling molecules reduces antigen sensitivity. While the TCR is capable of cytokine secretion and cytotoxicity upon recognition of a single pMHC, CARs require 100 to 1,000 times the amount of target antigen to elicit the same effector functions. One of the first examples of this was seen in 2015, where CD20-targeted CAR-T cells were only able to lyse target cells expressing ~200 molecules of CD20. At this same density, production of IL-2, TNFα, and IFNγ was not achieved [94].

Other studies have shown that ~1,000 molecules of CAR antigen were needed to induce comparable levels of ITAM phosphorylation and IFNγ secretion [93]. Taken together, these studies suggest that defects in recruitment and phosphorylation of early signaling molecules, such as LCK and ZAP-70, dull the CARs sensitivity to antigen.

While CARs containing either 4-1BB and CD28 costimulatory domains are both insensitive to target antigen compared to the TCR, comparative studies between costimulatory domains have revealed differences between their sensitivity and signaling strength, informing appropriate clinical use. CARs with CD28-based costimulation generally exhibit more intense activation, supported by higher phosphorylation of PLCγ1, ZAP-70, and CD3 ITAMs [95, 96]. This in part due to an increase of CAR-associated LCK that directly binds to the PYAPP motif found in the intracellular domain of CD28 [97, 98]. The lower intensity of signaling observed in CARs containing 4-1BB costimulatory domains is partially due to binding of the THEMIS:SHP1 complex, leading to dephosphorylation of CD3ζ ITAMs and CAR-associated LCK [99]. These differences in strength of activation impact sensitivity, with 4-1BB-containing CARs requiring roughly 10-times more antigen to reach similar levels of IL-2 production as CD28-containing CARs [100]. In summary, CD28-containing CAR designs tend to have higher levels of antigen-specific activation as well as antigen-independent tonic signaling. Despite being more sensitive to antigen than constructs using 4-1BB-based costimulation, CD28-containing CARs still have diminished ITAM phosphorylation and antigen sensitivity compared to the TCR. Although many clinical trials are focused on re-engineering second-generation CARs to target new surface antigens, it is clear there is still a great need for improving CAR-T signaling.

2. MATERIALS AND METHODS

2.1 Chimeric antigen receptor design and cloning

Gene blocks were generated *in silico* (SnapGene) and synthesized by IDT. CAR constructs housed within the second-generation lentiviral transfer plasmid pHR were assembled via a variety of molecular cloning methods including HiFi Assembly (NEB), restriction digest cloning, cloning by PCR, and site-directed mutagenesis. Assembled products were transformed into either Stbl3 (Invitrogen) or STABLE (NEB) chemically-competent cells. Individual colonies were selected off ampicillin or carbenicillin antibiotic plates, inoculated, and plasmid DNA isolated (Qiagen). Final colonies were chosen after size verification via restriction enzyme digestion and sanger sequencing spanning at minimum the transgene promoter through stop codon. Complete amino acid sequences for each construct can be found in Table 2.1.

2.2 Lentiviral production and titering

Lenti-X 293T cells (Takara) were plated at a density of $0.35e^6$/ml and grown overnight until at 85 to 95% confluence. Cells were transfected using Lipofectamine 3000 (Invitrogen) encapsulated with psPAX2, pmD2.G, and the desired transfer plasmid at a 1:1:1 molar ratio. After 48 to 72 hours of viral production, supernatant was filtered through a 0.45μm membrane and concentrated using 100kDa Amicon Ultra centrifugal filter units (Millipore Sigma). Concentrated lentiviral supernatant was aliquoted and stored at -80°C until use. Functional titers for each viral preparation were determined by transducing Jurkat T cells and assessing transgene fluorescence. Briefly, Jurkat cells were resuspended in RPMI supplemented with 10% FBS, 1X penicillin-streptomycin (Gibco), and 10μg/ml protamine sulfate and plated at a final concentration of $0.5e^6$ cells/ml. Dilutions of viral supernatant were added to each well and pipetted gently to mix. Cells were spinoculated at 800g for 1 hour at 22°C and incubated at 37°C

for 48 hours before assessing fluorescence via flow cytometry. Functional titer (FTU/ml) was calculated as: (number of cells transduced) x (percent of cells positive for transgene) / (volume of viral supernatant).

2.3 Generation of Nalm6 cell lines

Nalm6 Chili-Luc cells were generated by transducing Nalm6 cells (ATCC) with lentiviruses packaged with the Chili-Luciferase transgene (pUltra-Chili-Luc, Addgene Plasmid #48688). dTomato^{+} cells were sorted using FACS and returned to culture. For generating subclonal populations with differing CD22 antigen expression, Nalm6 cells were sorted as singlets into a 96-well plate and returned to culture. Each expanded single-cell was stained for CD22 using Quantitative Flow Cytometry and 11 were selected for coculture. Nalm6 CD22^{KO} cells were generated by the National Cancer Institute (NCI) and obtained under a material transfer agreement [81].

2.4 Isolation of peripheral blood mononuclear cells

Peripheral blood mononuclear cells (PBMCs) from healthy donors were isolated from blood filters obtained by the UChicago Medicine Blood Bank. Briefly, filters were obtained the day-of donation and washed with 1X PBS. PBMCs were isolated after separation by Ficoll-Paque PLUS density gradient media (Cytiva) and remaining red blood cells were lysed using ACK lysing buffer (Gibco). PBMCs were counted, resuspended in RPMI supplemented with 40% FBS and 10% DMSO, aliquoted into cryovials, and frozen at -150°C.

2.5 Generation of chimeric antigen receptor T cells

To generate Jurkat CAR-T cells, cells were stained using both acridine orange and propidium iodide dyes and counted on a LUNA-FL automatic cell counter (Logos Biosystems). Cells were resuspended in complete RPMI supplemented with 10% FBS, 1X penicillin-

streptomycin (Gibco), and 10μg/ml protamine sulfate and plated at a final concentration of $0.5e^6$ cells/ml. CAR viral particles were added dropwise to reach a multiplicity of infection (MOI) of 5 and if applicable, CoCAR viral particles at an MOI of 2.5. Cells were spinoculated at 800g for 1 hour at 22°C and then returned to the incubator for 48 to 72 hours before use.

Primary human CAR-T cells were generated from frozen PBMC aliquots as described previously. Each tube of primary human PBMCs was quickly thawed in a 37°C water bath and then transferred to 10ml of T cell media (TCM) consisting of RPMI supplemented with 10% FBS, 1X penicillin-streptomycin (Gibco), 50μM 2-Mercaptoethanol, and 100U/ml IL-2 (Miltenyi Biotec). Cells were centrifuged at 300g for 5 minutes at 22°C and supernatant was then removed. The cell pellet was resuspended in 2ml complete TCM, plated on a 6 well plate, and incubated at 37°C for 3 to 4 hours. The cell suspension was then passed through a 70μm stainer and transferred to a new well. Cells counts were obtained using a Luna-FL automatic cell counter. To maintain consistency between experiments, CD3% was determined through surface staining and analysis with flow cytometry. Concentrations were adjusted so that $5e^5$ $CD3^+$ cells and $5e^5$ anti-CD3/CD28 Dynabeads (Gibco) were plated at a final concentration of $0.5e^6$ cells/ml and incubated at 37°C overnight. Protamine sulfate was added to a final concentration of 10μg/ml and CAR viral particles were added dropwise to reach an MOI of 10 and if applicable, CoCAR viral particles at an MOI of 5. Cells were spinoculated at 800g for 1 hour at 22°C and then returned to the incubator for 24 hours. Cells were then washed with complete TCM and returned to the incubator for an additional 24 hours. Dynabeads were magnetically-removed and cells were incubated an additional 24 hours. Fresh TCM was then added every other day to maintain cell viability and growth. Expression of CAR and CoCAR molecules was assessed via

flow cytometry, either by mEGFP or FusionRed fluorescent proxies or by a surface-staining reagent.

2.6 Flow cytometry staining

Cells were kept on ice for the entirety of the protocol, unless otherwise stated. Cells were plated on a V-bottom 96 well plate and centrifuged at 300g for 5 minutes at 4°C. Supernatant was discarded and cells were resuspended in 50µl FACS buffer (1X PBS, 2% BSA, 0.05% NaN_3) with pre-titered amounts of surface-staining antibodies. Cells were then incubated for 30 minutes at 4°C before being washed twice with 200µl cold PBS. Cells were resuspended in 50µl Zombie NIR Viability Dye (Biolegend) diluted 1:1000 in PBS and incubated for 10 minutes at 22°C. Cells were then washed twice with 200µl FACS buffer. If only staining for surface antigen, cells were then resuspended in a final volume of 75µl FACS and assessed using flow cytometry. For samples being stained intracellularly, cells were resuspended in 100µl of fixation/permeabilization solution (BD) and incubated for 20 minutes at 4°C. Cells were then washed twice with 200µl perm/wash buffer (BD). Cells were resuspended in 50µl perm/wash solution with pre-titered amounts of intraceullar-staining antibodies and incubated for 30 minutes at 4°C. Cells were washed twice with 200µl perm/wash buffer (BD). Finally, cells were resuspended in 75µl FACS and assessed using flow cytometry. Antibody and staining reagent panels are listed in Table 2.2.

2.7 Quantitative flow cytometry

Nalm6 cells were stained with an AF647-CD22 antibody (Biolegend), using the same protocol as listed in Flow Cytometry Staining. Cells were then assessed using flow cytometry alongside Quantum AF647 MESF beads (Bangs Laboratories) on the same day with the same PMT settings. A calibration curve was established using the geometric mean fluorescence

intensity (gMFI) of MESF bead standards and the antibody binding capacity (ABC) of Nalm6 cells was determined by dividing the derived value from the calibration curve by the antibody's F/P ratio.

2.8 Cytokine assays

For intracellular staining, effector and target cells were stained using both acridine orange and propidium iodide dyes and counted on a LUNA-FL automatic cell counter (Logos Biosystems). $5e^5$ effector cells and $5e^5$ target cells were combined in a total volume of 100µl TCM with 1X Brefeldin A (Biolegend) and plated in a V-bottom 96-well plate. Cells were cocultured for 5 to 6 hours at 37°C before staining. For Legendplex or plate-based ELISA assays, effector and target cells were stained using both acridine orange and propidium iodide dyes and counted on a LUNA-FL automatic cell counter (Logos Biosystems). Effector counts were adjusted by mEGFP%$^+$, so to normalize the amount of CAR$^+$ cells between conditions. When noted, cells of equivalent mEGFP gMFI were sorted using FACS to ensure populations of uniform CAR expression. $5e^5$ effector cells and $5e^5$ target cells were combined in a total volume of 100µl TCM and plated in a 96-well plate. Cells were cocultured for 16 to 18 hours at 37°C, centrifuged at 300g for 5 min, and supernatant was transferred to clean tube strips. Supernatant was stored at -80°C until analyzed as per the manufacturer's recommendations (Biolegend).

2.9 Cytotoxicity assays

Effector and target cells were stained using both acridine orange and propidium iodide dyes and counted on a LUNA-FL automatic cell counter (Logos Biosystems). Effector counts were adjusted by mEGFP%$^+$, so to normalize the amount of CAR$^+$ cells between conditions. When noted, cells of equivalent mEGFP gMFI were sorted using FACS to ensure populations of uniform CAR expression. $16.7e^5$ effector cells and $5e^5$ target cells were combined in a total

volume of 100µl TCM in black-walled, clear-bottom 96-well plates and cocultured for 16 to 18 hours at 37°C. Following coculture, cytotoxicity was immediately assessed by ONE-Glo Luciferase Assay System (Promega) as per the manufacturer's recommendations.

2.10 Imaging

The following was largely based off a protocol published by Xiao and Su 2023 [101]. Briefly, Jurkat T cells expressing CAR and CoCAR were generated as previously described. Nalm6 cells were labelled with CellTrace Violet (CTV) as per the manufacturer's recommendations (Invitrogen). $2.5e^5$ Jurkat CAR-T cells were cocultured with $2.5e^5$ CTV-labeled Nalm6 cells in a total volume of 50µl RPMI supplemented with 10% FBS, 1X penicillin-streptomycin (Gibco) for 30 minutes at 37°C. To retain cell-cell interactions for imaging, PFA was then added to reach a final concentration of 4%. Cells were fixed for 15 minutes at 22°C, washed one with 1ml PBS, resuspended in 100µl PBS, and then mounted on a coverslip. Fluorescence images were acquired using a Leica DMI8 (Leica Microsystems) inverted microscope equipped with a HC PL APO 63x/1.40 OIL objective and Andor-Zyla-VSC03291 camera. CTV was detected by an excitation filter at 395/25nm and emission wavelength 440/40nm. mEGFP and FusionRed were observed by Ex/Em wavelength = 490/515 nm and Ex/Em wavelength = 570/590 nm, respectively. The data was processed using Leica Application Suite X v.1.4.6.

2.11 Mouse models

All mouse experiments were performed under UChicago Institutional Animal Care and Use Committee approval. NSG (NOD.Cg-*Prkdc*^{scid} *Il2rg*^{tm1Wjl}/SzJ) mice were either obtained from JAX or bred within UChicago animal facilities. Female NSG mice ages 6-10 weeks old were randomized and placed into fresh cages. On day 0, mice were intravenously injected with

$1e^6$ Nalm6 Chili-Luc cells in 100µl sterile PBS. On day 3, mice were intravenously injected with $5e^6$ CAR-T cells in 100µl PBS or with 100µl PBS as an untreated control. Survival of mice was monitored daily and mice were euthanized when pre-determined, appropriate experimental endpoints were met.

2.12 Statistical analysis

All statistical analyses were carried out in GraphPad Prism v.10.1.0. Statistical differences between groups were tested using unpaired, two-tailed t-tests except for *in vivo* survival which was tested using Kaplan-Meier nonparametric analysis. Statistical significance was set at $p < 0.05$ for all comparisons. In all figures, one asterisk indicates a p value of < 0.05, two asterisks indicates a p value of < 0.01, and three asterisks indicates a p value of < 0.001.

Table 2.1 Amino acid sequences of CAR and CoCAR constructs

As Described in Figure 3.1
SEQ1 (CAR): MALPVTALLLPLALLLHAARPDIQMTQTTSSLSASLGDRVTISCRASQDISKYLNWYQ QKPDGTVKLLIYHTSRLHSGVPSRFSGSGSGTDYSLTISNLEQEDIATYFCQQGNTLPY TFGGGTKLEITGGGGSGGGGSGGGGSEVKLQESGPGLVAPSQSLSVTCTVSGVSLPDY GVSWIRQPPRKGLEWLGVIWGSETTYYNSALKSRLTIIKDNSKSQVFLKMNSLQTDDT AIYYCAKHYYYGGSYAMDYWGQGTSVTVSSTTTPAPRPPTPAPTIASQPLSLRPEACR PAAGGAVHTRGLDFACDIYIWAPLAGTCGVLLLSLVITLYCKRGRKKLLYIFKQPFMR PVQTTQEEDGCSCRFPEEEEGGCELRVKFSRSADAPAYQQGQNQLYNELNLGRREEY DVLDKRRGRDPEMGGKPQRRKNPQEGLYNELQKDKMAEAYSEIGMKGERRRGKGH DGLYQGLSTATKDTYDALHMQALPPRHMVSKGEELFTGVVPILVELDGDVNGHKFS VSGEGEGDATYGKLTLKFICTTGKLPVPWPTLVTTLTYGVQCFSRYPDHMKQHDFFK SAMPEGYVQERTIFFKDDGNYKTRAEVKFEGDTLVNRIELKGIDFKEDGNILGHKLEY NYNSHNVYIMADKQKNGIKVNFKIRHNIEDGSVQLADHYQQNTPIGDGPVLLPDNHY LSTQSKLSKDPNEKRDHMVLLEFVTAAGITLGMDELYK **SEQ2 (CAR8α1):** MALPVTALLLPLALLLHAARPDIQMTQTTSSLSASLGDRVTISCRASQDISKYLNWYQ QKPDGTVKLLIYHTSRLHSGVPSRFSGSGSGTDYSLTISNLEQEDIATYFCQQGNTLPY TFGGGTKLEITGGGGSGGGGSGGGGSEVKLQESGPGLVAPSQSLSVTCTVSGVSLPDY GVSWIRQPPRKGLEWLGVIWGSETTYYNSALKSRLTIIKDNSKSQVFLKMNSLQTDDT AIYYCAKHYYYGGSYAMDYWGQGTSVTVSSTTTPAPRPPTPAPTIASQPLSLRPEACR PAAGGAVHTRGLDFACDIYIWAPLAGTCGVLLLSLVITLYCNHRNRRRVCKCPRPVV KSGDKPSLSARYVKRGRKKLLYIFKQPFMRPVQTTQEEDGCSCRFPEEEEGGCELRVK FSRSADAPAYQQGQNQLYNELNLGRREEYDVLDKRRGRDPEMGGKPQRRKNPQEGL YNELQKDKMAEAYSEIGMKGERRRGKGHDGLYQGLSTATKDTYDALHMQALPPRH MVSKGEELFTGVVPILVELDGDVNGHKFSVSGEGEGDATYGKLTLKFICTTGKLPVP WPTLVTTLTYGVQCFSRYPDHMKQHDFFKSAMPEGYVQERTIFFKDDGNYKTRAEV KFEGDTLVNRIELKGIDFKEDGNILGHKLEYNYNSHNVYIMADKQKNGIKVNFKIRHN IEDGSVQLADHYQQNTPIGDGPVLLPDNHYLSTQSKLSKDPNEKRDHMVLLEFVTAA GITLGMDELYK **SEQ3 (CAR8α2):** MALPVTALLLPLALLLHAARPDIQMTQTTSSLSASLGDRVTISCRASQDISKYLNWYQ QKPDGTVKLLIYHTSRLHSGVPSRFSGSGSGTDYSLTISNLEQEDIATYFCQQGNTLPY TFGGGTKLEITGGGGSGGGGSGGGGSEVKLQESGPGLVAPSQSLSVTCTVSGVSLPDY GVSWIRQPPRKGLEWLGVIWGSETTYYNSALKSRLTIIKDNSKSQVFLKMNSLQTDDT AIYYCAKHYYYGGSYAMDYWGQGTSVTVSSTTTPAPRPPTPAPTIASQPLSLRPEACR PAAGGAVHTRGLDFACDIYIWAPLAGTCGVLLLSLVITLYCKRGRKKLLYIFKQPFMR PVQTTQEEDGCSCRFPEEEEGGCELLYCNHRNRRRVCKCPRPVVKSGDKPSLSARYV RVKFSRSADAPAYQQGQNQLYNELNLGRREEYDVLDKRRGRDPEMGGKPQRRKNP

QEGLYNELQKDKMAEAYSEIGMKGERRRGKGHDGLYQGLSTATKDTYDALHMQAL
PPRHMVSKGEELFTGVVPILVELDGDVNGHKFSVSGEGEGDATYGKLTLKFICTTGKL
PVPWPTLVTTLTYGVQCFSRYPDHMKQHDFFKSAMPEGYVQERTIFFKDDGNYKTRA
EVKFEGDTLVNRIELKGIDFKEDGNILGHKLEYNYNSHNVYIMADKQKNGIKVNFKIR
HNIEDGSVQLADHYQQNTPIGDGPVLLPDNHYLSTQSKLSKDPNEKRDHMVLLEFVT
AAGITLGMDELYK

SEQ4 (CAR8*α3*):
MALPVTALLLPLALLLHAARPDIQMTQTTSSLSASLGDRVTISCRASQDISKYLNWYQ
QKPDGTVKLLIYHTSRLHSGVPSRFSGSGSGTDYSLTISNLEQEDIATYFCQQGNTLPY
TFGGGTKLEITGGGGSGGGGSGGGGSEVKLQESGPGLVAPSQSLSVTCTVSGVSLPDY
GVSWIRQPPRKGLEWLGVIWGSETTYYNSALKSRLTIIKDNSKSQVFLKMNSLQTDDT
AIYYCAKHYYYGGSYAMDYWGQGTSVTVSSTTTPAPRPPTPAPTIASQPLSLRPEACR
PAAGGAVHTRGLDFACDIYIWAPLAGTCGVLLLSLVITLYCKRGRKKLLYIFKQPFMR
PVQTTQEEDGCSCRFPEEEEGGCELRVKFSRSADAPAYQQGQNQLYNELNLGRREEY
DVLDKRRGRDPEMGGKPQRRKNPQEGLYNELQKDKMAEAYSEIGMKGERRRGKGH
DGLYQGLSTATKDTYDALHMQALPPRHLYCNHRNRRRVCKCPRPVVKSGDKPSLSA
RYVMVSKGEELFTGVVPILVELDGDVNGHKFSVSGEGEGDATYGKLTLKFICTTGKL
PVPWPTLVTTLTYGVQCFSRYPDHMKQHDFFKSAMPEGYVQERTIFFKDDGNYKTRA
EVKFEGDTLVNRIELKGIDFKEDGNILGHKLEYNYNSHNVYIMADKQKNGIKVNFKIR
HNIEDGSVQLADHYQQNTPIGDGPVLLPDNHYLSTQSKLSKDPNEKRDHMVLLEFVT
AAGITLGMDELYK

As Described in Figure 3.3

SEQ5 (CAR):
Identical to SEQ1

SEQ6 (CAR-IRES-CoCAR4):
MALPVTALLLPLALLLHAARPDIQMTQTTSSLSASLGDRVTISCRASQDISKYLNWYQ
QKPDGTVKLLIYHTSRLHSGVPSRFSGSGSGTDYSLTISNLEQEDIATYFCQQGNTLPY
TFGGGTKLEITGGGGSGGGGSGGGGSEVKLQESGPGLVAPSQSLSVTCTVSGVSLPDY
GVSWIRQPPRKGLEWLGVIWGSETTYYNSALKSRLTIIKDNSKSQVFLKMNSLQTDDT
AIYYCAKHYYYGGSYAMDYWGQGTSVTVSSTTTPAPRPPTPAPTIASQPLSLRPEACR
PAAGGAVHTRGLDFACDIYIWAPLAGTCGVLLLSLVITLYCKRGRKKLLYIFKQPFMR
PVQTTQEEDGCSCRFPEEEEGGCELRVKFSRSADAPAYQQGQNQLYNELNLGRREEY
DVLDKRRGRDPEMGGKPQRRKNPQEGLYNELQKDKMAEAYSEIGMKGERRRGKGH
DGLYQGLSTATKDTYDALHMQALPPRHMVSKGEELFTGVVPILVELDGDVNGHKFS
VSGEGEGDATYGKLTLKFICTTGKLPVPWPTLVTTLTYGVQCFSRYPDHMKQHDFFK
SAMPEGYVQERTIFFKDDGNYKTRAEVKFEGDTLVNRIELKGIDFKEDGNILGHKLEY
NYNSHNVYIMADKQKNGIKVNFKIRHNIEDGSVQLADHYQQNTPIGDGPVLLPDNHY
LSTQSKLSKDPNEKRDHMVLLEFVTAAGITLGMDELYK*SGRV*SRPAGMQACPSPSP
PPNVTGRSRLE*GRCAFVYMLFSTILPSFGNVRARKPGPVFLTSIPRGLSPLAKGMQGL
LNVVKEAVPLEAS*RQTTSVATLCRQRNPPPGDRCLCGQKPRV*DTPAKAAQPQCHV
VSWIVVERVKWLTSSVFNKGLKDAQKVPHCMGSDLGPRCTCFTCV*SRLKNV*APRT
TGTWFSFEKHDDNMLLLVTSLLLCELPHPAFLLIPQVQLQQSGPGLVKPSQTLSLTCAI

SGDSVSSNSAAWNWIRQSPSRGLEWLGRTYYRSKWYNDYAVSVKSRITINPDTSKNQ
FSLQLNSVTPEDTAVYYCAREVTGDLEDAFDIWGQGTMVTVSSGGGGSDIQMTQSPS
SLSASVGDRVTITCRASQTIWSYLNWYQQRPGKAPNLLIYAASSLQSGVPSRFSGRGS
GTDFTLTISSLQAEDFATYYCQQSYSIPQTFGQGTKLEIKTTTPAPRPPTPAPTIASQPLS
LRPEACRPAAGGAVHTRGLDFACMALIVLGGVAGLLLFIGLGIFFCVRCRHRRRQAER
MSQIKRLLSEKKTCQCPHRFQKTCSPIMVSELIKENMPMKLYMEGTVNNHHFKCTSE
GEGKPYEGTQTMRIKVVEGGPLPFAFDILATSFMYGSRTFIKHPPGIPDFFKQSFPEGFT
WERVTTYEDGGVLTATQDTSLQDGCLIYNVKVRGVNFPANGPVMQKKTLGWEASTE
TMYPADGGLEGACDMALKLVGGGHMICNLETTYRSKKPATNLKMPGVYNVDHRLE
RIKEADDETYVEQHEVAVARYSTGGAGDGGK

SEQ7 (CAR-IRES-CoCAR8*α*):
MALPVTALLLPLALLLHAARPDIQMTQTTSSLSASLGDRVTISCRASQDISKYLNWYQ
QKPDGTVKLLIYHTSRLHSGVPSRFSGSGSGTDYSLTISNLEQEDIATYFCQQGNTLPY
TFGGGTKLEITGGGGSGGGGSGGGGSEVKLQESGPGLVAPSQSLSVTCTVSGVSLPDY
GVSWIRQPPRKGLEWLGVIWGSETTYYNSALKSRLTIIKDNSKSQVFLKMNSLQTDDT
AIYYCAKHYYYGGSYAMDYWGQGTSVTVSSTTTPAPRPPTPAPTIASQPLSLRPEACR
PAAGGAVHTRGLDFACDIYIWAPLAGTCGVLLLSLVITLYCKRGRKKLLYIFKQPFMR
PVQTTQEEDGCSCRFPEEEEGGCELRVKFSRSADAPAYQQGQNQLYNELNLGRREEY
DVLDKRRGRDPEMGGKPQRRKNPQEGLYNELQKDKMAEAYSEIGMKGERRRGKGH
DGLYQGLSTATKDTYDALHMQALPPRHMVSKGEELFTGVVPILVELDGDVNGHKFS
VSGEGEGDATYGKLTLKFICTTGKLPVPWPTLVTTLTYGVQCFSRYPDHMKQHDFFK
SAMPEGYVQERTIFFKDDGNYKTRAEVKFEGDTLVNRIELKGIDFKEDGNILGHKLEY
NYNSHNVYIMADKQKNGIKVNFKIRHNIEDGSVQLADHYQQNTPIGDGPVLLPDNHY
LSTQSKLSKDPNEKRDHMVLLEFVTAAGITLGMDELYK*SGRV*SRPAGMQACPSPSP
PPNVTGRSRLE*GRCAFVYMLFSTILPSFGNVRARKPGPVFLTSIPRGLSPLAKGMQGL
LNVVKEAVPLEAS*RQTTSVATLCRQRNPPPGDRCLCGQKPRV*DTPAKAAQPQCHV
VSWIVVERVKWLTSSVFNKGLKDAQKVPHCMGSDLGPRCTCFTCV*SRLKNV*APRT
TGTWFSFEKHDDNMLLLVTSLLLCELPHPAFLLIPQVQLQQSGPGLVKPSQTLSLTCAI
SGDSVSSNSAAWNWIRQSPSRGLEWLGRTYYRSKWYNDYAVSVKSRITINPDTSKNQ
FSLQLNSVTPEDTAVYYCAREVTGDLEDAFDIWGQGTMVTVSSGGGGSDIQMTQSPS
SLSASVGDRVTITCRASQTIWSYLNWYQQRPGKAPNLLIYAASSLQSGVPSRFSGRGS
GTDFTLTISSLQAEDFATYYCQQSYSIPQTFGQGTKLEIKTTTPAPRPPTPAPTIASQPLS
LRPEACRPAAGGAVHTRGLDFACDIYIWAPLAGTCGVLLLSLVITLYCNHRNRRRVC
KCPRPVVKSGDKPSLSARYVMVSELIKENMPMKLYMEGTVNNHHFKCTSEGEGKPY
EGTQTMRIKVVEGGPLPFAFDILATSFMYGSRTFIKHPPGIPDFFKQSFPEGFTWERVTT
YEDGGVLTATQDTSLQDGCLIYNVKVRGVNFPANGPVMQKKTLGWEASTETMYPA
DGGLEGACDMALKLVGGGHMICNLETTYRSKKPATNLKMPGVYNVDHRLERIKEAD
DETYVEQHEVAVARYSTGGAGDGGK

As Described in Figure 3.5

SEQ8 (CAR):
MLLLVTSLLLCELPHPAFLLIPQVQLQQSGPGLVKPSQTLSLTCAISGDSVSSNSAAWN
WIRQSPSRGLEWLGRTYYRSKWYNDYAVSVKSRITINPDTSKNQFSLQLNSVTPEDTA

VYYCAREVTGDLEDAFDIWGQGTMVTVSSGGGGSDIQMTQSPSSLSASVGDRVTITC
RASQTIWSYLNWYQQRPGKAPNLLIYAASSLQSGVPSRFSGRGSGTDFTLTISSLQAED
FATYYCQQSYSIPQTFGQGTKLEIKTTTPAPRPPTPAPTIASQPLSLRPEACRPAAGGAV
HTRGLDFACIYIWAPLAGTCGVLLLSLVITKRGRKKLLYIFKQPFMRPVQTTQEEDGC
SCRFPEEEEGGCELRVKFSRSADAPAYQQGQNQLYNELNLGRREEYDVLDKRRGRDP
EMGGKPQRRKNPQEGLYNELQKDKMAEAYSEIGMKGERRRGKGHDGLYQGLSTAT
KDTYDALHMQALPPRGSGATNFSLLKQAGDVEENPGPMVSKGEELFTGVVPILVELD
GDVNGHKFSVSGEGEGDATYGKLTLKFICTTGKLPVPWPTLVTTLTYGVQCFSRYPD
HMKQHDFFKSAMPEGYVQERTIFFKDDGNYKTRAEVKFEGDTLVNRIELKGIDFKED
GNILGHKLEYNYNSHNVYIMADKQKNGIKVNFKIRHNIEDGSVQLADHYQQNTPIGD
GPVLLPDNHYLSTQSKLSKDPNEKRDHMVLLEFVTAAGITLGMDELYK

SEQ9 (CoCAR4):
MVLLVTSLLLCELPHPAFLLIPDTEVQLVESGGGLVKPGGSLKLSCAASGFAFSIYDMS
WVRQTPEKRLEWVAYISSGGGTYYPDTVKGRFTISRDNAKNTLYLQMSSLKSEDTAM
YYCARHSGYGTHWGVLFAYWGQGTLVTVSAGGGGSGGGGSGGGGSDIQMTQTTSS
LSASLGDRVTISCRASQDISNYLNWYQQKPDGTVKLLIYYTSILHSGVPSRFSGSGSGT
DYSLTISNLEQEDFATYFCQQGNTLPWTFGGGTKLEIKTTTPAPRPPTPAPTIASQPLSL
RPEACRPAAGGAVHTRGLDFACMALIVLGGVAGLLLFIGLGIFFCVRCRHRRRQAER
MSQIKRLLSEKKTCQCPHRFQKTCSPIGSGATNFSLLKQAGDVEENPGPMVSELIKEN
MPMKLYMEGTVNNHHFKCTSEGEGKPYEGTQTMRIKVVEGGPLPFAFDILATSFMYG
SRTFIKHPPGIPDFFKQSFPEGFTWERVTTYEDGGVLTATQDTSLQDGCLIYNVKVRGV
NFPANGPVMQKKTLGWEASTETMYPADGGLEGACDMALKLVGGGHMICNLETTYR
SKKPATNLKMPGVYNVDHRLERIKEADDETYVEQHEVAVARYSTGGAGDGGK

SEQ10 (CoCAR8*α*):
MVLLVTSLLLCELPHPAFLLIPDTEVQLVESGGGLVKPGGSLKLSCAASGFAFSIYDMS
WVRQTPEKRLEWVAYISSGGGTYYPDTVKGRFTISRDNAKNTLYLQMSSLKSEDTAM
YYCARHSGYGTHWGVLFAYWGQGTLVTVSAGGGGSGGGGSGGGGSDIQMTQTTSS
LSASLGDRVTISCRASQDISNYLNWYQQKPDGTVKLLIYYTSILHSGVPSRFSGSGSGT
DYSLTISNLEQEDFATYFCQQGNTLPWTFGGGTKLEIKTTTPAPRPPTPAPTIASQPLSL
RPEACRPAAGGAVHTRGLDFACIYIWAPLAGTCGVLLLSLVITLYCNHRNRRRVCKCP
RPVVKSGDKPSLSARYVGSGATNFSLLKQAGDVEENPGPMVSELIKENMPMKLYME
GTVNNHHFKCTSEGEGKPYEGTQTMRIKVVEGGPLPFAFDILATSFMYGSRTFIKHPP
GIPDFFKQSFPEGFTWERVTTYEDGGVLTATQDTSLQDGCLIYNVKVRGVNFPANGPV
MQKKTLGWEASTETMYPADGGLEGACDMALKLVGGGHMICNLETTYRSKKPATNL
KMPGVYNVDHRLERIKEADDETYVEQHEVAVARYSTGGAGDGGK

As Described in Figure 3.9

SEQ11 (CAR):
MLLLVTSLLLCELPHPAFLLIPQVQLQQSGPGLVKPSQTLSLTCAISGDSVSSNSAAWN
WIRQSPSRGLEWLGRTYYRSKWYNDYAVSVKSRITINPDTSKNQFSLQLNSVTPEDTA
VYYCAREVTGDLEDAFDIWGQGTMVTVSSGGGGSDIQMTQSPSSLSASVGDRVTITC
RASQTIWSYLNWYQQRPGKAPNLLIYAASSLQSGVPSRFSGRGSGTDFTLTISSLQAED
FATYYCQQSYSIPQTFGQGTKLEIKAAATTTPAPRPPTPAPTIASQPLSLRPEACRPAAG

GAVHTRGLDFACDIYIWAPLAGTCGVLLLSLVITLYCKRGRKKLLYIFKQPFMRPVQT
TQEEDGCSCRFPEEEEGGCELRVKFSRSADAPAYQQGQNQLYNELNLGRREEYDVLD
KRRGRDPEMGGKPRRKNPQEGLYNELQKDKMAEAYSEIGMKGERRRGKGHDGLYQ
GLSTATKDTYDALHMQALPPRMVSKGEELFTGVVPILVELDGDVNGHKFSVSGEGEG
DATYGKLTLKFICTTGKLPVPWPTLVTTLTYGVQCFSRYPDHMKQHDFFKSAMPEGY
VQERTIFFKDDGNYKTRAEVKFEGDTLVNRIELKGIDFKEDGNILGHKLEYNYNSHNV
YIMADKQKNGIKVNFKIRHNIEDGSVQLADHYQQNTPIGDGPVLLPDNHYLSTQSKLS
KDPNEKRDHMVLLEFVTAAGITLGMDELYK

SEQ12 (CoCAR):
MLLLVTSLLLCELPHPAFLLIPEVQLVESGGGLVKPGGSLKLSCAASGFAFSIYDMSW
VRQTPEKRLEWVAYISSGGGTYYPDTVKGRFTISRDNAKNTLYLQMSSLKSEDTAMY
YCARHSGYGTHWGVLFAYWGQGTLVTVSAGGGGSGGGGSGGGGSDIQMTQTTSSL
SASLGDRVTISCRASQDISNYLNWYQQKPDGTVKLLIYYTSILHSGVPSRFSGSGSGTD
YSLTISNLEQEDFATYFCQQGNTLPWTFGGGTKLEIKAAATTTPAPRPPTPAPTIASQPL
SLRPEACRPAAGGAVHTRGLDFACDIYIWAPLAGTCGVLLLSLVITLYCNHRNRRRVC
KCPRPVVKSGDKPSLSARYVMVSELIKENMPMKLYMEGTVNNHHFKCTSEGEGKPY
EGTQTMRIKVVEGGPLPFAFDILATSFMYGSRTFIKHPPGIPDFFKQSFPEGFTWERVTT
YEDGGVLTATQDTSLQDGCLIYNVKVRGVNFPANGPVMQKKTLGWEASTETMYPA
DGGLEGACDMALKLVGGGHMICNLETTYRSKKPATNLKMPGVYNVDHRLERIKEAD
DETYVEQHEVAVARYSTGGAGDGGK

As Described in Figure 3.15

SEQ13 (CAR):
MLLLVTSLLLCELPHPAFLLIPQVQLQQSGPGLVKPSQTLSLTCAISGDSVSSNSAAWN
WIRQSPSRGLEWLGRTYYRSKWYNDYAVSVKSRITINPDTSKNQFSLQLNSVTPEDTA
VYYCAREVTGDLEDAFDIWGQGTMVTVSSGGGGSDIQMTQSPSSLSASVGDRVTITC
RASQTIWSYLNWYQQRPGKAPNLLIYAASSLQSGVPSRFSGRGSGTDFTLTISSLQAED
FATYYCQQSYSIPQTFGQGTKLEIKTTTPAPRPPTPAPTIASQPLSLRPEACRPAAGGAV
HTRGLDFACIYIWAPLAGTCGVLLLSLVITKRGRKKLLYIFKQPFMRPVQTTQEEDGC
SCRFPEEEEGGCELRVKFSRSADAPAYQQGQNQLYNELNLGRREEYDVLDKRRGRDP
EMGGKPQRRKNPQEGLYNELQKDKMAEAYSEIGMKGERRRGKGHDGLYQGLSTAT
KDTYDALHMQALPPRMVSKGEELFTGVVPILVELDGDVNGHKFSVSGEGEGDATYG
KLTLKFICTTGKLPVPWPTLVTTLTYGVQCFSRYPDHMKQHDFFKSAMPEGYVQERTI
FFKDDGNYKTRAEVKFEGDTLVNRIELKGIDFKEDGNILGHKLEYNYNSHNVYIMAD
KQKNGIKVNFKIRHNIEDGSVQLADHYQQNTPIGDGPVLLPDNHYLSTQSKLSKDPNE
KRDHMVLLEFVTAAGITLGMDELYK

SEQ14 (CAR-IRES-CoCAR):
MLLLVTSLLLCELPHPAFLLIPQVQLQQSGPGLVKPSQTLSLTCAISGDSVSSNSAAWN
WIRQSPSRGLEWLGRTYYRSKWYNDYAVSVKSRITINPDTSKNQFSLQLNSVTPEDTA
VYYCAREVTGDLEDAFDIWGQGTMVTVSSGGGGSDIQMTQSPSSLSASVGDRVTITC
RASQTIWSYLNWYQQRPGKAPNLLIYAASSLQSGVPSRFSGRGSGTDFTLTISSLQAED
FATYYCQQSYSIPQTFGQGTKLEIKTTTPAPRPPTPAPTIASQPLSLRPEACRPAAGGAV
HTRGLDFACIYIWAPLAGTCGVLLLSLVITKRGRKKLLYIFKQPFMRPVQTTQEEDGC

SCRFPEEEEGGCELRVKFSRSADAPAYQQGQNQLYNELNLGRREEYDVLDKRRGRDP
EMGGKPQRRKNPQEGLYNELQKDKMAEAYSEIGMKGERRRGKGHDGLYQGLSTAT
KDTYDALHMQALPPRMVSKGEELFTGVVPILVELDGDVNGHKFSVSGEGEGDATYG
KLTLKFICTTGKLPVPWPTLVTTLTYGVQCFSRYPDHMKQHDFFKSAMPEGYVQERTI
FFKDDGNYKTRAEVKFEGDTLVNRIELKGIDFKEDGNILGHKLEYNYNSHNVYIMAD
KQKNGIKVNFKIRHNIEDGSVQLADHYQQNTPIGDGPVLLPDNHYLSTQSKLSKDPNE
KRDHMVLLEFVTAAGITLGMDELYK*PLSLPPP*RYWPKPLGIRPVCVCLYVIFHHIAV
FWQCEGPETWPCLLDEHS*GSFPSRQRNARSVECREGSSSSGSFLKTNNVCSDPLQAA
EPPTWRQVPLRPKATCIRYTCKGGTTPVPRCELDSCGKSQMALLKRIQQGAEGCPEGT
PLYGI*SGASVHMLYMCLVEVKKTSRPPEPRGRGFPLKNTMIIWPQMVLLVTSLLLCE
LPHPAFLLIPDTEVQLVESGGGLVKPGGSLKLSCAASGFAFSIYDMSWVRQTPEKRLE
WVAYISSGGGTYYPDTVKGRFTISRDNAKNTLYLQMSSLKSEDTAMYYCARHSGYG
THWGVLFAYWGQGTLVTVSAGGGGSGGGGSGGGGSDIQMTQTTSSLSASLGDRVTI
SCRASQDISNYLNWYQQKPDGTVKLLIYYTSILHSGVPSRFSGSGSGTDYSLTISNLEQ
EDFATYFCQQGNTLPWTFGGGTKLEIKTTTPAPRPPTPAPTIASQPLSLRPEACRPAAG
GAVHTRGLDFACIYIWAPLAGTCGVLLLSLVITLYCNHRNRRRVCKCPRPVVKSGDK
PSLSARYVMVSELIKENMPMKLYMEGTVNNHHFKCTSEGEGKPYEGTQTMRIKVVE
GGPLPFAFDILATSFMYGSRTFIKHPPGIPDFFKQSFPEGFTWERVTTYEDGGVLTATQ
DTSLQDGCLIYNVKVRGVNFPANGPVMQKKTLGWEASTETMYPADGGLEGACDMA
LKLVGGGHMICNLETTYRSKKPATNLKMPGVYNVDHRLERIKEADDETYVEQHEVA
VARYSTGGAGDGGK

SEQ15 (CAR-P2A-CoCAR):
MLLLVTSLLLCELPHPAFLLIPQVQLQQSGPGLVKPSQTLSLTCAISGDSVSSNSAAWN
WIRQSPSRGLEWLGRTYYRSKWYNDYAVSVKSRITINPDTSKNQFSLQLNSVTPEDTA
VYYCAREVTGDLEDAFDIWGQGTMVTVSSGGGGSDIQMTQSPSSLSASVGDRVTITC
RASQTIWSYLNWYQQRPGKAPNLLIYAASSLQSGVPSRFSGRGSGTDFTLTISSLQAED
FATYYCQQSYSIPQTFGQGTKLEIKTTTPAPRPPTPAPTIASQPLSLRPEACRPAAGGAV
HTRGLDFACIYIWAPLAGTCGVLLLSLVITKRGRKKLLYIFKQPFMRPVQTTQEEDGC
SCRFPEEEEGGCELRVKFSRSADAPAYQQGQNQLYNELNLGRREEYDVLDKRRGRDP
EMGGKPQRRKNPQEGLYNELQKDKMAEAYSEIGMKGERRRGKGHDGLYQGLSTAT
KDTYDALHMQALPPRMVSKGEELFTGVVPILVELDGDVNGHKFSVSGEGEGDATYG
KLTLKFICTTGKLPVPWPTLVTTLTYGVQCFSRYPDHMKQHDFFKSAMPEGYVQERTI
FFKDDGNYKTRAEVKFEGDTLVNRIELKGIDFKEDGNILGHKLEYNYNSHNVYIMAD
KQKNGIKVNFKIRHNIEDGSVQLADHYQQNTPIGDGPVLLPDNHYLSTQSKLSKDPNE
KRDHMVLLEFVTAAGITLGMDELYKGSGATNFSLLKQAGDVEENPGPMVLLVTSLLL
CELPHPAFLLIPDTEVQLVESGGGLVKPGGSLKLSCAASGFAFSIYDMSWVRQTPEKR
LEWVAYISSGGGTYYPDTVKGRFTISRDNAKNTLYLQMSSLKSEDTAMYYCARHSGY
GTHWGVLFAYWGQGTLVTVSAGGGGSGGGGSGGGGSDIQMTQTTSSLSASLGDRVT
ISCRASQDISNYLNWYQQKPDGTVKLLIYYTSILHSGVPSRFSGSGSGTDYSLTISNLEQ
EDFATYFCQQGNTLPWTFGGGTKLEIKTTTPAPRPPTPAPTIASQPLSLRPEACRPAAG
GAVHTRGLDFACIYIWAPLAGTCGVLLLSLVITLYCNHRNRRRVCKCPRPVVKSGDK
PSLSARYVMVSELIKENMPMKLYMEGTVNNHHFKCTSEGEGKPYEGTQTMRIKVVE
GGPLPFAFDILATSFMYGSRTFIKHPPGIPDFFKQSFPEGFTWERVTTYEDGGVLTATQ
DTSLQDGCLIYNVKVRGVNFPANGPVMQKKTLGWEASTETMYPADGGLEGACDMA

LKLVGGGHMICNLETTYRSKKPATNLKMPGVYNVDHRLERIKEADDETYVEQHEVA
VARYSTGGAGDGGK

As Described in Figure 3.16

SEQ16 (CAR):
MLLLVTSLLLCELPHPAFLLIPDYKDDDDKQVQLQQSGPGLVKPSQTLSLTCAISGDSV
SSNSAAWNWIRQSPSRGLEWLGRTYYRSKWYNDYAVSVKSRITINPDTSKNQFSLQL
NSVTPEDTAVYYCAREVTGDLEDAFDIWGQGTMVTVSSGGGGSDIQMTQSPSSLSAS
VGDRVTITCRASQTIWSYLNWYQQRPGKAPNLLIYAASSLQSGVPSRFSGRGSGTDFT
LTISSLQAEDFATYYCQQSYSIPQTFGQGTKLEIKTTTPAPRPPTPAPTIASQPLSLRPEA
CRPAAGGAVHTRGLDFACIYIWAPLAGTCGVLLLSLVITKRGRKKLLYIFKQPFMRPV
QTTQEEDGCSCRFPEEEEGGCELRVKFSRSADAPAYQQGQNQLYNELNLGRREEYDV
LDKRRGRDPEMGGKPQRRKNPQEGLYNELQKDKMAEAYSEIGMKGERRRGKGHDG
LYQGLSTATKDTYDALHMQALPPR

SEQ17 (CAR-P2A-CoCAR):
MLLLVTSLLLCELPHPAFLLIPDYKDDDDKQVQLQQSGPGLVKPSQTLSLTCAISGDSV
SSNSAAWNWIRQSPSRGLEWLGRTYYRSKWYNDYAVSVKSRITINPDTSKNQFSLQL
NSVTPEDTAVYYCAREVTGDLEDAFDIWGQGTMVTVSSGGGGSDIQMTQSPSSLSAS
VGDRVTITCRASQTIWSYLNWYQQRPGKAPNLLIYAASSLQSGVPSRFSGRGSGTDFT
LTISSLQAEDFATYYCQQSYSIPQTFGQGTKLEIKTTTPAPRPPTPAPTIASQPLSLRPEA
CRPAAGGAVHTRGLDFACIYIWAPLAGTCGVLLLSLVITKRGRKKLLYIFKQPFMRPV
QTTQEEDGCSCRFPEEEEGGCELRVKFSRSADAPAYQQGQNQLYNELNLGRREEYDV
LDKRRGRDPEMGGKPQRRKNPQEGLYNELQKDKMAEAYSEIGMKGERRRGKGHDG
LYQGLSTATKDTYDALHMQALPPRGSGATNFSLLKQAGDVEENPGPMVLLVTSLLLC
ELPHPAFLLIPDTEVQLVESGGGLVKPGGSLKLSCAASGFAFSIYDMSWVRQTPEKRL
EWVAYISSGGGTYYPDTVKGRFTISRDNAKNTLYLQMSSLKSEDTAMYYCARHSGY
GTHWGVLFAYWGQGTLVTVSAGGGGSGGGGSGGGGSDIQMTQTTSSLSASLGDRVT
ISCRASQDISNYLNWYQQKPDGTVKLLIYYTSILHSGVPSRFSGSGSGTDYSLTISNLEQ
EDFATYFCQQGNTLPWTFGGGTKLEIKEQKLISEEDLTTTPAPRPPTPAPTIASQPLSLR
PEACRPAAGGAVHTRGLDFACIYIWAPLAGTCGVLLLSLVITLYCNHRNRRRVCKCPR
PVVKSGDKPSLSARYV

As Described in Figure 4.3

SEQ18 (CAR):
Identical to SEQ11

SEQ19 (CoCAR):
Identical to SEQ12

SEQ20 (CoCAR^{BL22}):
MLLLVTSLLLCELPHPAFLLIPEVQLVESGGGLVKPGGSLKLSCAASGFAFSIYDMSW
VRQTPEKRLEWVAYISSGGGTYYPDTVKGRFTISRDNAKNTLYLQMSSLKSEDTAMY
YCARHSGYGSSYGVLFAYWGQGTLVTVSAGGGGSGGGGSGGGGSDIQMTQTTSSLS

ASLGDRVTISCRASQDISNYLNWYQQKPDGTVKLLIYYTSILHSGVPSRFSGSGSGTDY
SLTISNLEQEDFATYFCQQGNTLPWTFGGGTKLEIKAAATTTPAPRPPTPAPTIASQPLS
LRPEACRPAAGGAVHTRGLDFACDIYIWAPLAGTCGVLLLSLVITLYCNHRNRRRVC
KCPRPVVKSGDKPSLSARYVMVSELIKENMPMKLYMEGTVNNHHFKCTSEGEGKPY
EGTQTMRIKVVEGGPLPFAFDILATSFMYGSRTFIKHPPGIPDFFKQSFPEGFTWERVTT
YEDGGVLTATQDTSLQDGCLIYNVKVRGVNFPANGPVMQKKTLGWEASTETMYPA
DGGLEGACDMALKLVGGGHMICNLETTYRSKKPATNLKMPGVYNVDHRLERIKEAD
DETYVEQHEVAVARYSTGGAGDGGK

As Described in Figure 4.7

SEQ21 (CAR):
Identical to SEQ11

SEQ22 (CoCAR):
Identical to SEQ12

SEQ23 (CoCAR^{FMC63}):
MLLLVTSLLLCELPHPAFLLIPDIQMTQTTSSLSASLGDRVTISCRASQDISKYLNWYQ
QKPDGTVKLLIYHTSRLHSGVPSRFSGSGSGTDYSLTISNLEQEDIATYFCQQGNTLPY
TFGGGTKLEITGSTSGSGKPGSGEGSTKGEVKLQESGPGLVAPSQSLSVTCTVSGVSLP
DYGVSWIRQPPRKGLEWLGVIWGSETTYYNSALKSRLTIIKDNSKSQVFLKMNSLQTD
DTAIYYCAKHYYYGGSYAMDYWGQGTSVTVSSAAATTTPAPRPPTPAPTIASQPLSL
RPEACRPAAGGAVHTRGLDFACDIYIWAPLAGTCGVLLLSLVITLYCNHRNRRRVCK
CPRPVVKSGDKPSLSARYVMVSELIKENMPMKLYMEGTVNNHHFKCTSEGEGKPYE
GTQTMRIKVVEGGPLPFAFDILATSFMYGSRTFIKHPPGIPDFFKQSFPEGFTWERVTTY
EDGGVLTATQDTSLQDGCLIYNVKVRGVNFPANGPVMQKKTLGWEASTETMYPAD
GGLEGACDMALKLVGGGHMICNLETTYRSKKPATNLKMPGVYNVDHRLERIKEADD
ETYVEQHEVAVARYSTGGAGDGGK

As Described in Figure 4.11

SEQ24 (CAR):
Identical to SEQ11

SEQ25 (CoCAR):
Identical to SEQ12

SEQ26 (CoCAR^{AxAP}):
SEQ27 (CoCAR$^{\Delta}$):

As Described in Figure 5.1

SEQ28 (BCMA CAR):
MLLLVTSLLLCELPHPAFLLIPQVKLEESGGGLVQAGRSLRLSCAASEHTFSSHVMGW
FRQAPGKERESVAVIGWRDISTSYADSVKGRFTISRDNAKKTLYLQMNSLKPEDTAV
YYCAARRIDAADFDSWGQGTQVTVSSAAATTTPAPRPPTPAPTIASQPLSLRPEACRP

AAGGAVHTRGLDFACDIYIWAPLAGTCGVLLLSLVITLYCKRGRKKLLYIFKQPFMRP
VQTTQEEDGCSCRFPEEEEGGCELRVKFSRSADAPAYQQGQNQLYNELNLGRREEYD
VLDKRRGRDPEMGGKPRRKNPQEGLYNELQKDKMAEAYSEIGMKGERRRGKGHDG
LYQGLSTATKDTYDALHMQALPPRMVSKGEELFTGVVPILVELDGDVNGHKFSVSGE
GEGDATYGKLTLKFICTTGKLPVPWPTLVTTLTYGVQCFSRYPDHMKQHDFFKSAMP
EGYVQERTIFFKDDGNYKTRAEVKFEGDTLVNRIELKGIDFKEDGNILGHKLEYNYNS
HNVYIMADKQKNGIKVNFKIRHNIEDGSVQLADHYQQNTPIGDGPVLLPDNHYLSTQ
SKLSKDPNEKRDHMVLLEFVTAAGITLGMDELYK

SEQ29 (BCMA CoCAR):
MLLLVTSLLLCELPHPAFLLIPEVQLVESGGGLVQAGGSLRLSCAASGRTFTMGWFRQ
APGKEREFVAAISLSPTLAYYAESVKGRFTISRDNAKNTVVLQMNSLKPEDTALYYCA
ADRKSVMSIRPDYWGQGTQVTVSSAAATTTPAPRPPTPAPTIASQPLSLRPEACRPAA
GGAVHTRGLDFACDIYIWAPLAGTCGVLLLSLVITLYCNHRNRRRVCKCPRPVVKSG
DKPSLSARYVMVSELIKENMPMKLYMEGTVNNHHFKCTSEGEGKPYEGTQTMRIKV
VEGGPLPFAFDILATSFMYGSRTFIKHPPGIPDFFKQSFPEGFTWERVTTYEDGGVLTA
TQDTSLQDGCLIYNVKVRGVNFPANGPVMQKKTLGWEASTETMYPADGGLEGACD
MALKLVGGGHMICNLETTYRSKKPATNLKMPGVYNVDHRLERIKEADDETYVEQHE
VAVARYSTGGAGDGGK

As Described in Figure 5.4

SEQ30 (CD19 CAR):
MALPVTALLLPLALLLHAARPQSALTQPSSVSANPGETVKITCSGGYSSYYGWYQQK
SPGSAPVTLIYESNKRPSDIPSRFSGSASGSTATLTITGVQVEDEAVYYCGGLTPTHAGI
FGAGTTLTVLGGGGSGGGGSGGGGSAVTLDESGGGLQTPGGALSLVCKASGFTFSSY
DMGWVRQAPGKGLEFVAGIDDDGRYTSYGSAVDGRATISRDNGQSTVRLQLNNLRA
EDTATYYCTRGNAGWIDAWGHGTEVIVSSAAATTTPAPRPPTPAPTIASQPLSLRPEA
CRPAAGGAVHTRGLDFACDIYIWAPLAGTCGVLLLSLVITLYCKRGRKKLLYIFKQPF
MRPVQTTQEEDGCSCRFPEEEEGGCELRVKFSRSADAPAYQQGQNQLYNELNLGRRE
EYDVLDKRRGRDPEMGGKPRRKNPQEGLYNELQKDKMAEAYSEIGMKGERRRGKG
HDGLYQGLSTATKDTYDALHMQALPPRMVSKGEELFTGVVPILVELDGDVNGHKFS
VSGEGEGDATYGKLTLKFICTTGKLPVPWPTLVTTLTYGVQCFSRYPDHMKQHDFFK
SAMPEGYVQERTIFFKDDGNYKTRAEVKFEGDTLVNRIELKGIDFKEDGNILGHKLEY
NYNSHNVYIMADKQKNGIKVNFKIRHNIEDGSVQLADHYQQNTPIGDGPVLLPDNHY
LSTQSKLSKDPNEKRDHMVLLEFVTAAGITLGMDELYK

SEQ31 (CD19 CoCAR):
Identical to SEQ23

Table 2.2 Antibodies and reagents used for flow cytometry staining

Panel for Figures 3.2 and 3.6				
Target	**Clone**	**Fluorophore**	**Vendor**	**Catalog**
CD69	FN50	BV421	BioLegend	310929
Zombie	---	NIR	BioLegend	423105
Panel for Figure 3.9				
Target	**Clone**	**Fluorophore**	**Vendor**	**Catalog**
CD22-Fc	---	AF647	R&D Systems	AFR1968
Panel for Figures 3.10-3.13, 4.1, 4.2, 4.4, 4.5, 4.8-4.10, 4.12, 4.13, 5.2, 5.3, 5.5, 5.6				
Target	**Clone**	**Fluorophore**	**Vendor**	**Catalog**
CD3	SK7	BUV395	BD Biosciences	564000
CD4	SK3	BUV496	BD Biosciences	612937
CD8	SK1	BV510	BioLegend	612937
IL-2	MQ1-17H12	AF647	BioLegend	500315
TNFα	MAb11	BV650	BioLegend	502938
IFNγ	4S.B3	BV421	BioLegend	502532
Zombie	---	NIR	BioLegend	423105
Panel for Figure 3.13				
Target	**Clone**	**Fluorophore**	**Vendor**	**Catalog**
CD22	HIB22	AF647	BioLegend	302518
Panel for Figure 3.16				
Target	**Clone**	**Fluorophore**	**Vendor**	**Catalog**
FLAG Tag	L5	BV421	BioLegend	637322
MYC Tag	9B11	AF647	Cell Signaling Technology	2233S

3. ITERATIVE DESIGN AND FUNCTIONAL EVALUATION OF A NOVEL CHIMERIC CORECEPTOR

Driven by the clinical need for more sensitive chimeric antigen receptors (CARs) and inspired by the interactions between the coreceptor and T cell receptor (TCR), we sought to design a novel CAR with increased sensitivity to antigen through incorporation of LCK-binding domains derived from CD4 or CD8. We first approached this challenge by inserting coreceptor cytoplasmic domains directly into a second-generation CD19-targeted CAR. Whether new CAR constructs will express properly is hard to predict and we assumed a higher probability of stability if we kept the number of molecules from which we sourced domains as low as possible. Therefore, although CD4 is capable of binding LCK we selected domains from the CD8 coreceptor as our CAR already contained hinge and transmembrane domains derived from CD8α. We chose to incorporate the full length CD8α cytoplasmic sequence over CD8β as the latter has been shown to become palmitoylated and aggregate in lipid rafts [102]. Therefore, use of CD8β cytoplasmic domains could potentially lead to unwanted interactions with endogenous CD8 molecules.

Briefly, the anti-CD19 scFv FMC63 was combined with CD8α hinge and transmembrane, 4-1BB costimulatory, and CD3ζ stimulatory domains [103]. Monomeric EGFP (mEGFP) was then fused to the C-terminus to track CAR expression [104]. Three novel constructs - CAR8α1, CAR8α2, and CAR8α3 - were generated by inserting the full CD8α cytoplasmic sequence between existing domains (Figure 3.1.A). We hypothesized that LCK, bound to the CD8α domain, would be able to increase CD3ζ phosphorylation and therefore, functionality (Figure 3.1.B).

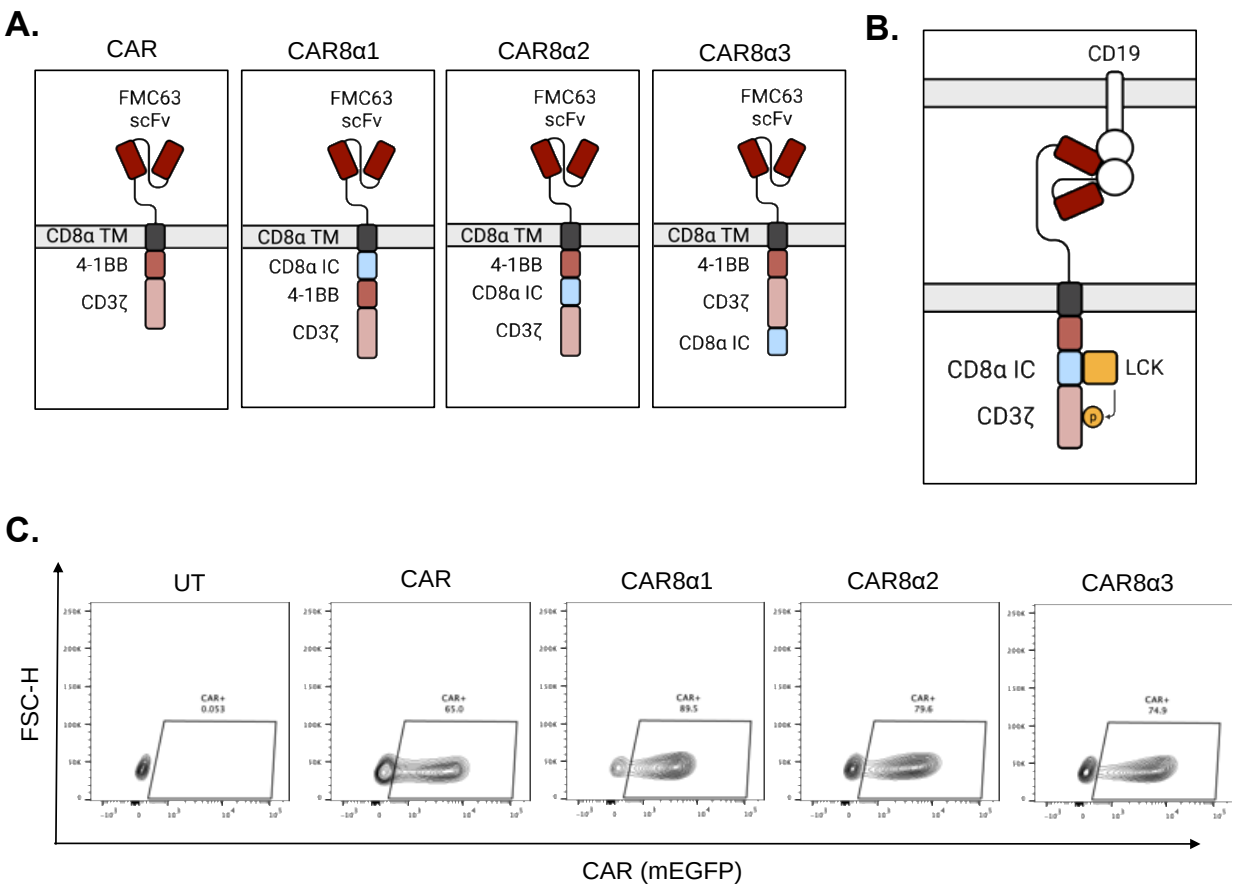

Figure 3.1 Design, rationale, and expression of CAR8α constructs
A. Schematics of a conventional anti-CD19-BBζ CAR and three novel variants with the insertion of the full-length CD8α cytoplasmic domain. All molecules are tagged with a C-terminal mEGFP (not depicted). **B.** Mechanistic hypothesis behind design in which CD8α-bound LCK phosphorylates ITAMs present in the CD3ζ cytoplasmic domain. **C.** Representative flow cytometric plots showing expression of CAR constructs in the Jurkat cell line or untransduced (UT) controls.

Each construct was cloned into replication-deficient lentiviral transfer plasmids, packaged, and expressed in the Jurkat human T cell line through viral transduction (Figure 3.1.C). We then used fluorescence-activated cell sorting (FACS) to sort populations with equivalent mEGFP gMFI to normalize CAR expression and ensure a fair comparison. Sorted Jurkat cells expressing CAR, CAR8α1, CAR8α2, and CAR8α3, or untransduced controls were then cocultured with Nalm6 cells, a $CD19^{+}CD22^{+}$ human B-ALL cell line. Functionality was assessed through surface staining for the early-activation marker CD69 and by IL-2 secretion.

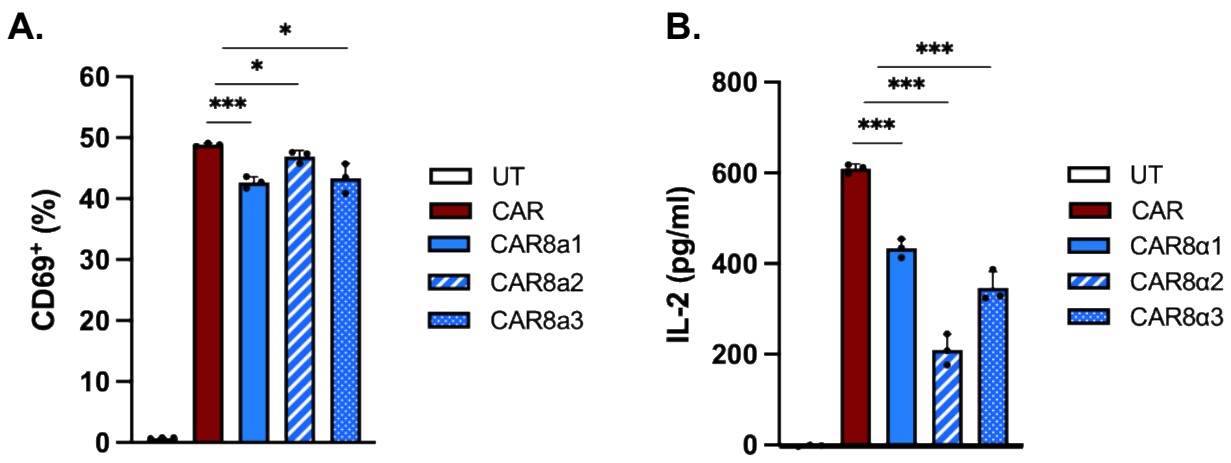

Figure 3.2 CAR8α cells are less functional than conventional CARs
In vitro activity of CAR-expressing Jurkat T cells after stimulation with the Nalm6 cell line, measured by **A.** surface staining for CD69 and **B.** ELISA of IL-2 in the supernatant. CAR expression across effector lines were normalized before coculture using fluorescence-activated cell sorting (FACS).

Compared to the state-of-the-art, all three novel designs exhibited slight decreases in CD69 expression and major impairments to IL-2 secretion (Figure 3.2). Since we did not observe defects in CAR expression after incorporation of the CD8α domain, we hypothesized that the decrease in functionality was likely due to the inhibition of stimulatory signaling, perhaps due to changes in protein conformation after introduction of the CD8α cytoplasmic domain.

Seeing little promise with linearly incorporating the cytoplasmic domain of CD8α into an existing CAR, we turned to the design and evaluation of a dual-CAR system. Mimicking the two-molecule nature of the TCR and coreceptor, our system would contain both a second-generation CAR and a novel chimeric coreceptor, or CoCAR. We decided to have CAR and CoCAR target unique antigen, since using the same scFv would lead to competition during binding. CD19 and CD22 were chosen as antigen targets since both are highly expressed in B-ALL and scFvs for both have been well validated for CAR use. We used our previously described anti-CD19 CAR and generated two CoCAR variants by fusing the anti-CD22 scFv HA22 to a CD8α hinge and the transmembrane and cytoplasmic domains of either CD4 or CD8α

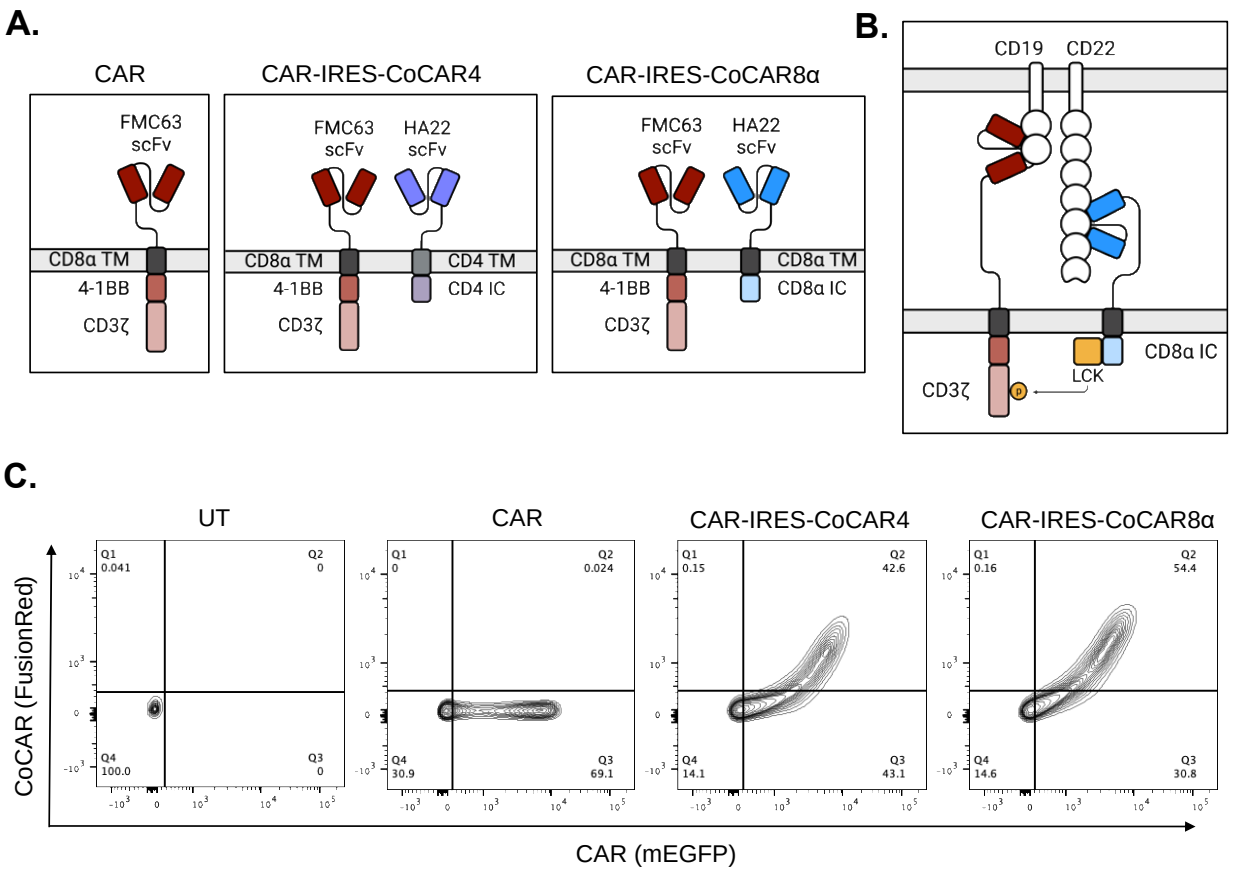

Figure 3.3 Design, rationale, and expression of CAR-IRES-CoCAR constructs
A. Schematics of a conventional anti-CD19-BBζ CAR and two novel dual-CAR systems with the addition of a chimeric coreceptor containing the HA22 scFv and either transmembrane domains (TM) and cytoplasmic domains from either CD4 or CD8α. All molecules are tagged with a C-terminal mEGFP or FusionRed (not depicted). **B.** Mechanistic hypothesis in which CoCAR-bound LCK phosphorylates ITAMs present in the CD3ζ cytoplasmic domain after antigen binding and colocalization of CAR and CoCAR. **C.** Representative flow cytometric plots showing expression of CAR constructs in the Jurkat cell line or untransduced (UT) controls.

(Figure 3.3.A) [105]. FusionRed was fused to the C-terminus of either CoCAR to monitor expression [106]. Three lentiviral transfer plasmids were generated containing CAR only, both CAR and CoCAR4, or both CAR and CoCAR8α. An IRES was inserted between CAR and CoCAR of the latter two designs so that both molecules could be expressed bicistronically. We hypothesized that cells coexpressing CAR-IRES-CoCAR4 or CAR-IRES-CoCAR8α would have

increased functionality compared to cells expressing CAR alone, due to colocalization of CAR and CoCAR and increased ITAM phosphorylation by CoCAR-bound LCK (Figure 3.3.B).

All three constructs were successfully cloned, packaged, and transduced into Jurkat cells (Figure 3.3.C). FACS was again used to normalize the expression of both CAR and CoCAR molecules between the three lines. After coculture with Nalm6 cells, we observed that neither CoCAR4 nor CoCAR8α positively contributed to overall CAR function. Interestingly, while CAR-IRES-CoCAR4 cells expressed similar levels of IL-2 to CAR, CAR-IRES-CoCAR8α cells showed a significant decrease in IL-2 secretion (Figure 3.4). Although neither design showed promise, we were encouraged by these results as the decrease in functionality implied some level of interaction, although deleterious, between the CAR and CoCAR8α. We hypothesized that CoCAR8α molecules were interacting with CAR molecules through their shared transmembrane domain, but sequestering CAR molecules away from CD19, decreasing binding and activation. This theory was further supported by previous studies showing that CD19 and CD22 do not readily colocalize on B cells, perhaps due to their opposing functions to amplify and dampen B cell activation [107-109].

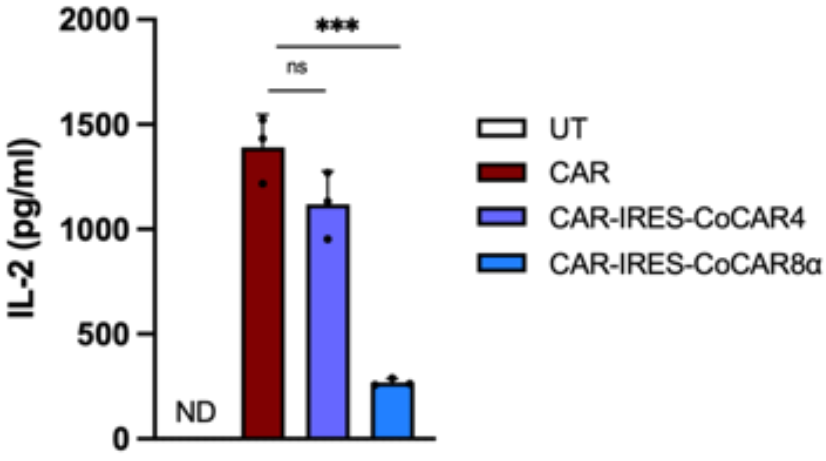

Figure 3.4 CAR-IRES-CoCAR cells are less functional than conventional CARs
In vitro activity of CAR-expressing Jurkat T cells after stimulation with the Nalm6 cell line, measured by ELISA of IL-2 in the supernatant. CAR expression across effector lines were normalized before coculture using fluorescence-activated cell sorting (FACS).

We iterated upon our dual-CAR design so that both CARs would bind the same antigen target. We identified the anti-CD22 scFv m971 that noncompetetively binds CD22 at Ig domains 3, while the HA22 scFv binds at Ig domains 5-7 [79, 80]. Briefly, we formed the CAR by fusing the m971 scFv to CD8α hinge and transmembrane, 4-1BB costimulatory, and CD3ζ stimulatory domains. Two CoCARs were formed by fusing the HA22 scFv to a CD8α hinge and the transmembrane and cytoplasmic domains of either CD4 or CD8α (Figure 3.5.A). In order to

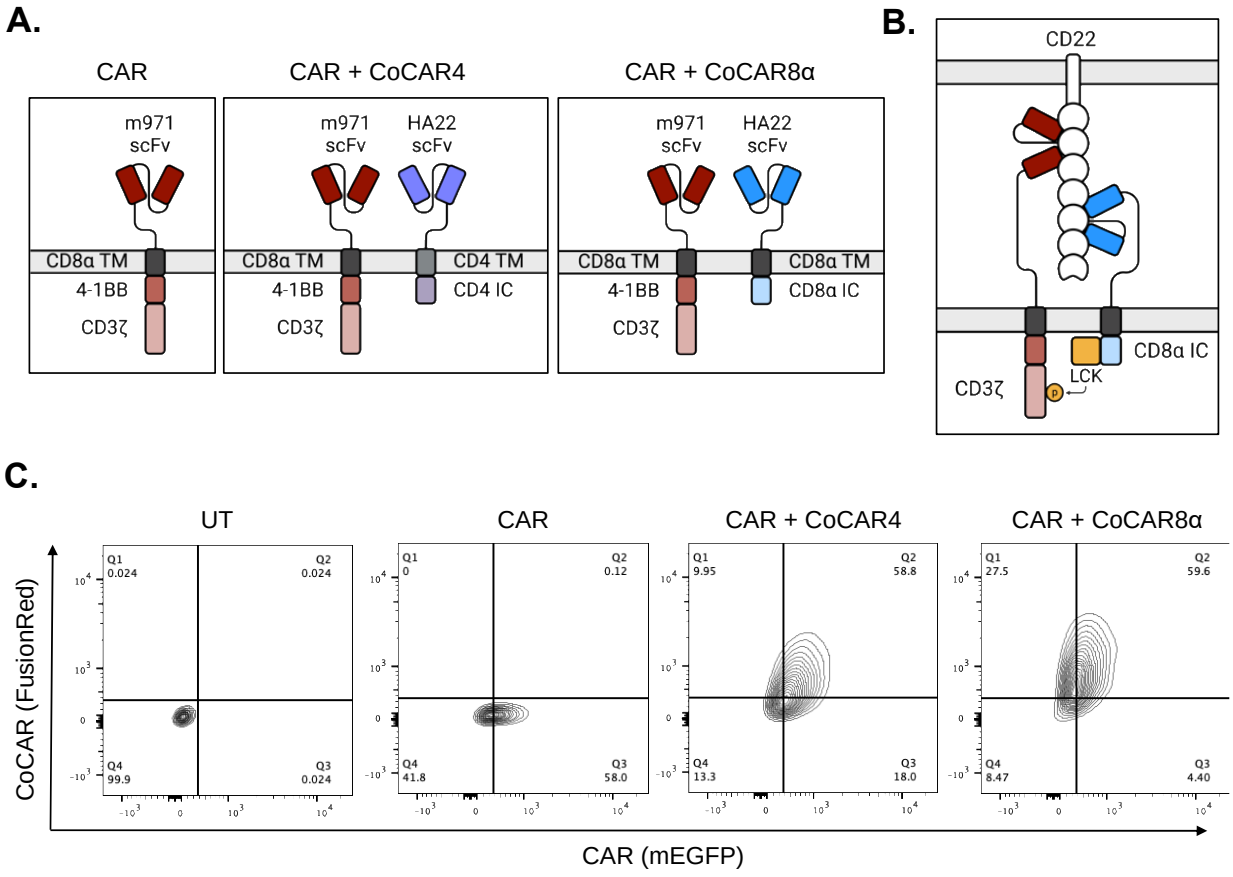

Figure 3.5 Design, rationale, and expression of CAR + CoCAR constructs
A. Schematics of a conventional anti-CD22-BBζ CAR and two novel dual-CAR systems with the addition of a chimeric coreceptor containing the HA22 scFv and either transmembrane domains (TM) and cytoplasmic domains from either CD4 or CD8α. All molecules are tagged with a C-terminal P2A-mEGFP or P2A-FusionRed (not depicted). **B.** Mechanistic hypothesis in which CoCAR-bound LCK phosphorylates ITAMs present in the CD3ζ cytoplasmic domain after non-competitive antigen binding to CD22. **C.** Representative flow cytometric plots showing expression of CAR constructs in the Jurkat cell line or untransduced (UT) controls.

facilitate more efficient screening and improve viral titers, we split CAR and CoCAR molecules into their own respective lentiviral vectors. Additionally, to rule out possible steric inhibition between C-terminal fused mEGFP and FusionRed as a cause of failure, a P2A cleavage sequence was inserted before mEGFP on the CAR or FusionRed on the CoCAR. CAR expression could therefore still be monitored through fluorescent proxies, although the molecules would now be localized cytoplasmically, versus membrane-bound through fusion with the CAR or CoCAR. We hypothesized that by noncompetitively targeting the same antigen, CAR and CoCAR molecules would be able to colocalize and interact as designed without impeding CAR binding and stimulation (Figure 3.5.B).

Coexpression was achieved in a subset of Jurkat cells after cotransduction with lentiviruses encoding CAR and either CoCAR variant (Figure 3.5.C). Like before, FACS was used to normalize CAR and CoCAR expression between the three lines. After coculture with Nalm6 cells, Jurkat cells expressing CAR + CoCAR4 or CAR + CoCAR8α expressed more CD69 and secreted more IL-2 (Figure 3.6). While these results indicated that coexpression of

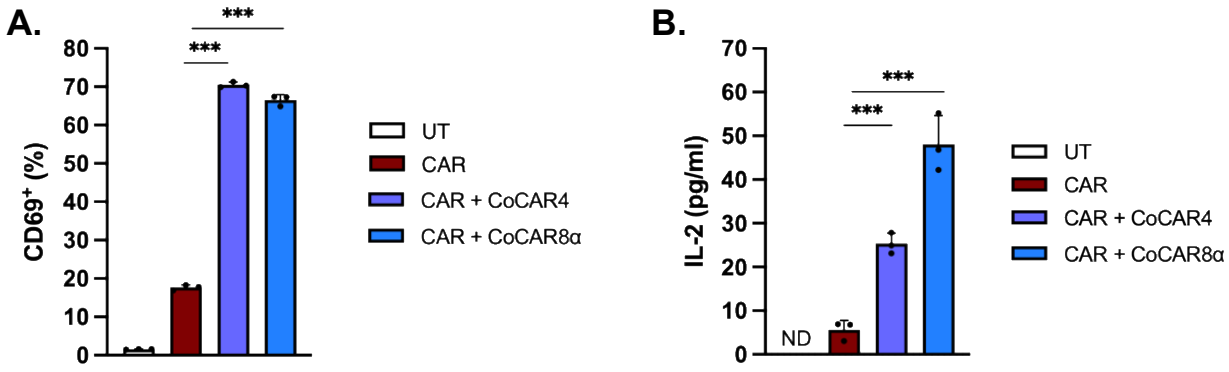

Figure 3.6 CAR + CoCAR constructs increase functionality of conventional CARs
In vitro activity of CAR-expressing Jurkat T cells after stimulation with the Nalm6 cell line, measured by **A.** surface staining for CD69 and **B.** ELISA of IL-2 in the supernatant. CAR expression across effector lines were normalized before coculture using fluorescence-activated cell sorting (FACS).

CAR and CoCAR increased anti-tumor functionality in Jurkat cells, it was yet to be seen if system would also function in primary human T cells. Seeing that CAR + CoCAR8α Jurkat cells outperformed those expressing CAR + CoCAR4, only the former was carried forward for testing in primary cells.

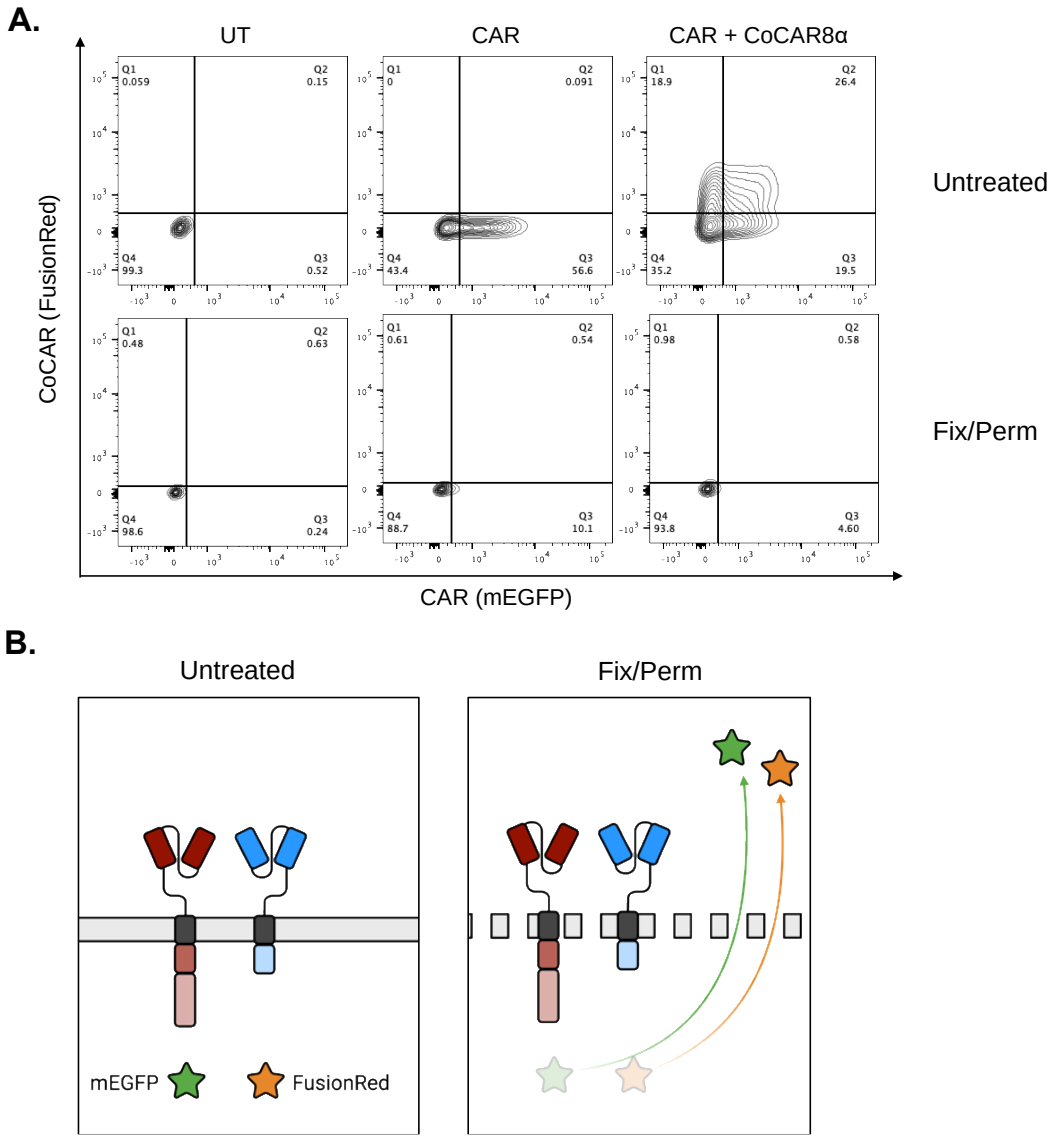

Figure 3.7 Fixation and permeabilization leads to loss of mEGFP and FusionRed signal
A. Representative flow cytometric plots showing expression of CAR constructs in primary human T cells before and after fixation and permeabilization. Untransduced (UT) cells were used as gating controls. **B.** Mechanistic hypothesis behind loss of fluorescent signal, in which cytoplasmically-localized P2A-fluorescent proteins are washed out of the cell during permeabilization.

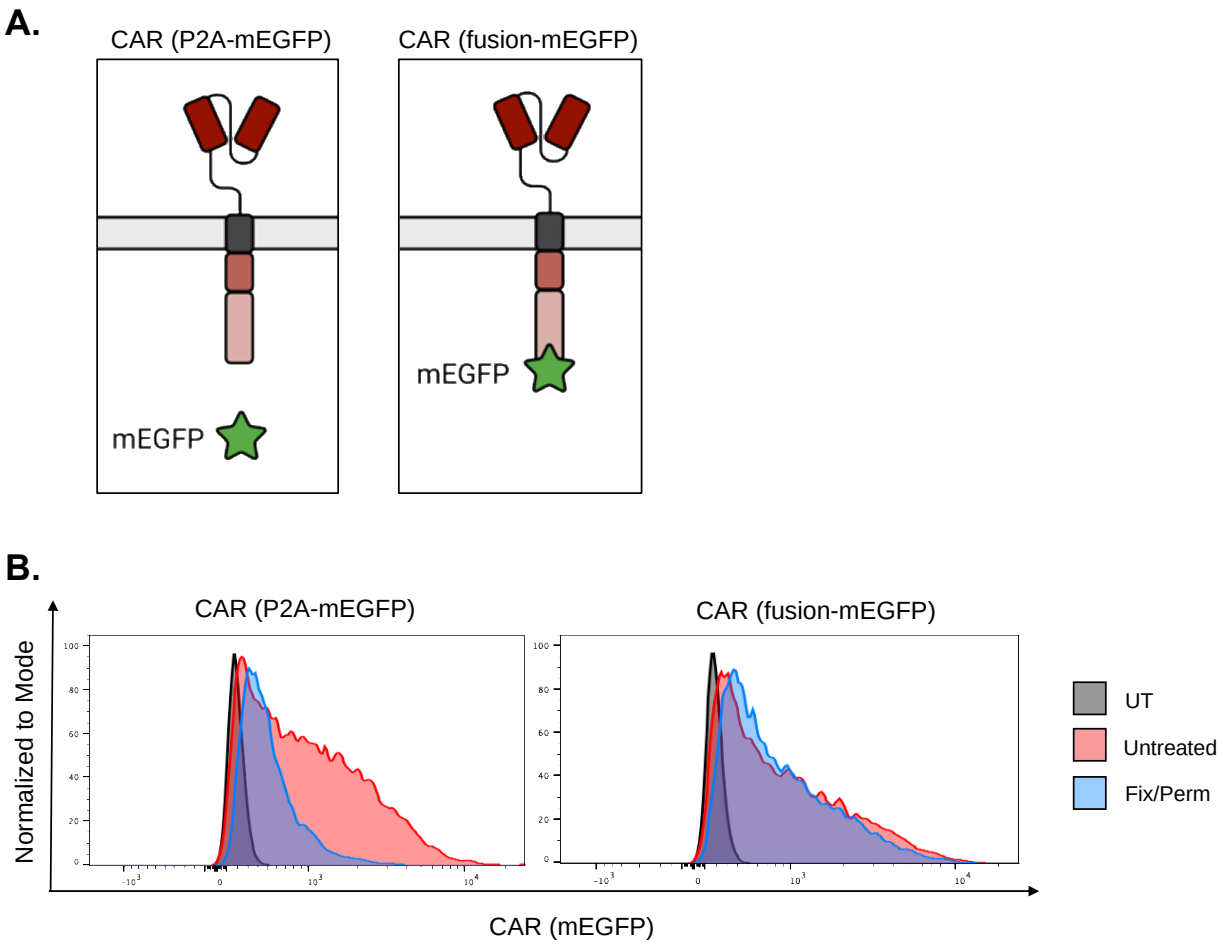

Figure 3.8 mEGFP bound to CAR molecules better withstand fixation and permeabilization
A. Schematics of a conventional anti-CD22-BBζ CAR with C-terminal mEGFP expressed via P2A or direct fusion to the CAR. **B.** Representative flow cytometric expression of mEGFP before and after fixation and permeabilization. Untransduced (UT) controls are shown for reference.

We were pleased to see that like in Jurkat cells, coexpression of CAR and CoCAR was achieved in a subset of cells after cotransduction with lentiviruses (Figure 3.7.A). Normalization of CAR expression between conditions proved difficult, as FACS adversely affected the viability of primary T cells. With this limitation in mind, we chose to assess cytokine production via intracellular staining, so that CAR expression could be normalized through gating during analysis. Primary T cells were cocultured with Nalm6 cells and subsequently fixed,

permeabilized, and stained for prototypical inflammatory T cell cytokines IL-2, TNFα, and IFNγ. Unfortunately, we found that fixation and permeabilization greatly reduced expression of mEGFP and FusionRed (Figure 3.7.B). We hypothesized that our fluorescent proxies, no longer membrane bound, were being washed out of our cells during intracellular staining (Figure 3.7.C). To test this hypothesis, we compared fluorescence retention in Jurkat cells transduced with either CAR or a CAR variant with mEGFP fused to the C-terminus (Figure 3.8.A). After fixation and permeabilization, we observed that fusion to the C-terminus of the CAR was necessary for retention of mEGFP signal (Figure 3.8.B).

Detection of both CAR and CoCAR was optimized for fixation and permeabilization by fusing mEGFP to the C-terminus of the CAR and FusionRed to the CoCAR. Coexpression of both molecules in a subset of primary human T cells was achieved after cotransduction with lentiviruses encoding either CAR or CoCAR (Figure 3.9.C). Additionally, to validate the use of mEGFP and FusionRed as reliable proxy for surface expression, primary T cells were transduced with either CAR or CoCAR virus and then stained with AF647-conjugated CD22-Fc. Both fluorescent proteins exhibited similar expression as CD22-Fc, verifying their use as proxies for surface expression (Figure 3.9.D).

We first evaluated anti-tumor functionality through coculture with Nalm6 cells and intracellular staining for IL-2, TNFα, and IFNγ. We found that CAR^+CoCAR^+ cells had both a higher percentage of cytokine positivity and cytokine gMFI (Figure 3.10, Figure 3.11.A, and Figure 3.11.B). Similarly, we found an increase in polyfunctional, cytokine triple-positive cells when comparing CAR^+CoCAR^+ to CAR^+ (Figure 3.11.C) [110-112]. Next, to assess if the CoCAR impacted other anti-tumor functions we evaluated cell-mediated killing. FACS was used to normalize CAR expression between the conditions and sorted cells were then put into

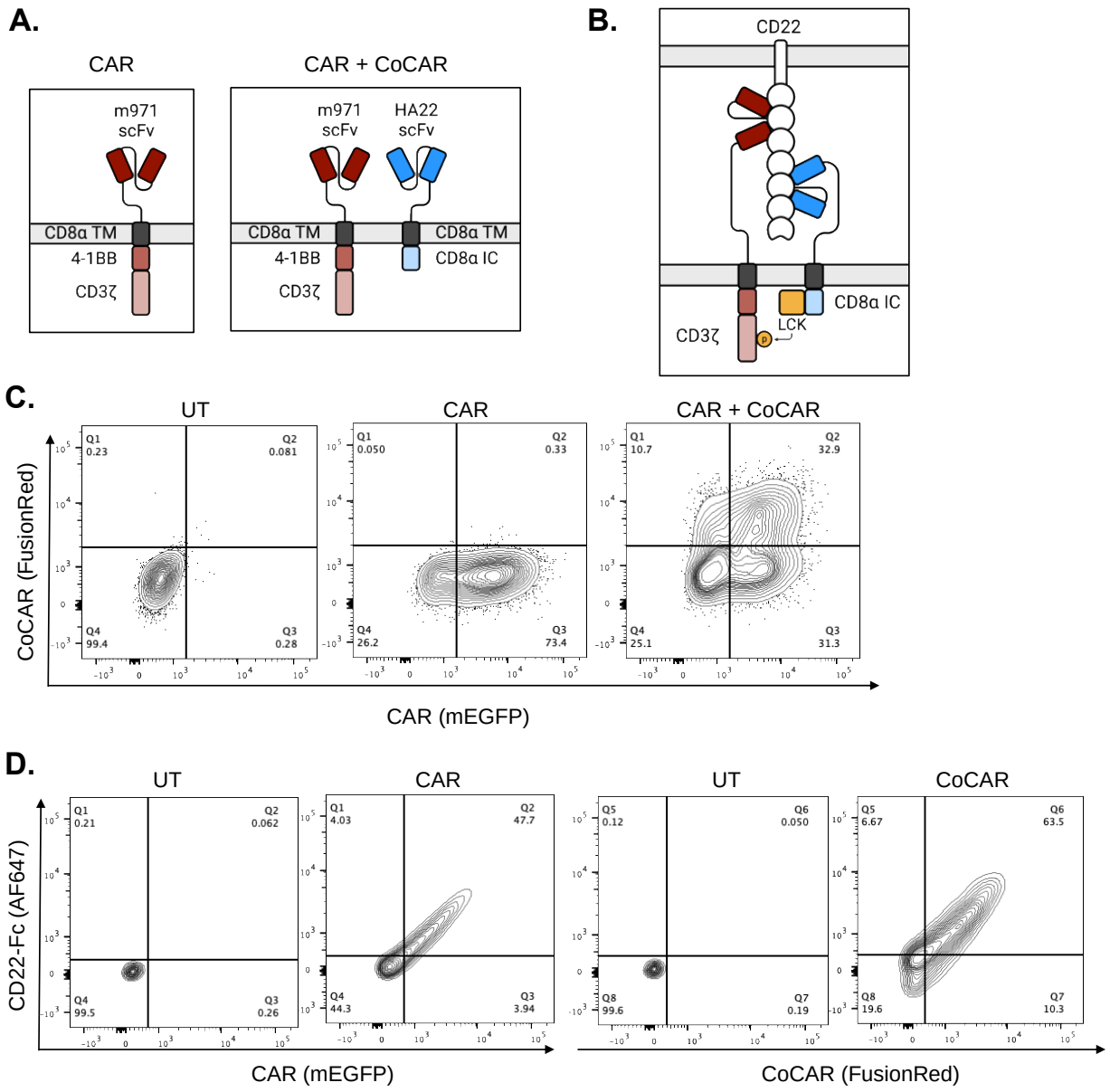

Figure 3.9 Design, rationale, and expression of optimized CAR + CoCAR constructs
A. Schematics of a conventional anti-CD22-BBζ CAR and our novel dual-CAR system with additional chimeric coreceptor containing the HA22 scFv, CD8α transmembrane domain (TM), and CD8α cytoplasmic domain. All molecules are tagged with a C-terminal mEGFP or FusionRed (not depicted). **B.** Mechanistic hypothesis in which CoCAR-bound LCK phosphorylates ITAMs present in the CD3ζ cytoplasmic domain after non-competitive antigen binding to CD22. **C.** Representative flow cytometric plots showing expression of CAR constructs in primary human T cells or untransduced (UT) controls. **D.** Secondary staining of untransduced, CAR-transduced, or CoCAR-transduced primary human T cells with AF647-conjugated CD22-Fc.

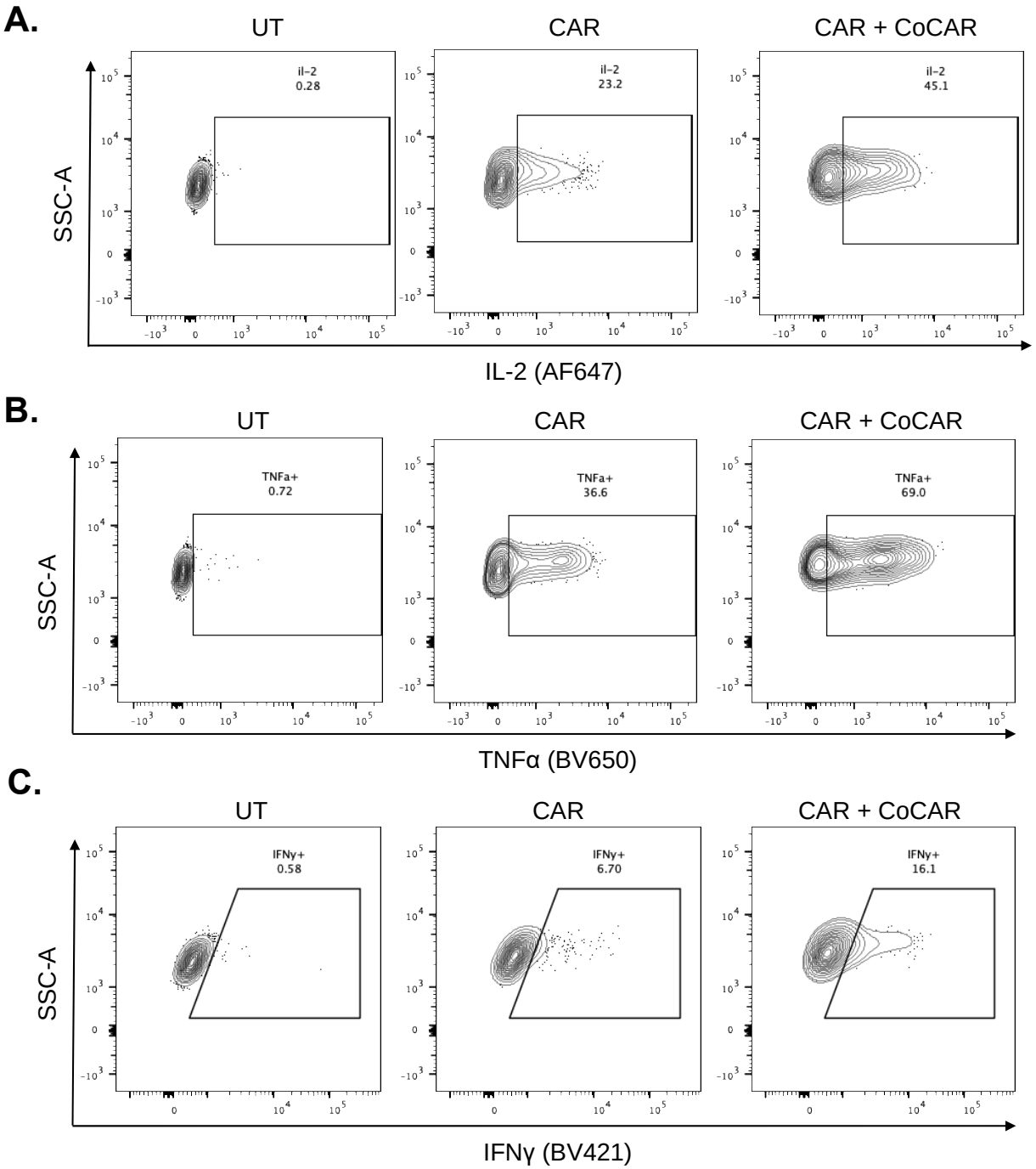

Figure 3.10 Dual-expression of CAR and CoCAR increase cytokine production
In vitro activity of CAR-expressing primary human T cells after stimulation with the Nalm6 cell line measured by intracellular staining of prototypical cytokines induced upon T cell activation. Representative flow cytometric plots for **A.** IL-2 **B.** TNFα **C.** IFNγ after gating of CAR^+ or CAR^+CoCAR^+ populations. Baseline T cell activation in untransduced (UT) cells is shown for reference.

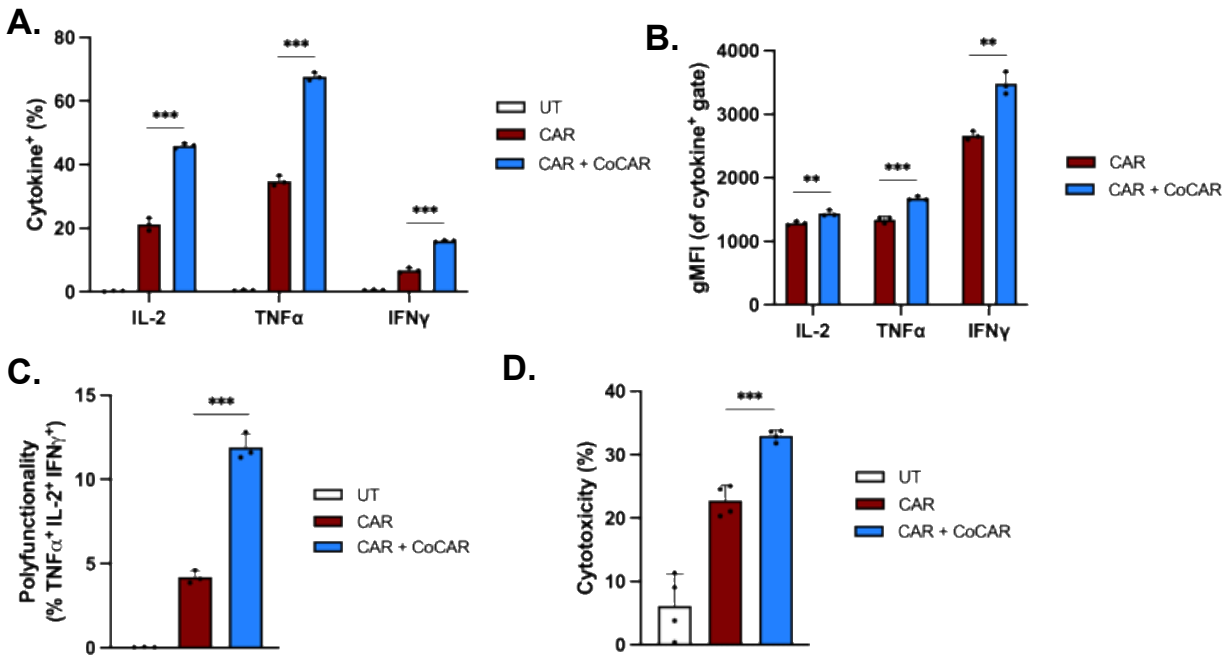

Figure 3.11 CAR$^+$CoCAR$^+$ cells exhibit improved antitumor functionality
A-C. Summarized *in vitro* activity of CAR-transduced primary human T cells after stimulation with the Nalm6 cell line measured by intracellular staining IL-2, TNFα, and IFNγ. Baseline T cell activation in untransduced (UT) cells is shown for reference. **A.** Percent cytokine positivity **B.** gMFI of cytokine-positive cells **C.** percent of TNFα $^+$IL-2$^+$ IFNγ$^+$ cells within CAR$^+$ or CAR$^+$CoCAR$^+$ gates. **D.** Cytotoxic abilities of CAR-transduced primary human T cells after coculture with luciferase-expressing Nalm6 cells. CAR expression across effector lines were normalized before coculture using fluorescence-activated cell sorting (FACS). Baseline T cell killing in UT cells is shown for reference.

coculture with Nalm6 cells. Sorted CAR + CoCAR cells were significantly more cytotoxic towards target cells compared to those only expressing CAR (Figure 3.11.D). To ensure that the improved functionality was not a donor-specific anomaly, we repeated intracellular staining for cytokines with three additional healthy donors. In all donors, coexpression of both CAR and CoCAR was achieved and CAR$^+$CoCAR$^+$ T cells derived from each additional donor showed increased cytokine positivity over CAR$^+$ cells (Figure 3.12).

We further evaluated the sensitivity of the CoCAR system by assessing cytokine production after coculture with Nalm6 populations of different antigen densities. FACS was used

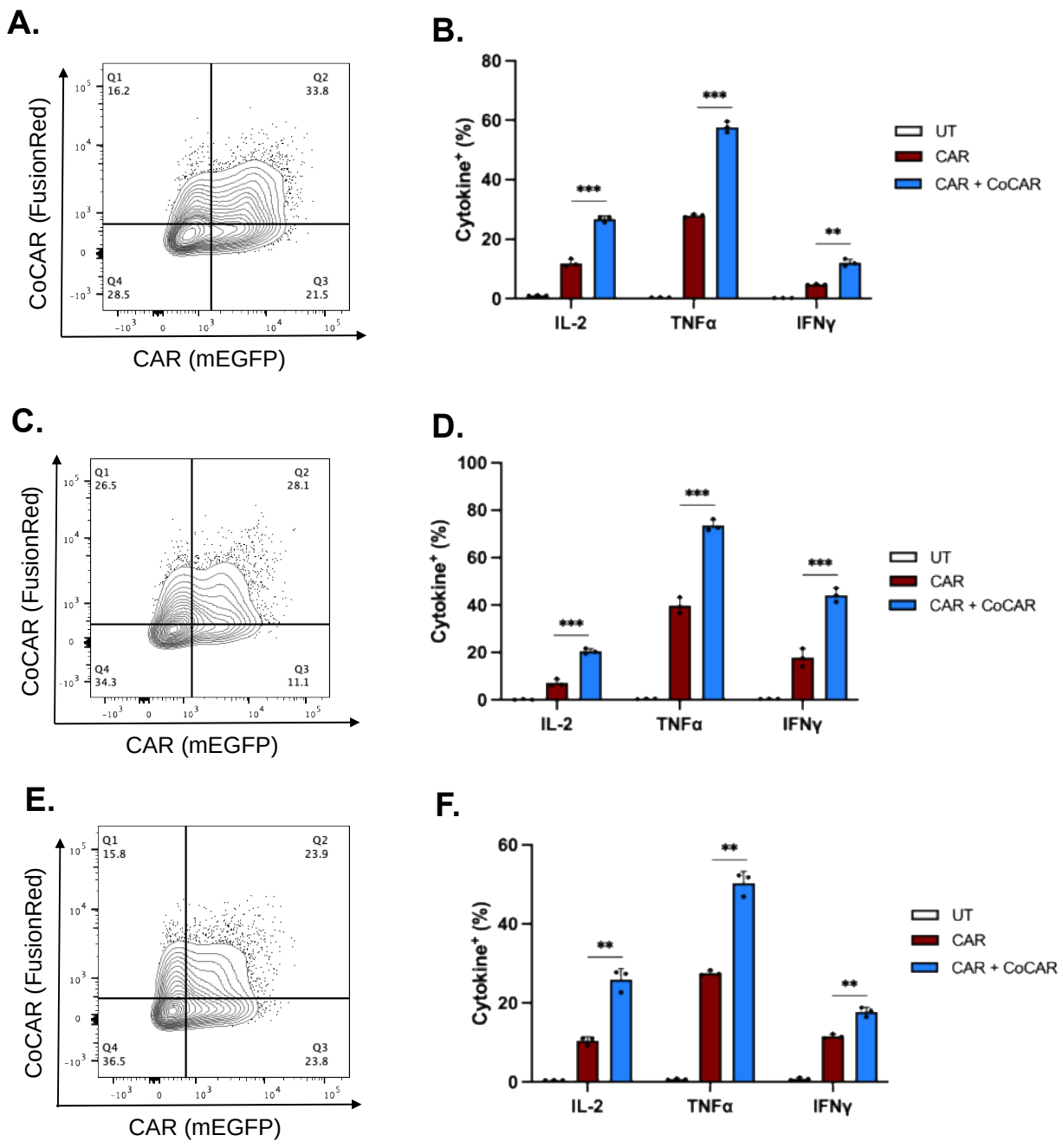

Figure 3.12 The CoCAR system is not donor-restricted
Expression of CAR and CoCAR molecules in additional healthy donors and summarized *in vitro* activity of CAR-transduced primary human T cells after stimulation with the Nalm6 cell line measured by intracellular staining IL-2, TNFα, and IFNγ. Percent cytokine positivity is shown for cells within CAR^+ or CAR^+CoCAR^+ gates. Untransduced (UT) cells are shown for reference. **A,B.** Donor 1. **C,D.** Donor 2. **E,F.** Donor 3.

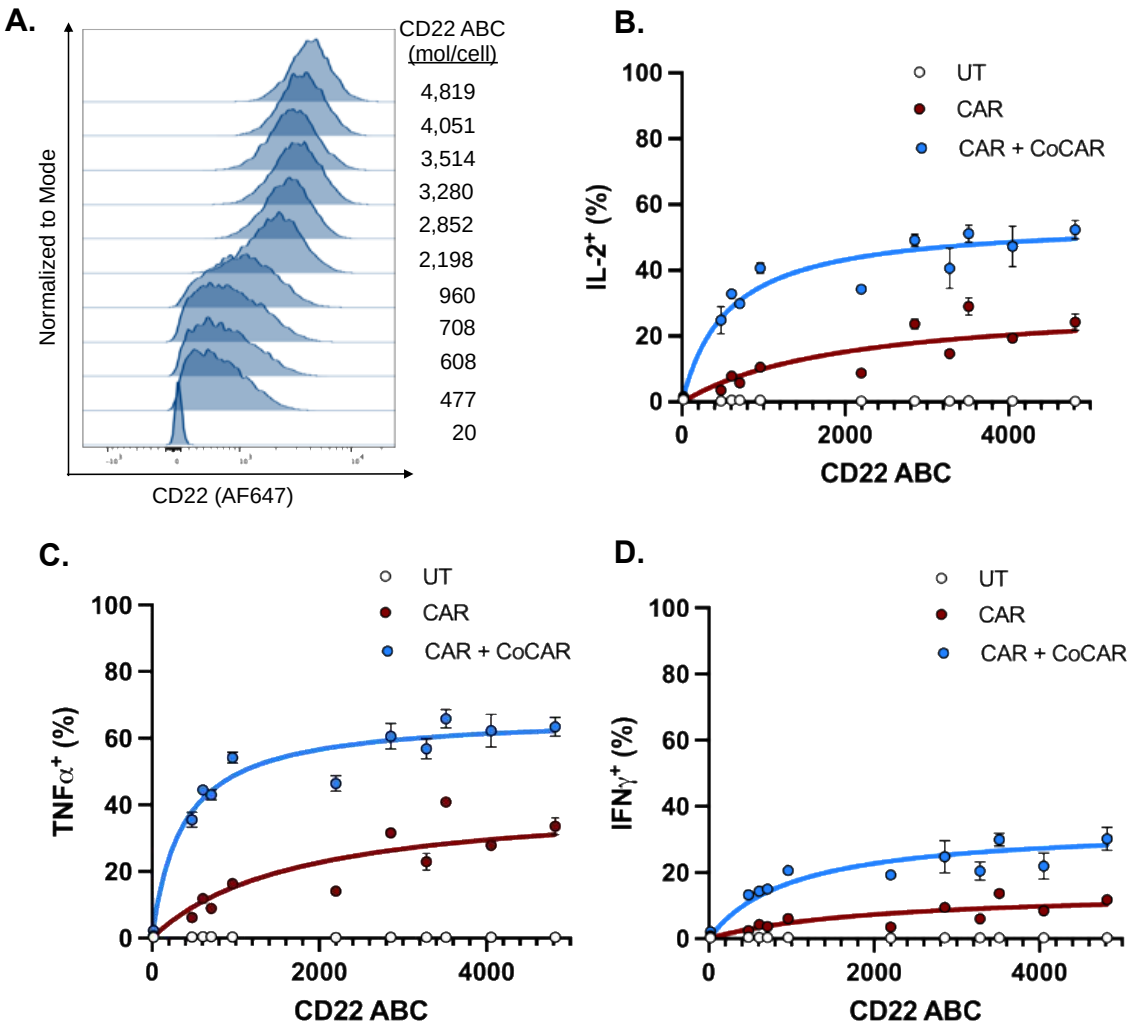

Figure 3.13 CAR$^+$CoCAR$^+$ cells are more functional across clinically-relevant antigen densities

A. Flow cytometric analysis of CD22 antibody binding capacity (ABC) of Nalm6 cell lines after single-cell sorting and expansion of individual clones. Summarized *in vitro* activity of CAR-transduced primary human T cells after stimulation with one of 11 Nalm6 cell line measured by intracellular staining of **B.** IL-2, **C.** TNFα, and **D.** IFNγ. Percent cytokine positivity is shown for cells within CAR$^+$ or CAR$^+$CoCAR$^+$ gates. Untransduced (UT) cells are shown for reference.

to sort out single Nalm6 cells from the parental line. Single cells were expanded, yielding 11 distinct populations with measured antibody binding capacities (ABC) ranging from 19 molecules of CD22 per cell to 4,819 molecules of CD22 per cell (Figure 3.13.A). Across all antigen densities, a higher percentage of CAR$^+$CoCAR$^+$ cells were capable of producing

cytokines compared to CAR^+ (Figure 3.13.B, Figure 3.13.C, and Figure 3.13.D). Differences in cytokine production were most apparent at lower levels of CD22 expression, such as at ~500 molecules/cell where coexpression of CAR and CoCAR increased the percent of cytokine producing cells approximately five- to seven-fold. Importantly, the reported average ABC of CD22 on primary B-ALL cells post-relapse is ~1,200 molecules of CD22 per cell, which comfortably falls within the range of antigen densities we tested, indicating that our dual-molecule system performs better *in vitro* at these failure points [81, 82]. In conclusion, these data provide evidence for both increased antitumor functionality and antigen sensitivity allowed by the CAR + CoCAR system compared to the conventional CAR.

In order to assess *in vivo* persistence and anti-tumor killing, we injected immunodeficient, NOD.Cg-*Prkdc*^{scid} *Il2rg*^{tm1Wjl}/SzJ (NSG) mice with Nalm6 cells and then treated them with CAR or CAR + CoCAR primary human T cells (Figure 3.14.A). Mice treated with CAR + CoCAR cells showed a median increase of 3 days survival compared to mice injected with CAR cells (Figure 3.14.B). While the increase in survival was modest, our results show that CAR^+CoCAR^+ cells are functional *in vivo*. We hypothesized that our current expression strategy is to blame for underwhelming *in vivo* performance. Cotransduction of CAR and CoCAR viruses produces a heterogenous expression pattern, with only ~50% of the CAR^+ population expressing the CoCAR as well (Figure 3.14.C). It is likely that increasing the percent and purity of CAR^+CoCAR^+ cells would further increase differences between conditions.

Having shown that CAR^+CoCAR^+ cells were highly functional, we next sought to implement bicistronic expression to further optimize the dual-molecule system. Previously described CAR and CoCAR constructs were combined into single lentiviral transfer plasmids

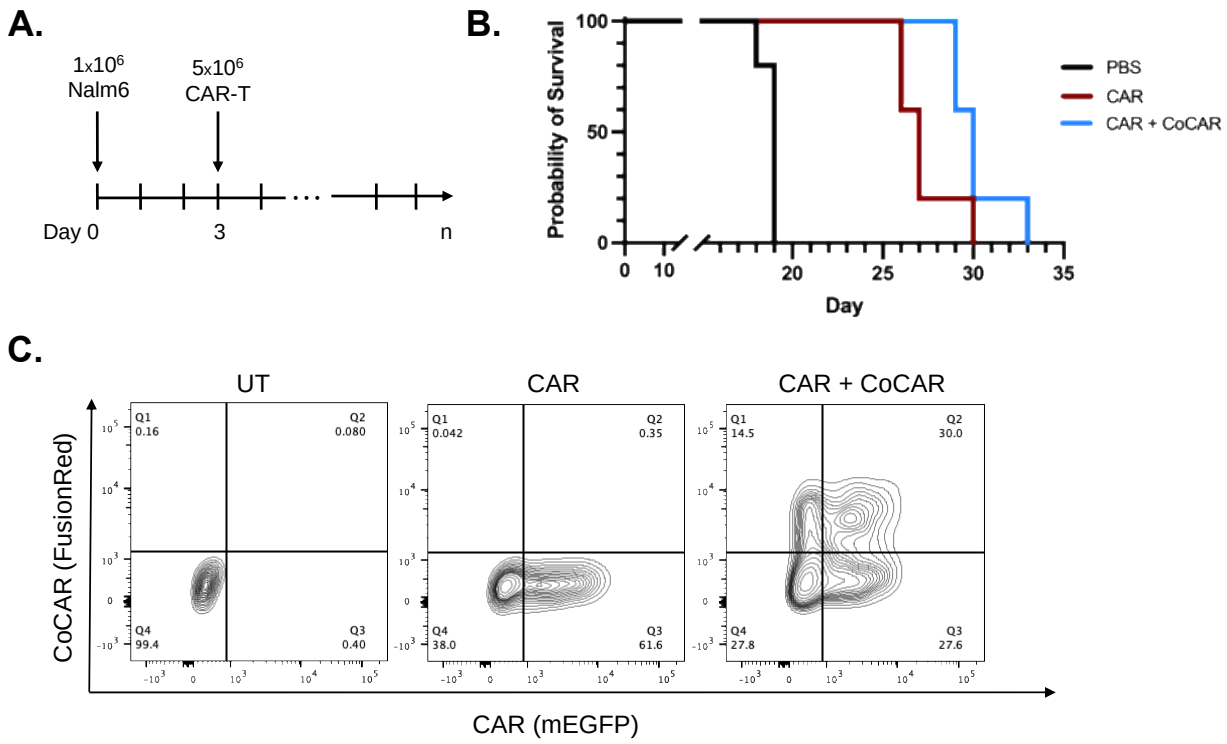

Figure 3.14 CAR + CoCAR cells modestly improve *in vivo* survival
A. Schematic of IV injections for assessing *in vivo* activity of CAR-transduced cells in NSG mice. **B.** Survival curve of mice receiving different experimental treatments C. Flow cytometric plots showing expression of CAR constructs in primary human T cells or untransduced (UT) controls pre-administration on Day 3.

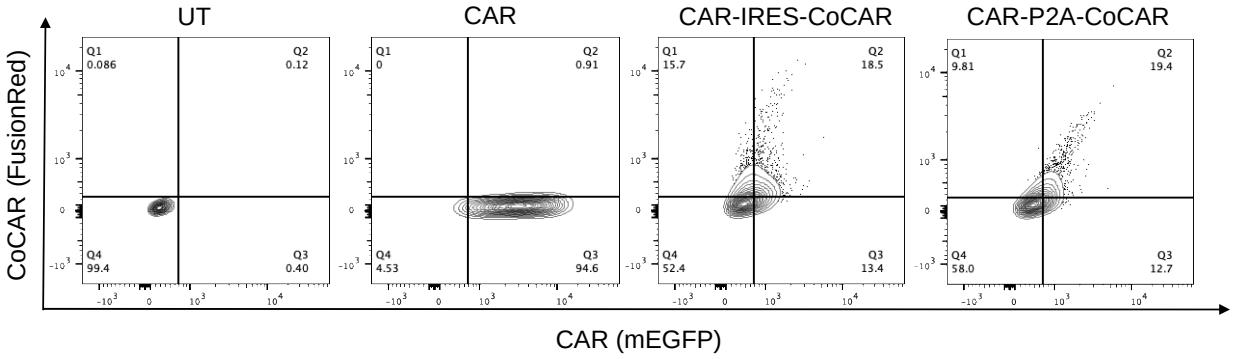

Figure 3.15 Bicistronic expression of fluorescently-tagged molecules via P2A leads to better expression distribution than IRES
Representative flow cytometric plots showing expression of CAR constructs in the Jurkat cell line or untransduced (UT) controls.

separated by either IRES or P2A. Both bicistronic vectors were successfully cloned, packaged, and transduced into Jurkat cells. While both bicistronic elements led to a subset of $CAR^{+}CoCAR^{+}$ Jurkat cells, use of the P2A led to a more equimolar distribution (Figure 3.15) [113]. Unfortunately, we were not able to test the expression of either bicistronic vector in primary human T cells as the large transgene size prevented production of practically useful viral titers [114].

We next altered our detection strategy to decrease transgene size and increase viral titers. C-term fused fluorescent proteins, each around 700bp in length, were replaced with small epitope tags, each around 30bp in length. Briefly, the CAR construct was altered by removing mEGFP and adding a FLAG tag at the 5' end of the m971 scFv [115]. The CoCAR was altered by removing FusionRed and adding a MYC tag at the 3' end of the HA22 scFv (Figure 3.16.A) [116]. By inserting unique epitope tags into the CAR and CoCAR, each molecule could still be uniquely identified by surface staining. CAR and CoCAR genes were again combined into a single lentiviral transfer plasmid and separated by P2A. This smaller bicistronic vector was capable of being produced at high titers and primary cells expressed a more favorable distribution of CAR and CoCAR than with cotransduction of split viruses (Figure 3.16.B).

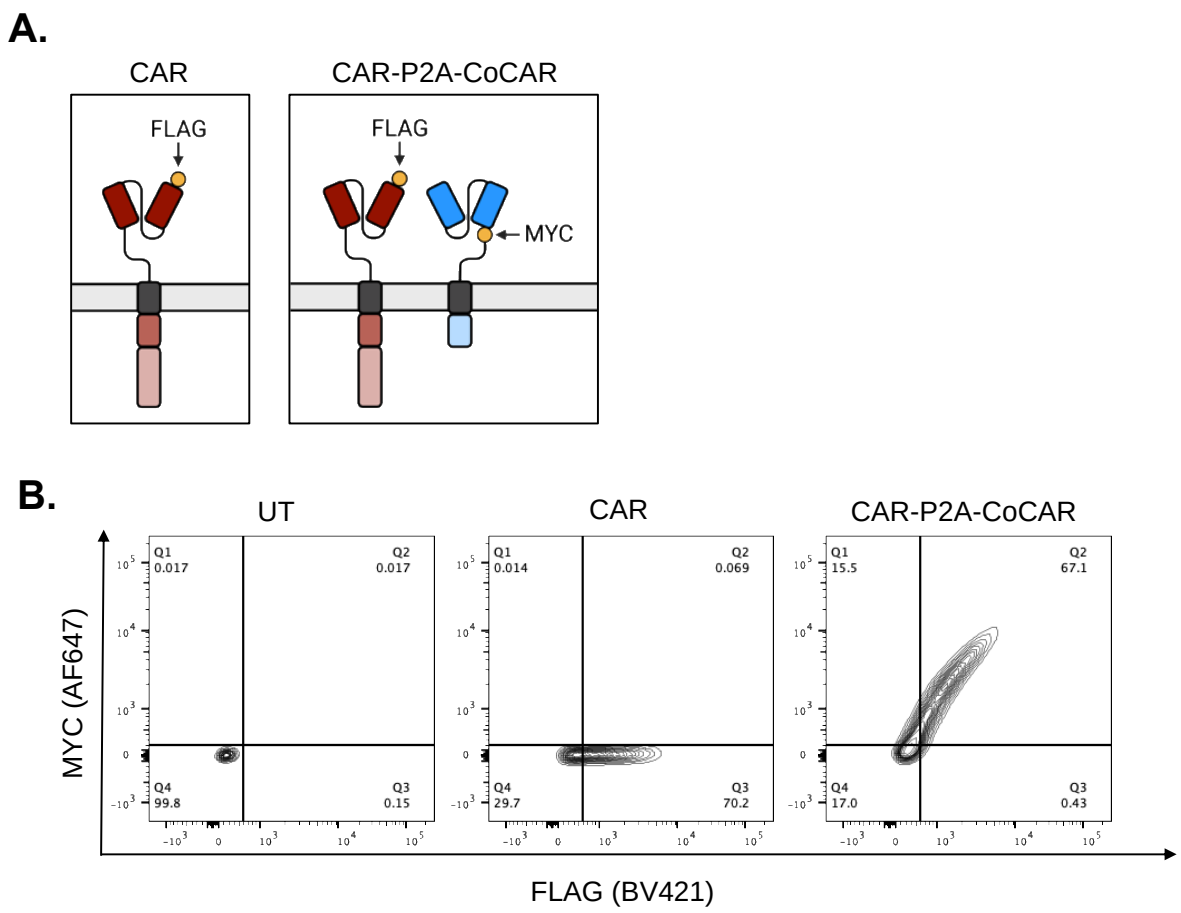

Figure 3.16 Bicistronic expression of epitope-tagged molecules via P2A improve coexpression of CAR and CoCAR

A. Schematics of a conventional anti-CD22-BBζ CAR and our novel dual-CAR system with additional chimeric coreceptor containing the HA22 scFv, CD8α transmembrane domain (TM), and CD8α cytoplasmic domain. CAR and CoCAR are tagged with FLAG or MYC tags, respectively. **B.** Representative flow cytometric plots showing expression of epitope-tagged CAR constructs in primary human T cells or untransduced (UT) controls after surface staining.

4. MECHANISTIC UNDERSTANDING

Considering the unpredictable nature of synthetic receptors and the novelty of our dual-CAR system, we sought to assess the role of various antigen-independent and antigen-dependent factors that might contribute to the CoCAR's function. We first assessed sources of antigen-independent activation, undesirable for our system. Tonic signaling, or activation in the absence of antigen, can be caused by CAR aggregation and can be identified by secretion of IFNγ by resting CAR-T cells. Although resting CAR + CoCAR cells secreted more IFNγ compared to CAR, this increase appears trivial when compared to the amount of IFNγ produced after coculture with Nalm6 cells (Figure 4.1.A). Next, we sought to verify that CAR-induced activation was due to CD22 and not non-specific binding to another molecule on Nalm6 cells.

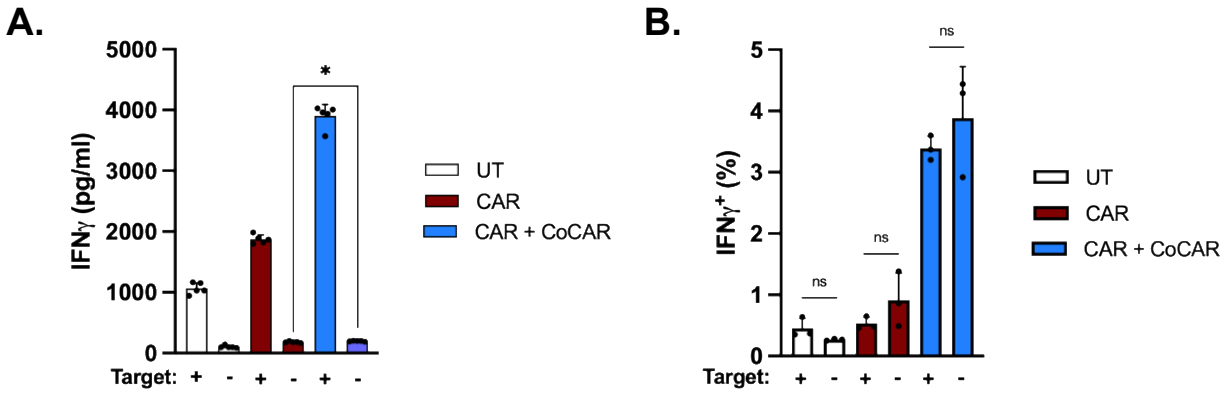

Figure 4.1 Activation through the CoCAR system is CD22-dependent
A. CAR-transduced primary human T cells were either cocultured with Nalm6 target cells (+) or left as effector-only controls (-). Pre-coculture effector counts were adjusted by mEGFP%$^{+}$, so to normalize the amount of CAR^{+} cells between conditions. Cytokine secretion was then measured by Legendplex of IFNγ in the supernatant. Baseline T cell activation in untransduced (UT) cells is shown for reference. **B.** Summarized *in vitro* activity of CAR-transduced primary human T cells after stimulation with a modified Nalm6^{CD22KO} cell line (+) or as effector-only controls (-). Cytokine production was measured by intracellular staining of IFNγ. Baseline T cell activation in untransduced (UT) cells is shown for reference.

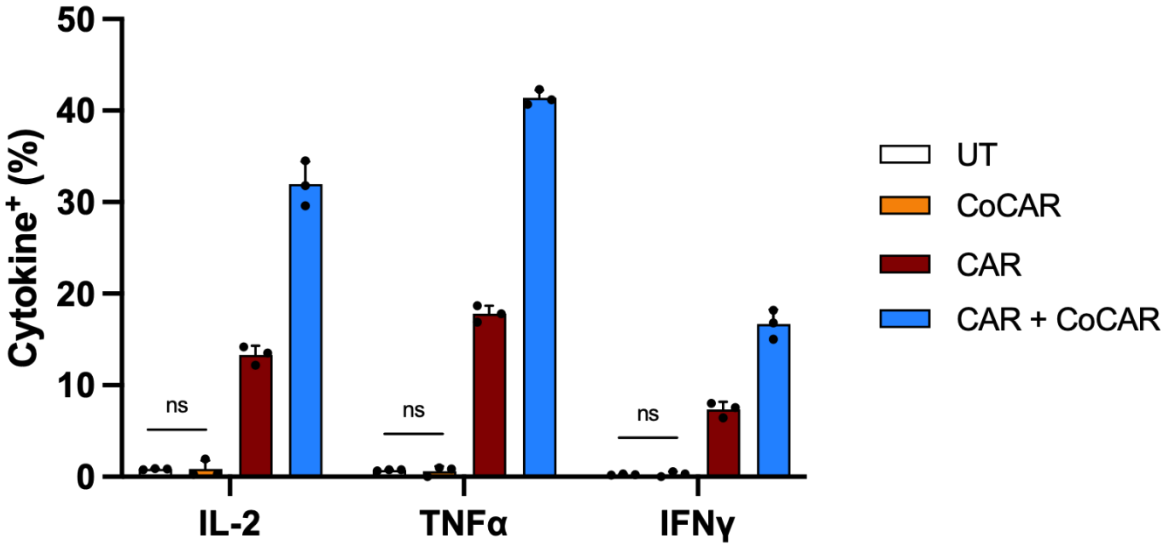

Figure 4.2 The CoCAR is incapable of inducing T cell activation by itself
Summarized *in vitro* activity of CAR-transduced primary human T cells after stimulation with the Nalm6 cell line measured by intracellular staining of IL-2, TNFα, and IFNγ. Percent cytokine positivity is shown for cells within $CoCAR^+$, CAR^+, or CAR^+CoCAR^+ gates. Untransduced (UT) cells are shown for reference.

Coculture with $Nalm6^{CD22KO}$ cells did not induce activation beyond the baseline attributed to tonic signaling (Figure 4.1.B). In conclusion, we show that the CoCAR system is dependent on CD22 and induces a negligible increase in tonic signaling compared to CAR alone.

These results led us to next evaluate antigen-dependent mechanisms. We first asked if the CoCAR alone was able to induce activation or if it was only supplementing CAR activation as designed. After coculture with Nalm6 cells, we observed no significant differences in cytokine production between untransduced cells and those expressing CoCAR alone, showing its inability to initiate T cell activation (Figure 4.2). We next sought to assess the role of avidity, as both CAR and CoCAR bind epitopes of CD22. We generated a CoCAR variant with decreased binding strength by replacing the HA22 scFv with BL22. While both scFvs bind the same epitope, a three amino acid substitution in the V_H decreases scFv affinity (K_d) from 2.3nM to

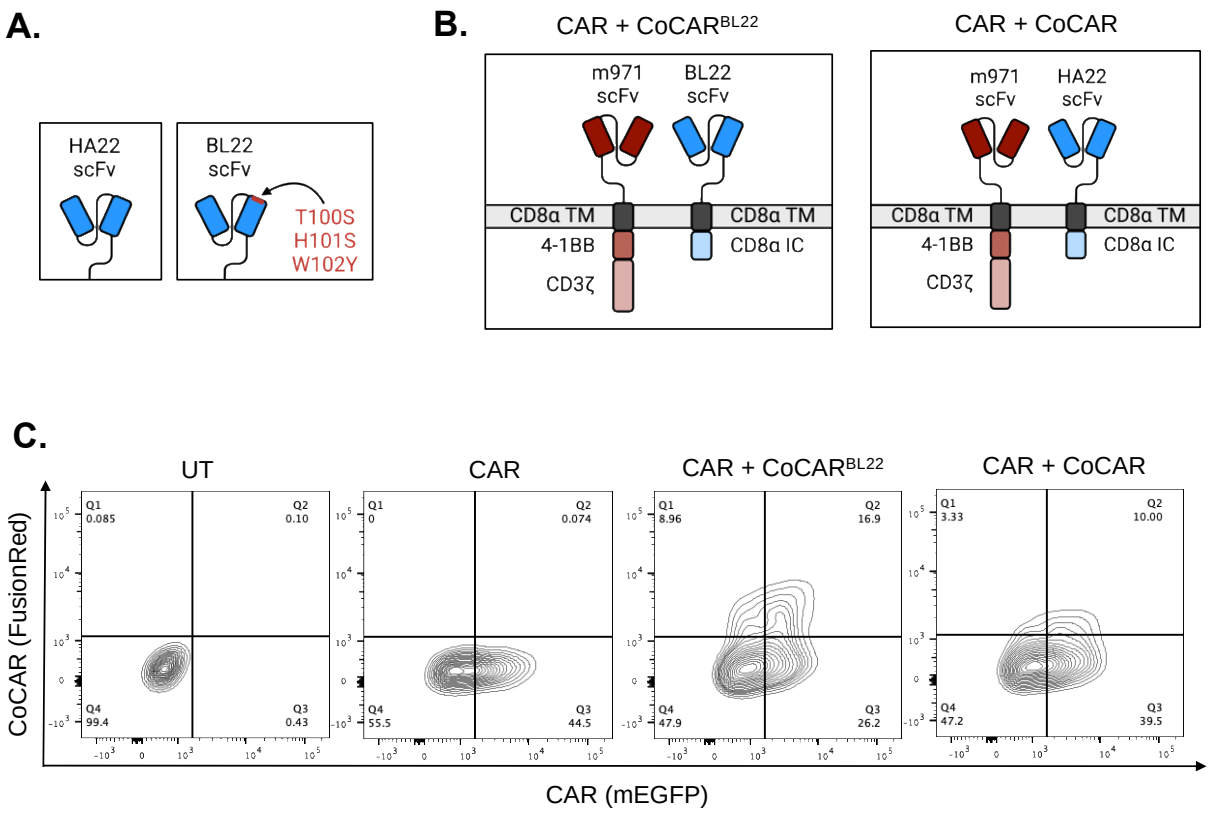

Figure 4.3 Design and expression of a lower-affinity CoCAR variant)
A. Schematic depicting amino acid mutations in the V_H domain of HA22 scFv necessary to generate the lower-affinity BL22 scFv. **B.** Schematics of the CoCAR^{BL22} system compared to the WT CoCAR system. All molecules are tagged with a C-terminal mEGFP or FusionRed (not depicted). **C.** Representative flow cytometric plots showing expression of CAR constructs in primary human T cells or untransduced (UT) controls.

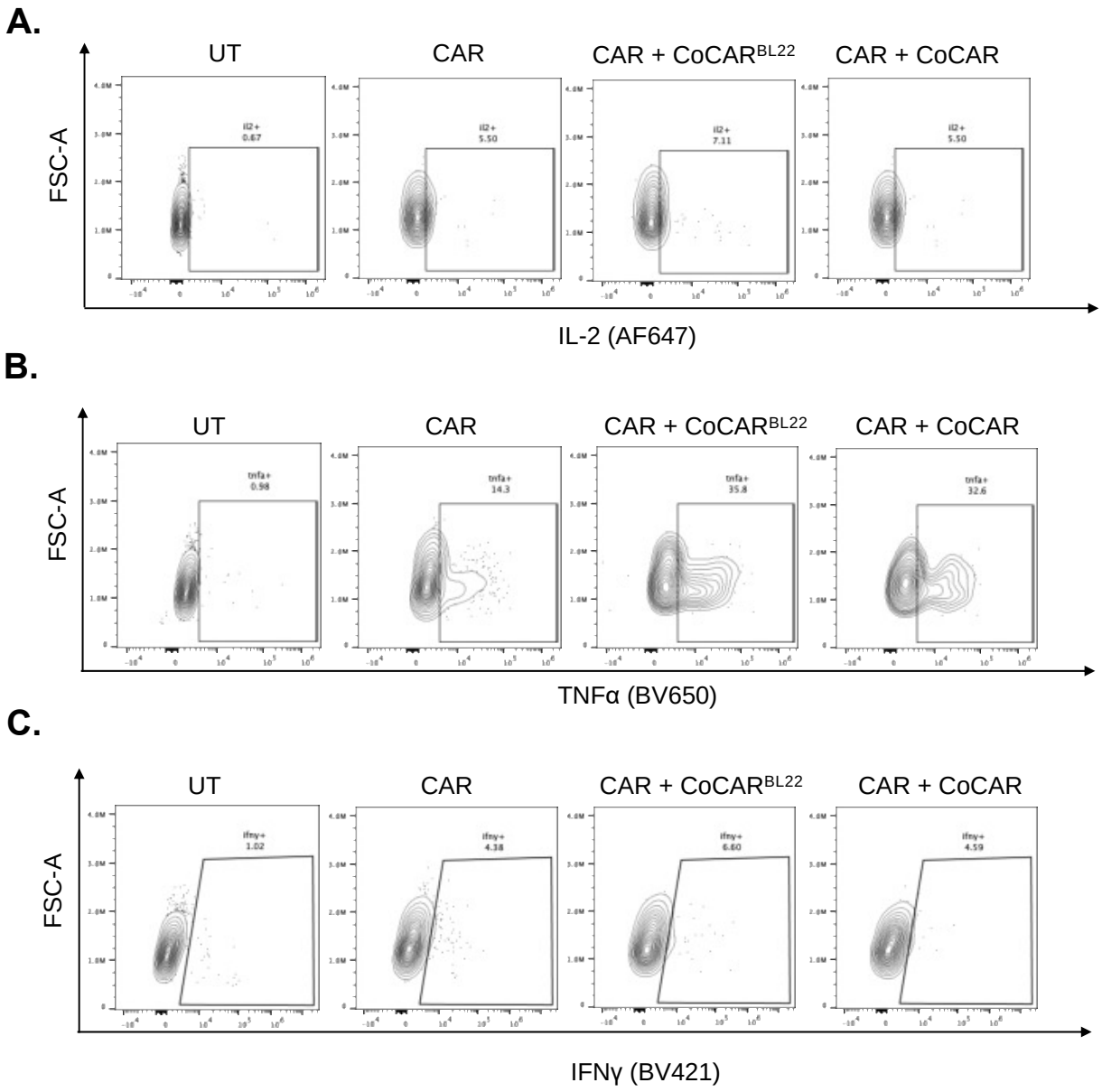

Figure 4.4 Dual-expression of CAR and CoCAR or CoCAR^{BL22} provide similar functional benefits

In vitro activity of CAR-expressing primary human T cells after stimulation with the Nalm6 cell line measured by intracellular staining of prototypical cytokines induced upon T cell activation. Representative flow cytometric plots for **A.** IL-2 **B.** TNFα **C.** IFNγ after gating of CAR$^+$, CAR$^+$CoCAR$^{BL22+,}$ CAR$^+$CoCAR$^+$ populations of equivalent gMFIs. Baseline T cell activation in untransduced (UT) cells is shown for reference.

5.8nM (Figure 4.3) [79]. Cytokine responses of $CAR^{+}CoCAR^{+}$ cells after coculture with Nalm6 cells were similar, regardless if the CoCAR contained the HA22 or BL22 (Figure 4.4 and Figure 4.5). While these results indicate that avidity is not a driving factor in CoCAR function it does not completely absolve it as a contributor, as CoCAR affinity may need to by multiple orders of magnitude in order to impair function.

These results led us to believe that the CAR and CoCAR were likely interacting with each other and we therefore sought to determine the importance of colocalization. Jurkat cells were cotransduced with CAR and CoCAR viruses and then cultured with or without Nalm6 cells. Each well was carefully fixed to retain cell-cell interactions, washed, and then transferred to a coverslip for imaging. We observed colocalization of mEGFP and FusionRed signal, especially in CAR-T cells bound to Nalm6 targets (Figure 4.6). Seeing that CAR and CoCAR molecules occupied similar regions of the T cell membrane during antigen recognition, we asked what

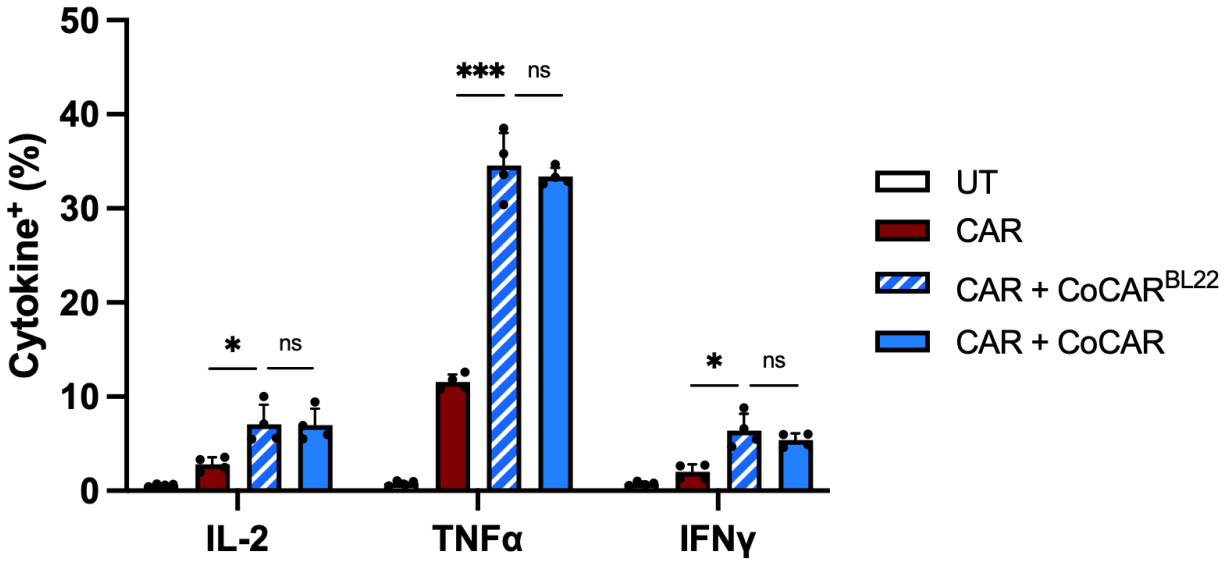

Figure 4.5 $CAR^{+}CoCAR^{BL22+}$ cells exhibit similar antitumor functionality as $CAR^{+}CoCAR^{+}$ cells
Summarized *in vitro* activity of CAR-transduced primary human T cells after stimulation with the Nalm6 cell line measured by intracellular staining of IL-2, TNFα, and IFNγ. Percent cytokine positivity is shown for cells within CAR^{+}, $CAR^{+}CoCAR^{BL22+,}$ or $CAR^{+}CoCAR^{+}$ gates of equivalent gMFIs. Untransduced (UT) cells are shown for reference.

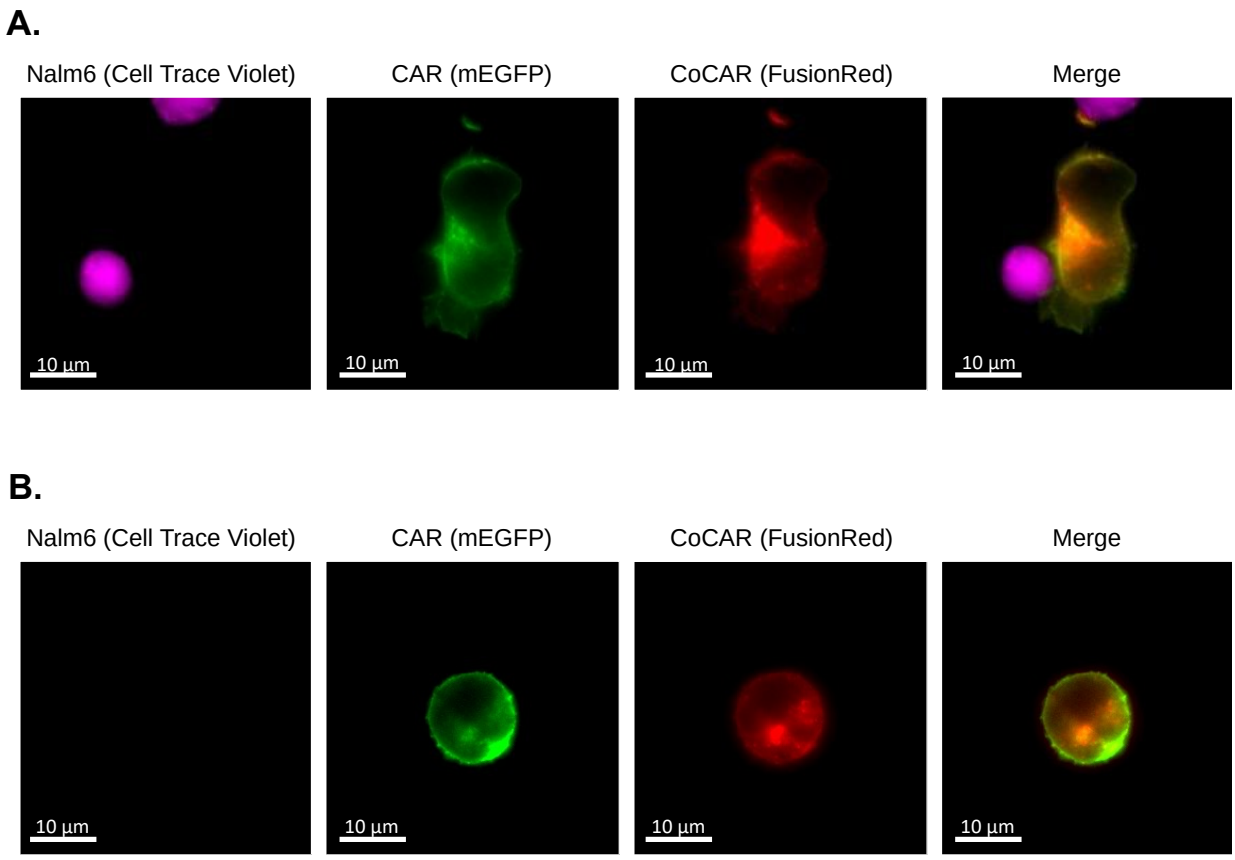

Figure 4.6 CAR and CoCAR molecules are colocalized during antigen recognition
Representative images of a $CAR^{+}CoCAR^{+}$ Jurkat T cell **A.** during recognition of a Nalm6 target cell or **B.** at rest. CAR molecules were detected via C-terminal fused mEGFP (green), CoCAR by C-terminal fused FusionRed (Red), and Nalm6 cells by labeling with Cell Trace Violet (pink). Overlap of CAR and CoCAR signal can be observed in orange.

would happen if we forced the CAR and CoCAR apart. By having the CAR and CoCAR target antigens known to inhabit different locations in the B membrane, we could further probe the necessity of CAR and CoCAR colocalization. Briefly, we generated a CoCAR variant targeting by swapping the anti-CD22 scFv HA22 with the anti-CD19 scFv FMC63 (Figure 4.7). HA22 and FMC63 have affinities of 5.8nM and 0.3nM, respectively, ensuring any increase in target cell avidity would not be lost. After coculture with Nalm6 cells, we found that redirecting the CoCAR to target CD19 led to large decreases in cytokine production (Figure 4.8 and Figure 4.9). $CAR^{+}CoCAR^{FMC63+}$ cells showed similar functionality to CAR^{+} cells, indicating that the

expression of the CD19-targeted CoCAR did nothing to improve activation induced by the CAR. Together, these data show that the CoCAR is a supplementary signaling molecule, only capable of enhancing activation when colocalized with the CAR.

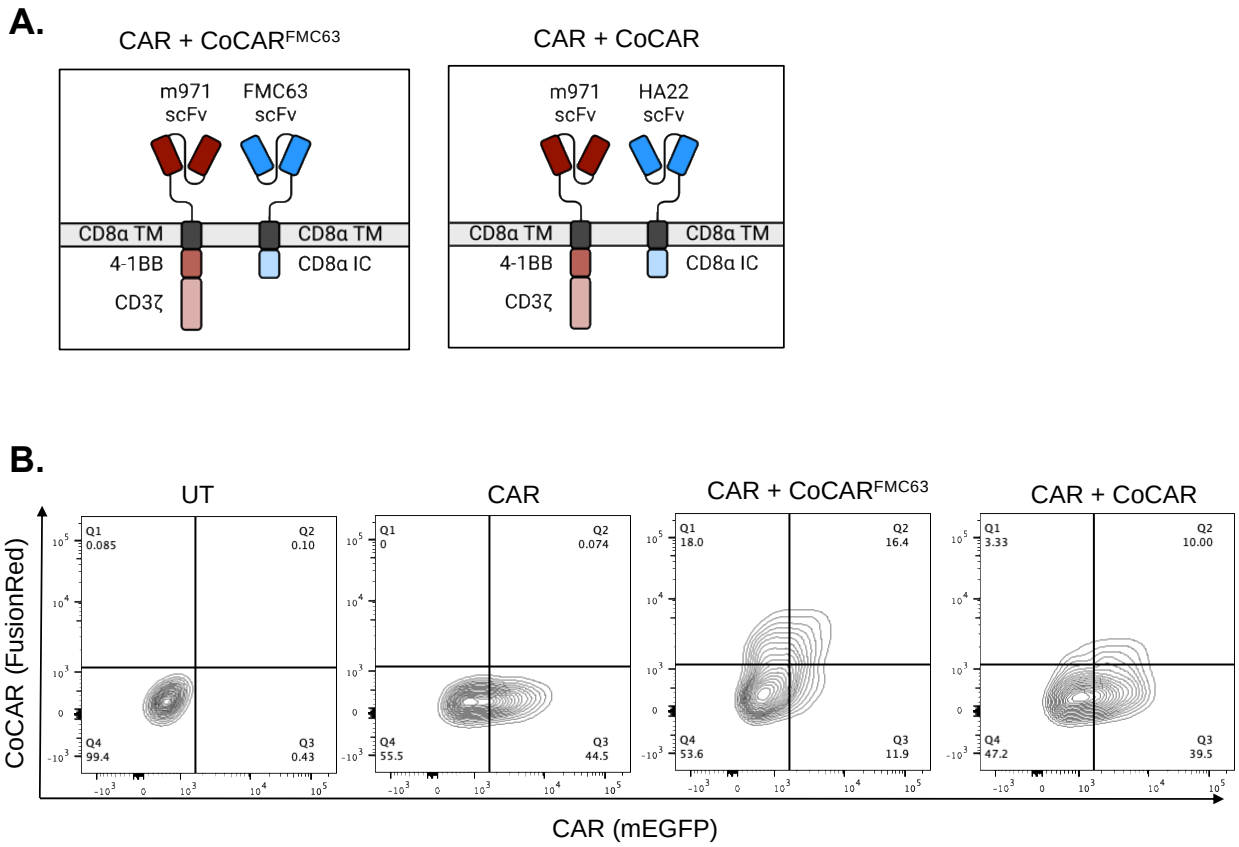

Figure 4.7 Design and expression of a CoCAR variant targeting CD19
A. Schematics of the CoCAR^{FMC63} system compared to the WT CoCAR system. All molecules are tagged with a C-terminal mEGFP or FusionRed (not depicted). **B.** Representative flow cytometric plots showing expression of CAR constructs in primary human T cells or untransduced (UT) controls.

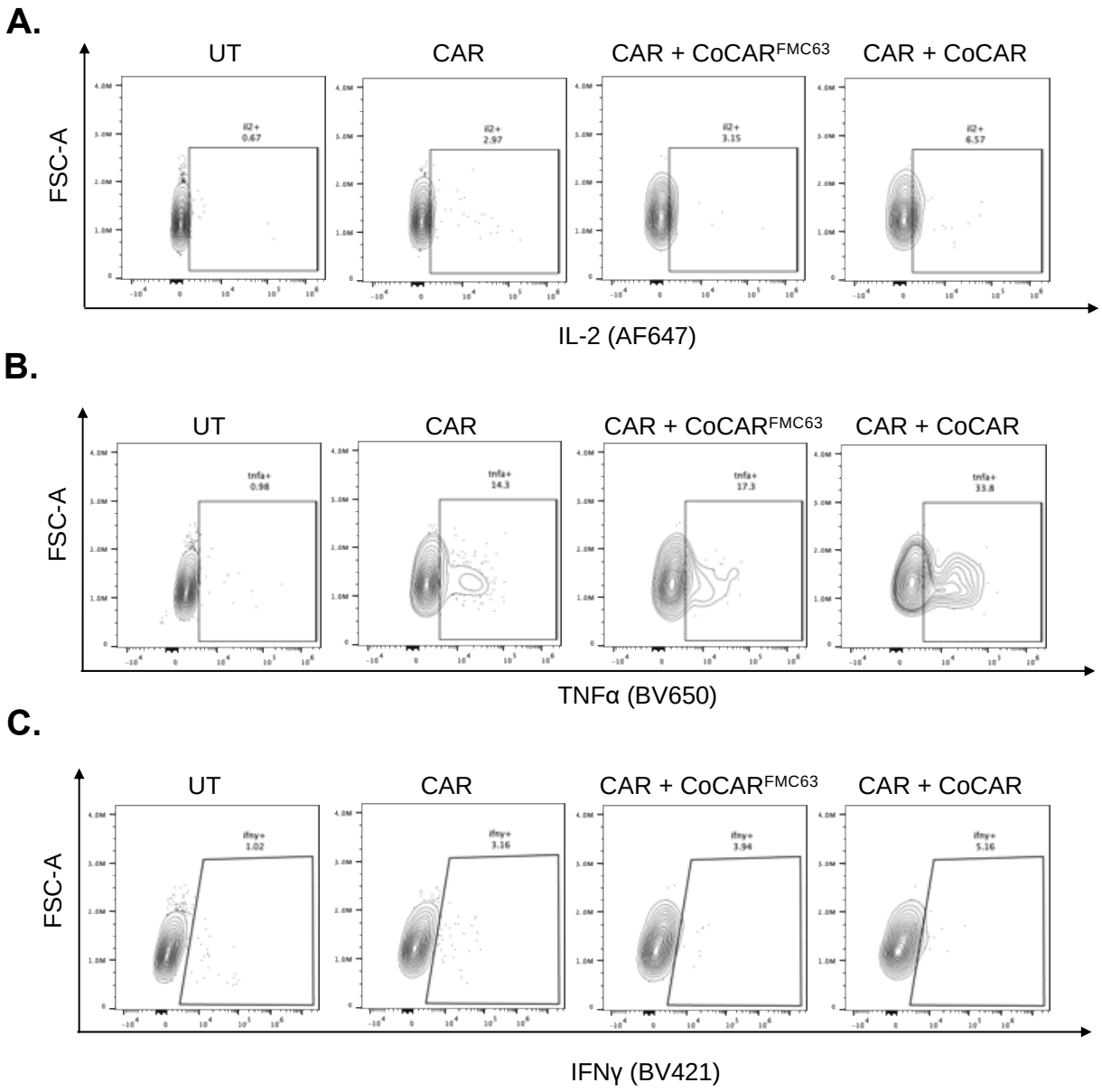

Figure 4.8 Dual-expression of CAR and CoCAR^{FMC63} do not increase functionality
In vitro activity of CAR-expressing primary human T cells after stimulation with the Nalm6 cell line measured by intracellular staining of prototypical cytokines induced upon T cell activation. Representative flow cytometric plots for **A.** IL-2 **B.** TNFα **C.** IFNγ after gating of CAR$^+$, CAR$^+$CoCAR^{FMC63+}, CAR$^+$CoCAR$^+$ populations of equivalent gMFIs. Baseline T cell activation in untransduced (UT) cells is shown for reference.

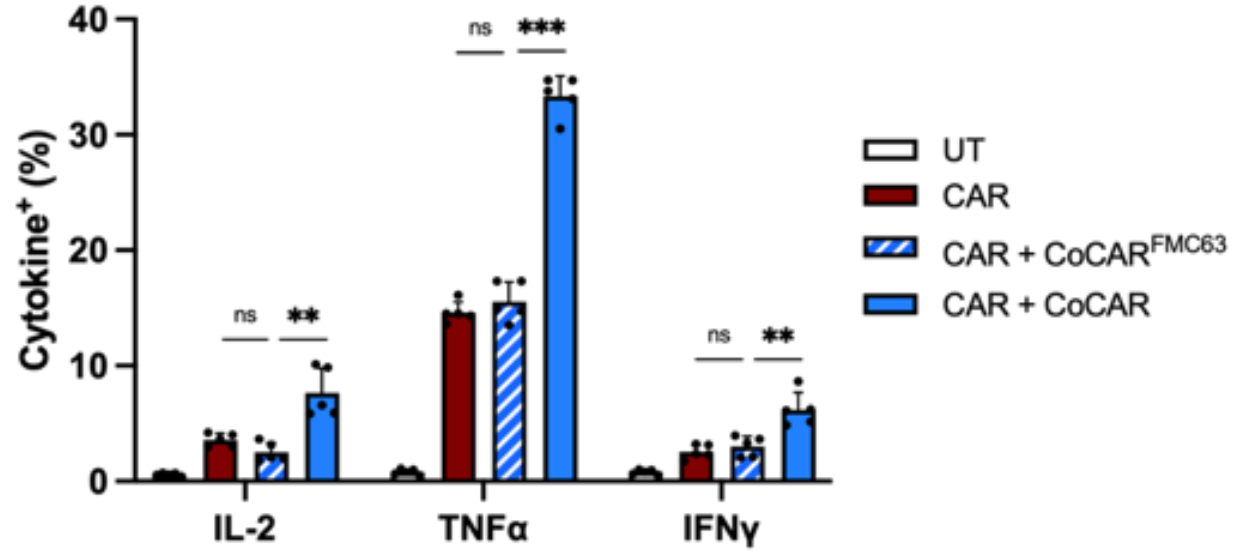

Figure 4.9 CAR$^+$CoCAR^{FMC63+} cells exhibit similar antitumor functionality as CAR$^+$ cells

Summarized *in vitro* activity of CAR-transduced primary human T cells after stimulation with the Nalm6 cell line measured by intracellular staining of IL-2, TNFα, and IFNγ. Percent cytokine positivity is shown for cells within CAR$^+$, CAR$^+$CoCAR^{FMC63+}, or CAR$^+$CoCAR$^+$ gates of equivalent gMFIs. Untransduced (UT) cells are shown for reference.

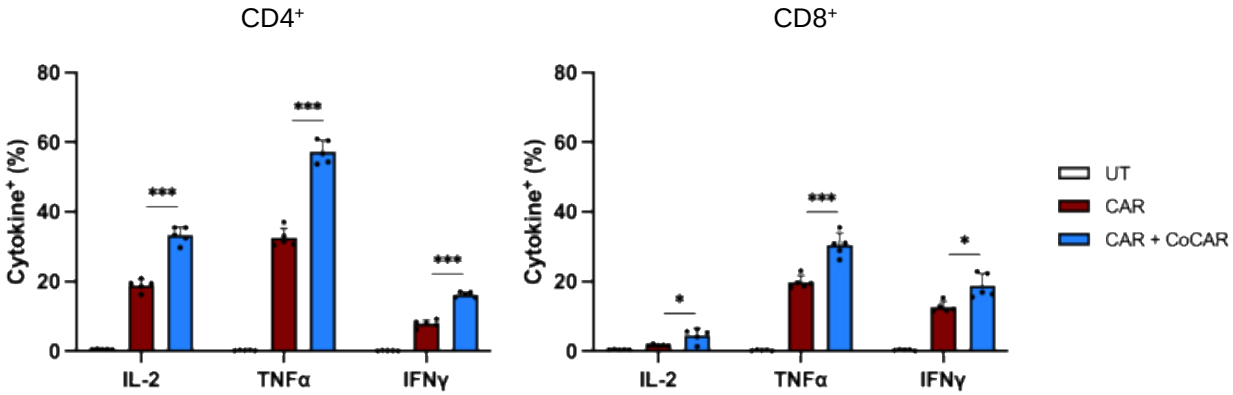

Figure 4.10 The CoCAR system works in both CD4$^+$ and CD8$^+$ T cell subtypes

Summarized *in vitro* activity of CAR-transduced primary human T cells after stimulation with the Nalm6 cell line measured by intracellular staining of IL-2, TNFα, and IFNγ. Percent cytokine positivity is shown for cells within CD4$^+$ or CD8$^+$ followed by CAR$^+$ or CAR$^+$CoCAR$^+$ gates. Untransduced (UT) cells are shown for reference.

As the CoCAR contains components borrowed from the CD8 coreceptor, we next asked if system properly functions in both $CD4^+$ and $CD8^+$ subtypes, or if the endogenous CD8 coreceptor would interfere with or sequester CoCAR function. After gating into $CD4^+$ or $CD8^+$ subtypes, we observed that the CoCAR system was able to properly function in both subtypes, showing that coreceptor subtype is largely irrelevant (Figure 4.10).

We next asked whether the intracellular domain of the CoCAR was necessary for its function and hypothesized that abrogation of LCK binding would negatively impact anti-tumor functionality. We generated two variants of the CoCAR, the first containing targeted cysteine to alanine mutations in the CxCP motif responsible for binding LCK through a zinc-clasp ($CoCAR^{AxAP}$) and a second in which the entire intracellular region was removed to rule out the binding of other molecules such as LAT to alternative motifs ($CoCAR^{\Delta}$) (Figure 4.11) [117-120]. As we hypothesized, cytokine expression was significantly impaired by abrogating LCK binding or by deletion of the cytoplasmic region (Figure 4.12 and Figure 4.13). Interestingly, CAR^+CoCAR^{AxAP+} and $CAR^+CoCAR^{\Delta+}$ cells still showed functional improvements over CAR^+ cells, indicating that the LCK-binding domain in the CoCAR is a contributor to function but not the only mechanism in play. While it appears that the CoCAR system largely behaves as designed, further interrogation into other factors such as CAR stability and synapse structure would likely provide greater insight into the CoCAR's mechanism.

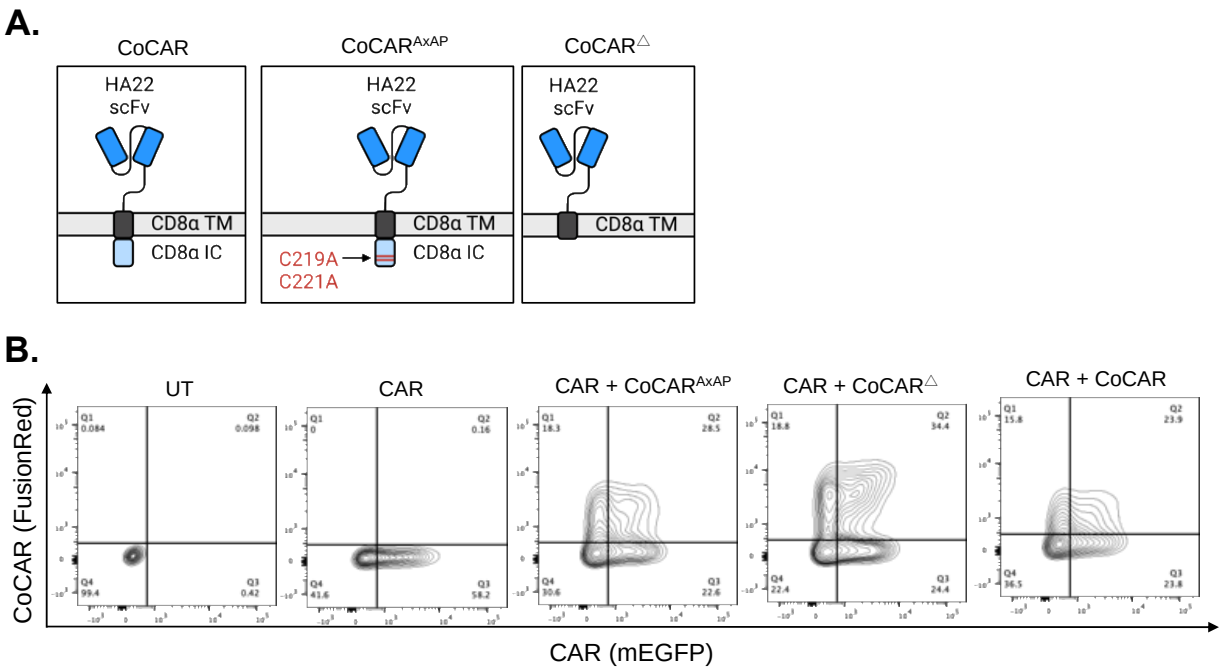

Figure 4.11 Design and expression of CoCAR variants with mutated LCK-binding domains

A. Schematics of the CoCAR^{AxAP} and CoCAR$^{\triangle}$ LCK-binding mutants compared the WT CoCAR system. All molecules are tagged with a C-terminal FusionRed (not depicted). **B.** Representative flow cytometric plots showing expression of CAR constructs in primary human T cells or untransduced (UT) controls.

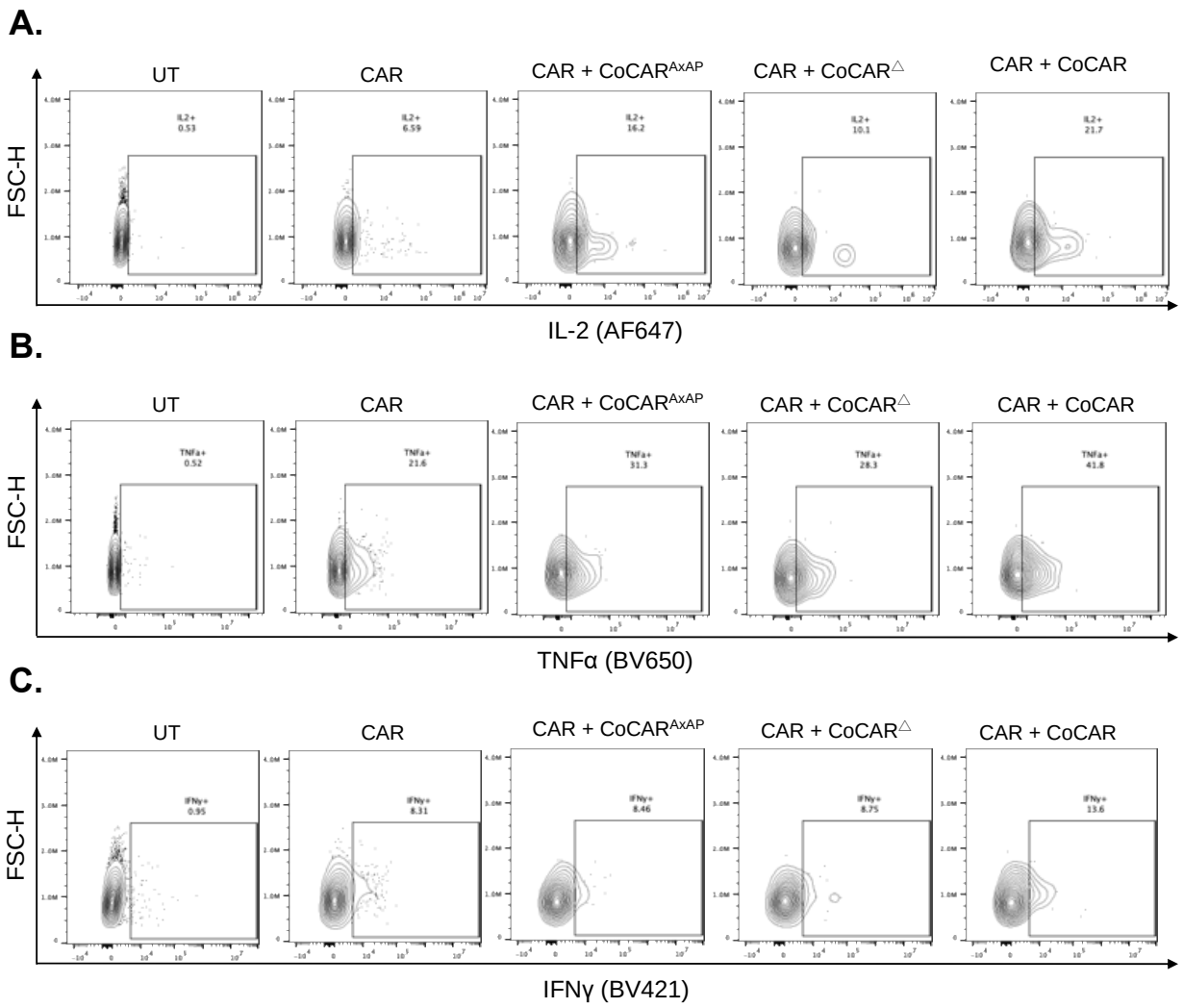

Figure 4.12 Dual-expression of CAR and CoCAR^{AxAP} or CoCAR$^{\Delta}$ are less functional than CoCAR

In vitro activity of CAR-expressing primary human T cells after stimulation with the Nalm6 cell line measured by intracellular staining of prototypical cytokines induced upon T cell activation. Representative flow cytometric plots for **A.** IL-2 **B.** TNFα **C.** IFNγ after gating of CAR^{+}, CAR^{+}CoCAR^{AxAP+}, CAR^{+}CoCAR$^{\Delta+}$, or CAR^{+}CoCAR^{+} populations of equivalent gMFIs. Baseline T cell activation in untransduced (UT) cells is shown for reference.

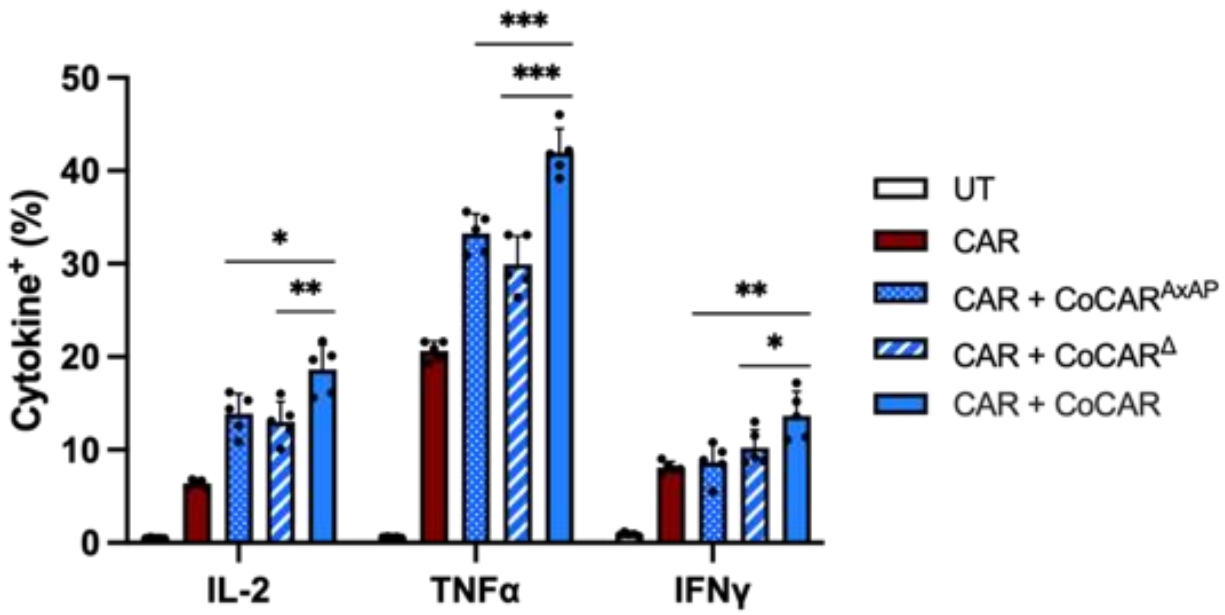

Figure 4.13 LCK plays a role in CoCAR function, but is not necessary for functional benefit

Summarized *in vitro* activity of CAR-transduced primary human T cells after stimulation with the Nalm6 cell line measured by intracellular staining of IL-2, TNFα, and IFNγ. Percent cytokine positivity is shown for cells within CAR^+, CAR^+CoCAR^{AxAP+}, $CAR^+CoCAR^{\Delta+}$, or CAR^+CoCAR^+ gates of equivalent gMFIs. Untransduced (UT) cells are shown for reference.

5. APPLICABILITY TO OTHER ANTIGEN TARGETS

Seeing that the CoCAR could be implemented to improve the functionality of a pre-existing CD22 CAR, we asked if the system was CD22-restricted or if it was capable of being adapted to other antigen targets. We selected BCMA as an alternative target and identified

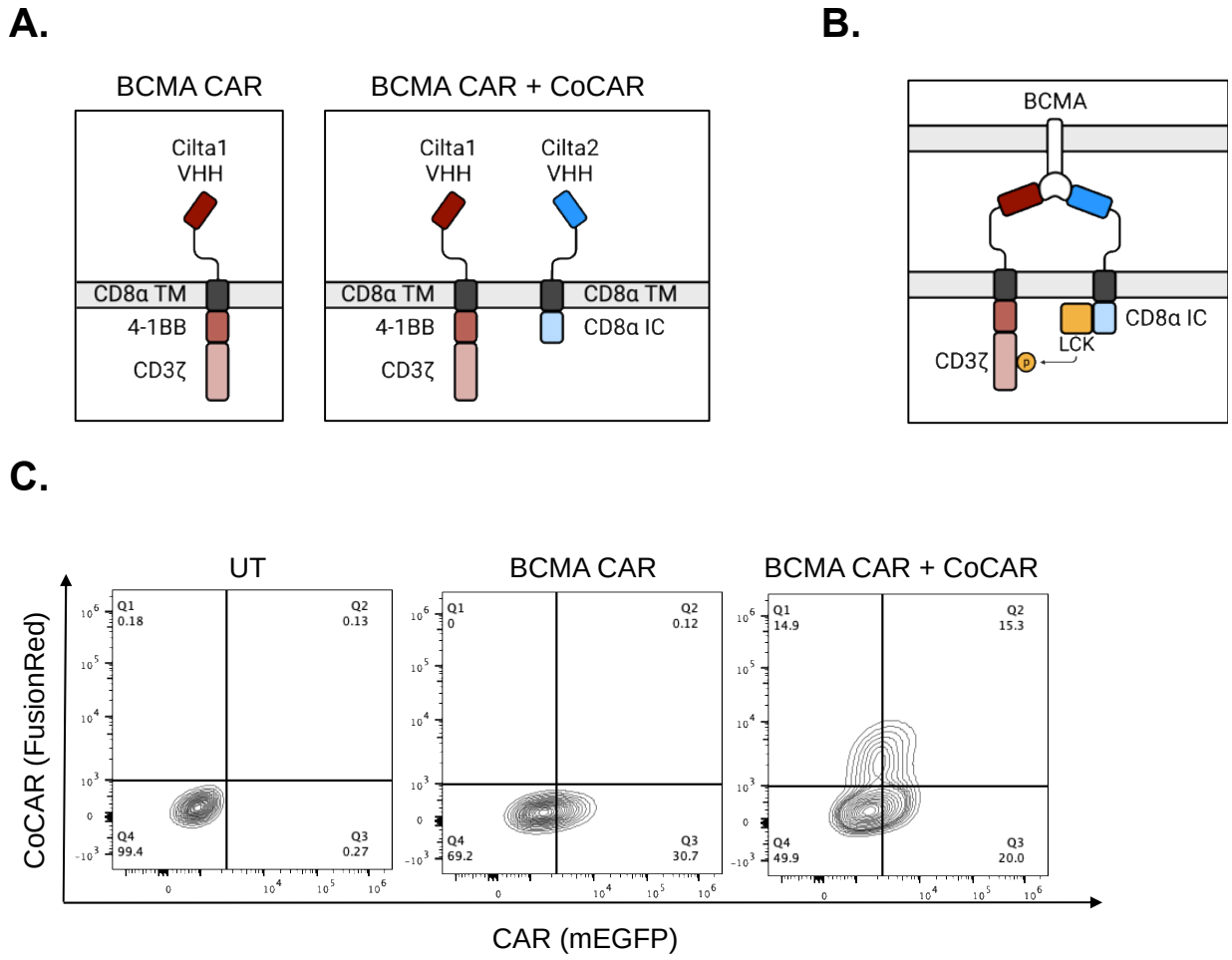

Figure 5.1 Design, rationale, and expression of re-engineeed CAR + CoCAR constructs targeting BCMA

A. Schematics of a second-generation anti-BCMA-BBζ CAR and our novel dual-CAR system targeting BCMA with additional chimeric coreceptor containing the Cilta2 VHH, CD8α transmembrane domain (TM), and CD8α cytoplasmic domain. All molecules are tagged with a C-terminal mEGFP or FusionRed (not depicted). **B.** Mechanistic hypothesis in which BCMA CoCAR-bound LCK phosphorylates ITAMs present in the CD3ζ cytoplasmic domain after non-competitive antigen binding to BCMA. **C.** Representative flow cytometric plots showing expression of BCMA CAR constructs in primary human T cells or untransduced (UT) controls.

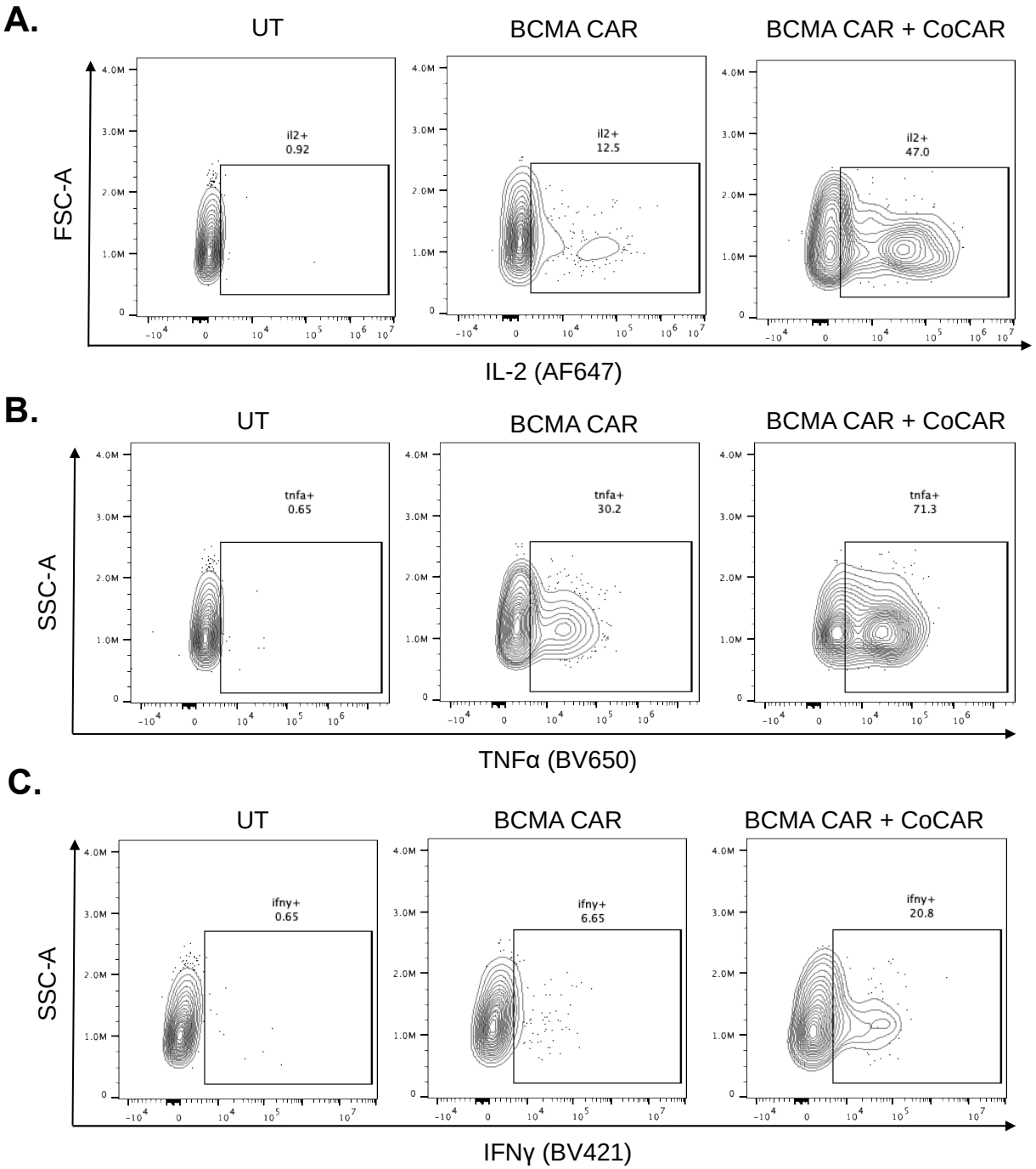

Figure 5.2 Dual-expression of BCMA CAR and CoCAR increase cytokine production
In vitro activity of BCMA CAR-expressing primary human T cells after stimulation with the MM.1s cell line measured by intracellular staining of prototypical cytokines induced upon T cell activation. Representative flow cytometric plots for **A.** IL-2 **B.** TNFα **C.** IFNγ after gating of BCMA CAR^+ or BCMA CAR^+CoCAR^+ populations. Baseline T cell activation in untransduced (UT) cells is shown for reference.

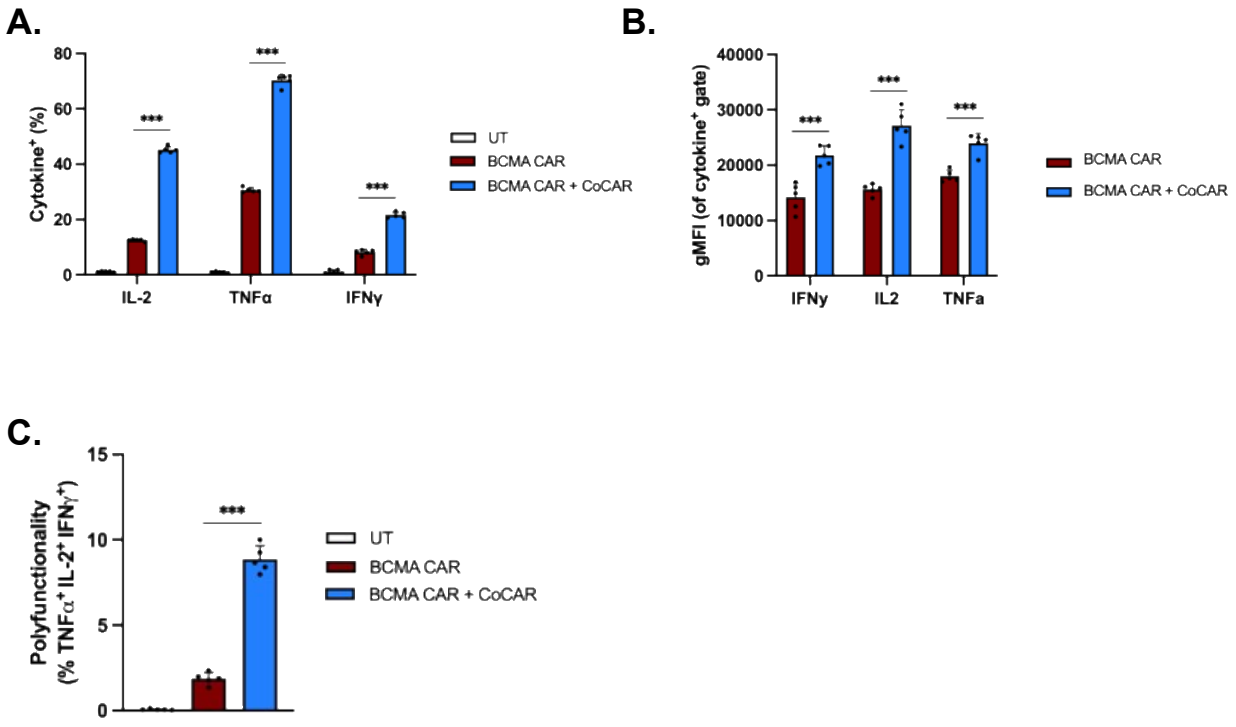

Figure 5.3 BCMA CAR$^+$CoCAR$^+$ cells exhibit improved antitumor functionality
Summarized *in vitro* activity of BCMA CAR-transduced primary human T cells after stimulation with the MM.1s cell line measured by intracellular staining of IL-2, TNFα, and IFNγ. Baseline T cell activation in untransduced (UT) cells is shown for reference. Analyzed by **A.** Percent cytokine positivity **B.** gMFI of cytokine-positive cells **C.** percent of TNFα $^+$IL-2$^+$ IFNγ$^+$ cells within BCMA CAR$^+$ or BCMA CAR$^+$CoCAR$^+$ gates.

BCMA-binding nanobodies derived from cilta-cel, known to bind distinct epitopes of BCMA [121, 122]. Briefly, we replaced the CAR's m971 scFv with Cilta1 VHH and the CoCAR's HA22 scFv with Cilta2 VHH (Figure 5.1.A and Figure 5.1.B). Coexpression of both BCMA CAR and BCMA CoCAR was achieved in a subset of primary T cells after cotransduction with split viruses (Figure 5.1.C). BCMA CAR, BCMA CAR + CoCAR, or untransduced controls were then cocultured with MM.1s cells, a BCMA$^+$ human multiple myeloma cell line. We found that BCMA CAR$^+$CoCAR$^+$ cells had both a higher percentage of cytokine positivity as well as cytokine gMFI (Figure 5.2, Figure 5.3.A, and Figure 5.3.B). Additionally, we found an increase

in polyfunctional, cytokine triple-positive cells when comparing BCMA CAR^+CoCAR^+ to CAR^+ cells (Figure 5.3.C).

Seeing that the CAR-CoCAR system could be re-engineered to target BCMA, we asked if it could be further adapted to other antigen targets. We identified previously reported scFvs that noncompetitively bind proximal (h1218) and distal domains (FMC63) of CD19 and cloned them into CAR and CoCAR vectors, respectively (Figure 5.4.A and Figure 5.4.B) [123]. Coexpression of both molecules was achieved after cotransduction with lentiviruses encoding CD19 CAR and CD19 CoCAR (Figure 5.4.C). After coculture with Nalm6 cells, we were surprised to see that CD19 CAR^+CoCAR^+ cells produced significantly less IL-2, TNFα, and IFNγ than $CD19^+$ CAR cells (Figure 5.5 and Figure 5.6). Together this data shows that the while the CoCAR system is capable of being re-engineered to target other antigens, it is selectively so. The use of any two non-competive scFvs is not a guarantee for success and other factors, such as CAR conformation, hinge length, and access to the target epitope likely play a role.

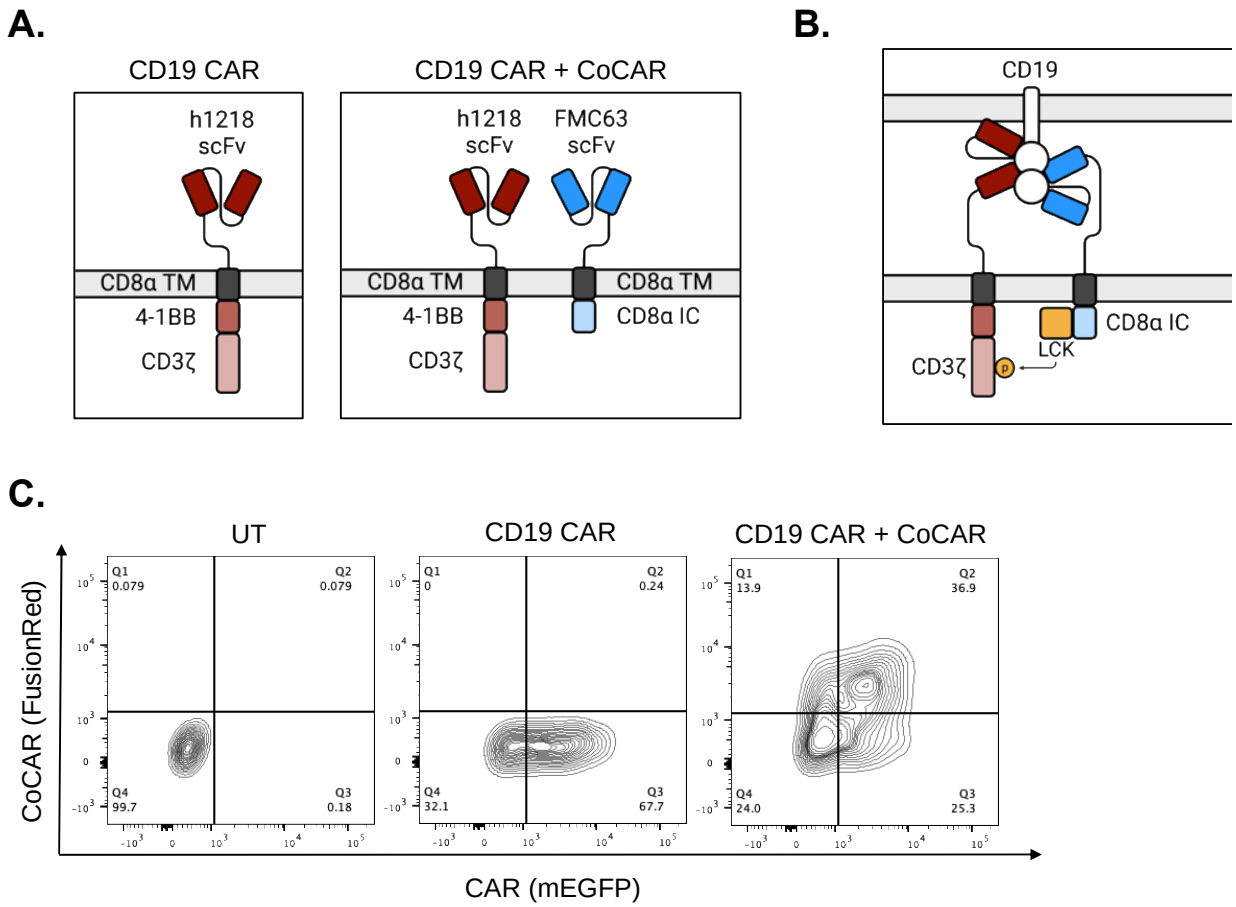

Figure 5.4 Design, rationale, and expression of re-engineeed CAR + CoCAR constructs targeting CD19

A. Schematics of a second-generation anti-CD19-BBζ CAR and our novel dual-CAR system targeting CD19 with additional chimeric coreceptor containing the FMC63 scFv, CD8α transmembrane domain (TM), and CD8α cytoplasmic domain. All molecules are tagged with a C-terminal mEGFP or FusionRed (not depicted). **B.** Mechanistic hypothesis in which CD19 CoCAR-bound LCK phosphorylates ITAMs present in the CD3ζ cytoplasmic domain after non-competitive antigen binding to CD19. **C.** Representative flow cytometric plots showing expression of CD19 CAR constructs in primary human T cells or untransduced (UT) controls.

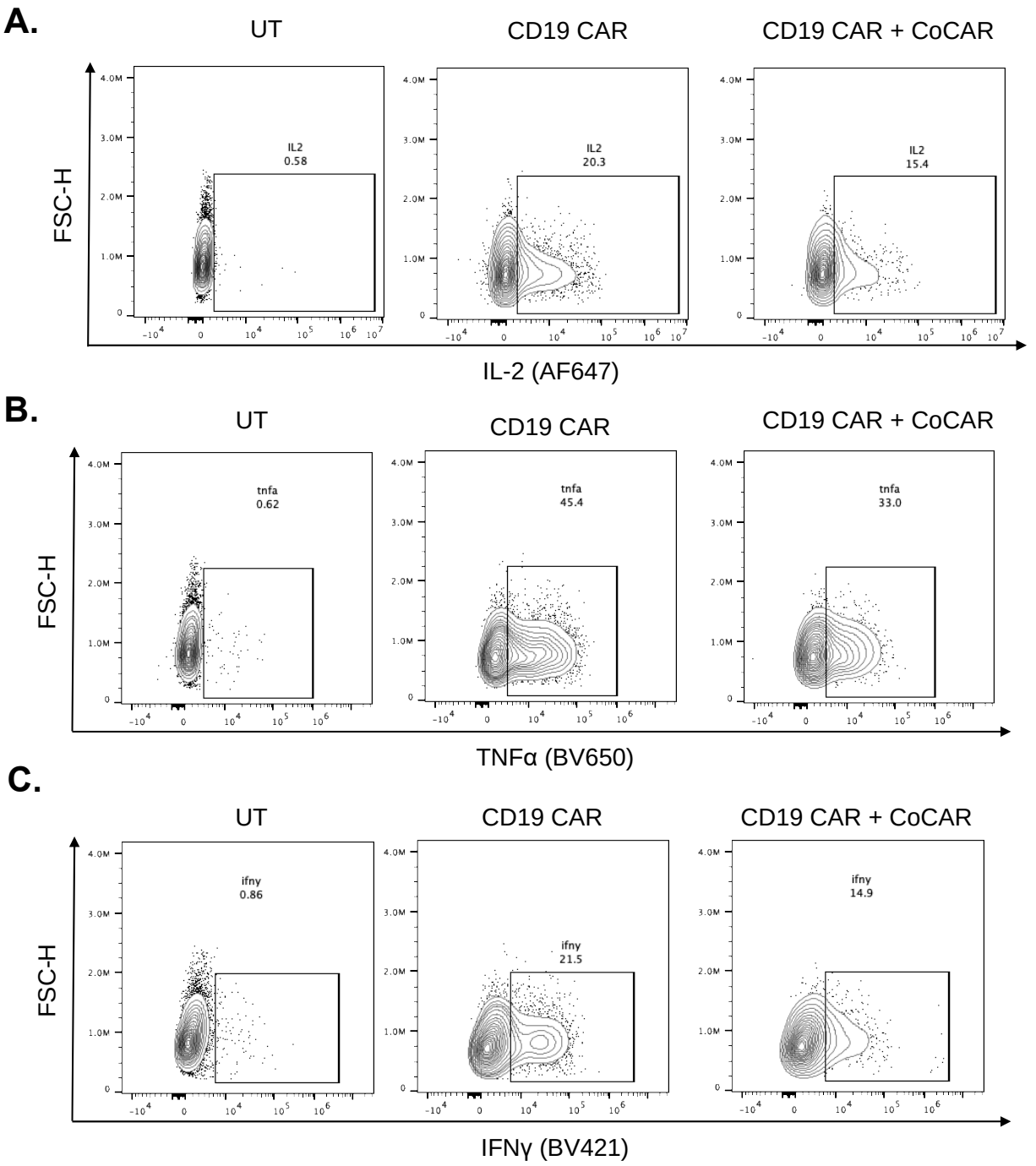

Figure 5.5 Dual-expression of CD19 CAR and CoCAR does not increase cytokine production

In vitro activity of CD19 CAR-expressing primary human T cells after stimulation with the Nalm6 cell line measured by intracellular staining of prototypical cytokines induced upon T cell activation. Representative flow cytometric plots for **A.** IL-2 **B.** TNFα **C.** IFNγ after gating of CD19 CAR^+ or CD19 CAR^+CoCAR^+ populations. Baseline T cell activation in untransduced (UT) cells is shown for reference.

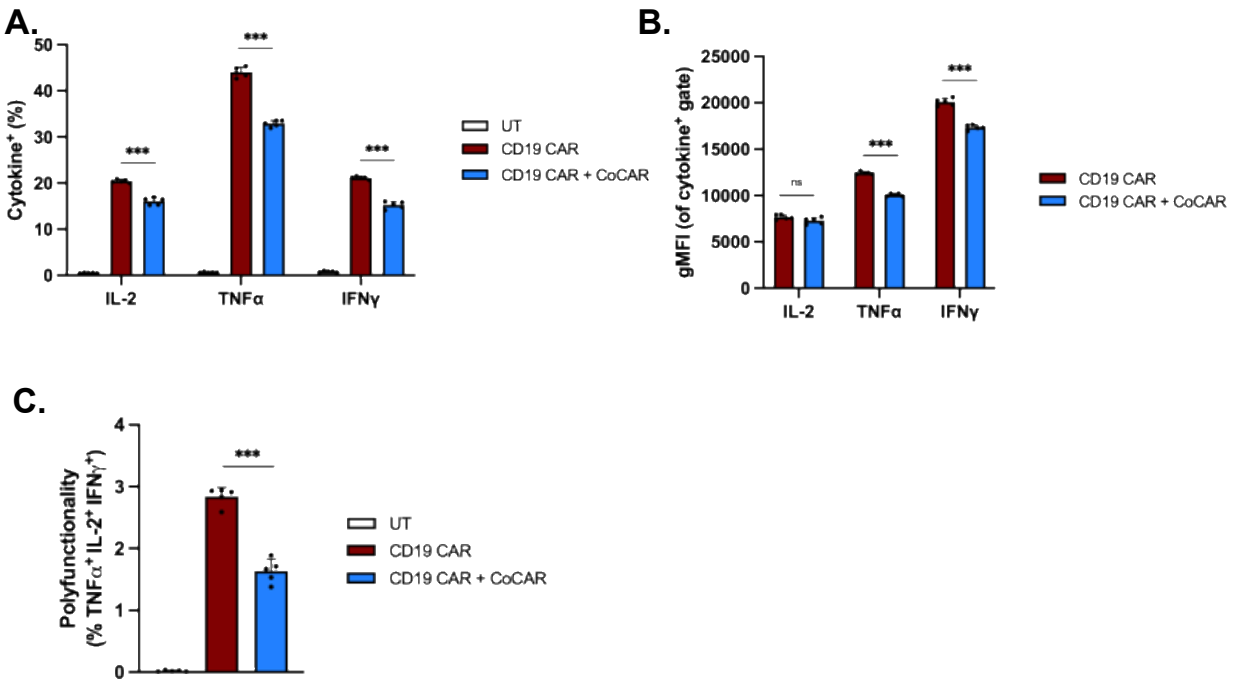

Figure 5.6 CD19 CAR$^+$CoCAR$^+$ cells exhibit worse antitumor functionality compared to CD19 CAR$^+$ cells

Summarized *in vitro* activity of CD19 CAR-transduced primary human T cells after stimulation with the Nalm6 cell line measured by intracellular staining IL-2, TNFα, and IFNγ. Baseline T cell activation in untransduced (UT) cells is shown for reference. Analyzed by **A.** Percent cytokine positivity **B.** gMFI of cytokine-positive cells **C.** percent of TNFα $^+$IL-2$^+$ IFNγ$^+$ cells within CD19 CAR$^+$ or CD19 CAR$^+$CoCAR$^+$ gates.

6. DISCUSSION

6.1 Combatting relapse of chimeric antigen receptor T cell therapy

While chimeric antigen receptor (CAR) T cell therapies have completely changed the landscape of treating lymphoid-derived cancers, relapse is still a common occurrence in complete responders. While this can be partially attributed to inefficiencies of second-generation CAR signaling, downregulation of target antigen by tumor cells plays a role in immunoevasion. One strategy undertaken to combat relapse has been administration of a second CAR-T cell therapy, typically targeting a different antigen than the first dose. The most common antigen pairing investigated in the clinic has been CD19 and CD22. In a review of clinical trials investigating the efficacy of sequential administration, the authors identified a set of studies in which B cell acute lymphoblastic lymphoma (B-ALL) patients received 4-1BB-based, anti-CD19 CAR-T therapy, had a complete response, relapsed, and then received 4-1BB-based, anti-CD22 CAR-T therapy (Figure 6.1.A) [124]. 65% of patients had a complete response to the second

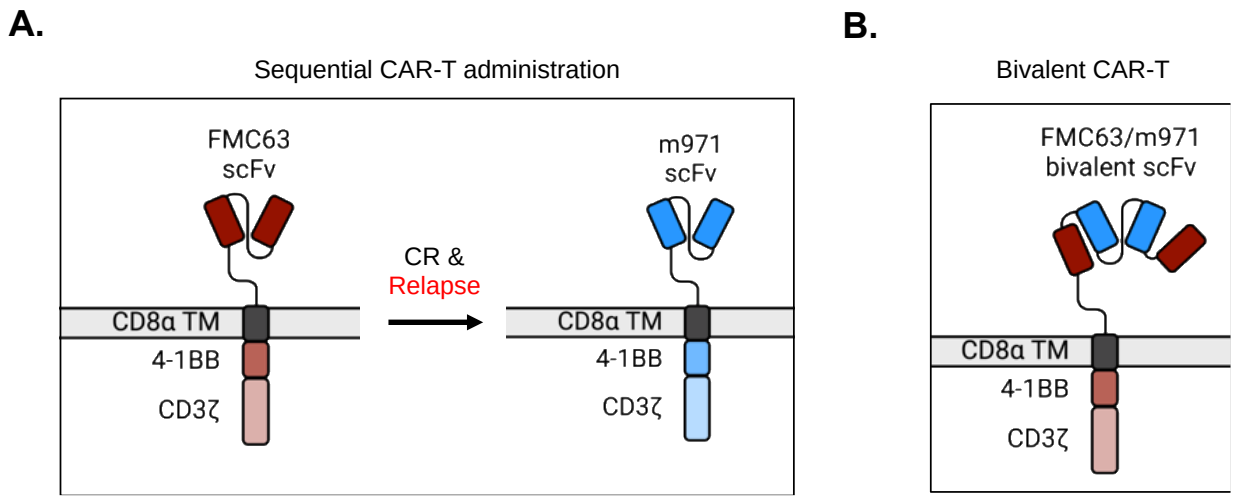

Figure 6.1 Sequential CAR-T administration and bivalent CAR-T therapies for combatting relapse
Schematics of **A.** sequential administration of typical anti-CD19 and anti-CD22 targeted CAR-T therapies or **B.** a bivalent anti-CD19/22 CAR using both FMC63 and m971 scFvs.

CAR dose but unfortunately 70% relapsed, similarly to rates observed in patients only receiving one dose of anti-CD22 CAR-T therapy.

An alternative strategy undertaken has been the use of bivalent CAR-T therapy, in which two scFvs are joined into one continuous binding domain capable of recognizing two different antigen targets. Clinically, the most common bivalent CAR for treating B-ALL contains a tandem FMC63/m971 scFv capable of binding CD19 and CD22 (Figure 6.1.B). In clinical trials, 75% of B-ALL patients receiving bivalent anti-CD19/CD22 CAR-T therapy achieved complete responses and 53% of those responders relapsed [125-128]. In conclusion, current clinical data suggests that neither sequentially administered or bivalent CAR therapies fully prevent relapse. While more data is needed to prove mechanisms of failure behind both approaches, inefficient CAR signaling most likely plays a role in both. Neither strategy prevent antigen downregulation nor increase sensitivity to antigen. Lastly, while targeting two antigens is a feasible approach for treating B-ALL, many tumor types do not have multiple highly conserved and highly expressed antigens that can be safely targeted without risk of 'on-target, off-tumor' toxicities [129].

6.2 Next-generation chimeric antigen receptors for increased antigen sensitivity

Other groups have sought to address relapse by engineering next-generation CARs with increased sensitivity. These novel constructs can be broadly separated into two categories: second-generation CARs with additional signaling domains and chimeric TCRs (cTCRs).

The εRKζ CAR, BBε$_{PRS+ITAM}$ζ CAR, and BBζlinkGRB2$_{SH2}$ CAR are three examples of next-generation CAR constructs with increased sensitivity. The εRKζ CAR includes an LCK-binding RK motif from CD3ε, inserted between 4-1BB and CD3ζ cytoplasmic domains [130]. Mechanistically, the authors hypothesized that by increasing CAR-associated LCK, antigen sensitivity would be improved. Impressively, their design increased CD3ζ-associated LCK and

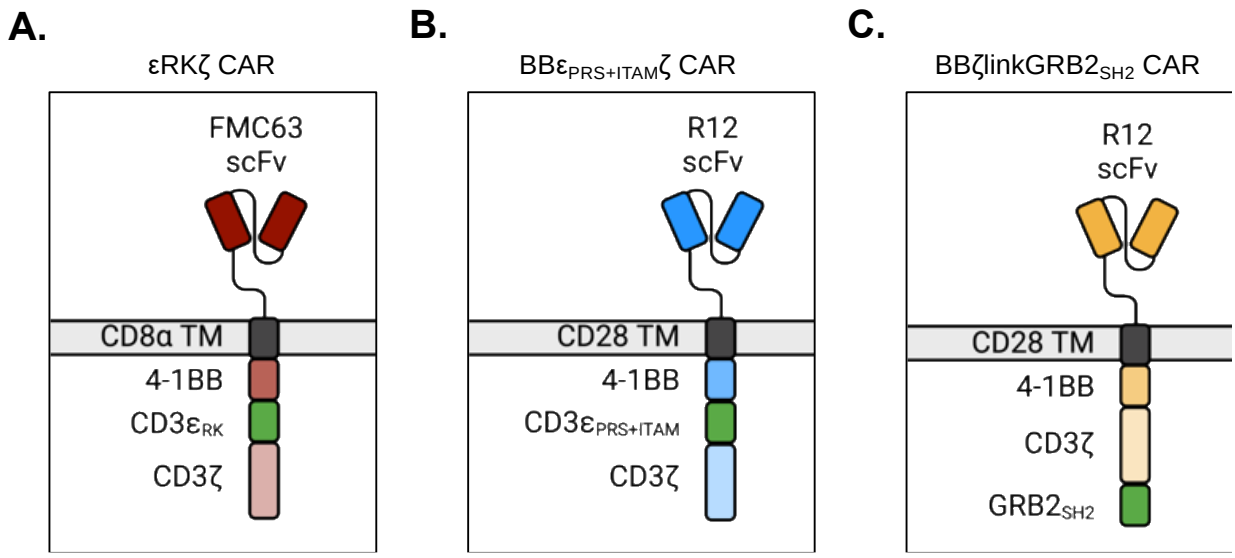

Figure 6.2 Design of next-generation chimeric antigen receptors for increased antigen sensitivity
Schematics of **A.** the εRKζ CAR containing the FMC63 scFv, CD8α transmembrane (TM) domain, 4-1BB cytoplasmic domain, $CD3\varepsilon_{RK}$ LCK-binding domain, and CD3ζ cytoplasmic domain. **B.** the $BB\varepsilon_{PRS+ITAM}\zeta$ CAR containing the R12 scFv, CD28 TM domain, 4-1BB cytoplasmic domain, $CD3\varepsilon_{PRS+ITAM}$ Nck1-binding domain, and CD3ζ cytoplasmic domain, or **C.** $BB\zeta linkGRB2_{SH2}$ CAR containing the R12 scFv, CD28 TM domain, 4-1BB cytoplasmic domain, CD3ζ cytoplasmic domain, and $GRB2_{SH2}$ LAT-binding domain attached by flexible linker (not depicted).

antigen sensitivity without introducing additional tonic signaling. Both $BB\varepsilon_{PRS+ITAM}\zeta$ and $BB\zeta linkGRB2_{SH2}$ CARs were rationally-designed to increase the phosphorylation of LAT or PLCγ1, as both molecules were found to be downregulated in CAR signaling [92]. The $BB\varepsilon_{PRS+ITAM}\zeta$ CAR was generated by inserting a Nck1-binding PRS domain and an additional ITAM from CD3ε between 4-1BB and CD3ζ cytoplasmic domains. The $BB\zeta linkGRB2_{SH2}$ CAR contained a LAT-binding SH2 domain from GRB2 at the C-terminus. Compared to conventional 4-1BB-based CARs, both novel designs increased cytokine production and calcium flux *in vitro* and increased survival against antigen-low cells *in vivo*. Significant increases in tonic signaling were not observed with either novel construct.

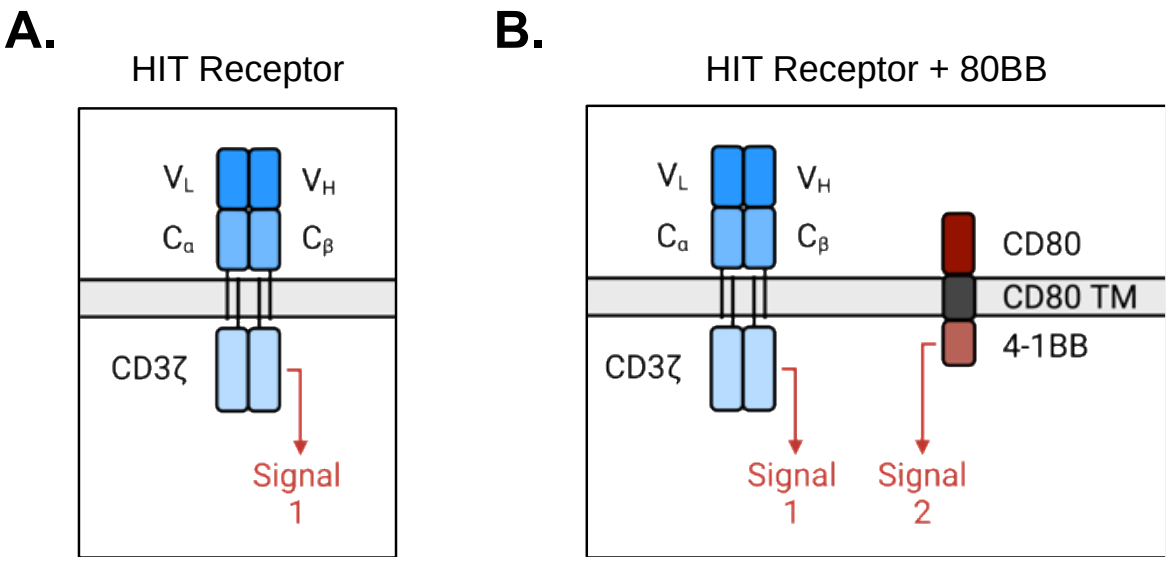

Figure 6.3 Design of next-generation chimeric T cell receptors for increased antigen sensitivity
Schematics of A. the HIT receptor showing V_L-C_α and V_H-C_β molecules complexed with endogenous CD3ζ and B. the HIT receptor and the 80BB receptor, containing CD80 extracellular and transmembrane (TM) domains and a 4-1BB cytoplasmic domain.

cTCRs emerged as the first chimeric receptor but quickly fell out of favor to the CAR. No longer hindered by prior technical limitations regarding expression, the cTCR has revived in recent years in part due to their ability to better interact with endogenous components of the TCR complex. Two recently described cTCRs are the synthetic T cell receptor and antigen receptor (STAR) and the HLA-independent T cell (HIT) receptor [131, 132]. The structure of each cTCR is identical, with V_α and V_β domains of the TCR being replaced with V_L and V_H domains derived from a monoclonal antibody. While only anti-EGFR targeting was validated with the STAR, the HIT receptor was re-engineered multiple times to target CD19, CD22, BCMA, and CD70. Both STAR and HIT receptors displayed increased sensitivity to antigen and higher phosphorylation of CD3ζ ITAMs and ZAP-70. Unlike the STAR and past cTCRs, the HIT receptor introduced a major improvement in regard to transgene expression. While the STAR is randomly integrated into the genome of modified T cells, the HIT receptor employs *TRAC* locus editing to replace

chromosomal TCR variable regions, reducing possible competition between the HIT receptor and the endogenous TCR for CD3 components. Anticipating that *in vivo* persistence of HIT receptor T cells may be negatively affected by lack of costimulation, the chimeric costimulatory molecule 80BB has recently been described [133]. Consisting of the extracellular domain of CD80 and the intracellular domain of 4-1BB, the chimeric costimulatory molecule functions by providing or receiving CD28-based costimulation through binding endogenous CD28 receptors or by providing 4-1BB-based costimulation by binding endogenous CD28 receptors in *trans* or CTLA-4 molecules expressed by target cells. T cells coexpressing both HIT receptor and 80BB performed better *in vivo* compared to cells solely expressing the HIT receptor.

6.3 Strengths and limitations of the chimeric coreceptor

Here, we present another approach for increasing the antigen sensitivity of CD22-targeted CARs through the coexpression of the CoCAR, an anti-CD22 chimeric coreceptor. Our novel approach increased *in vitro* antitumor functionality of 4-1BB-based CARs at clinically-relevant antigen densities of CD22, without inducing problematic levels of tonic signaling. While there are outstanding questions regarding its mechanism, we showed that as designed the CoCAR is a supplementary signaling molecule, incapable of inducing T cell activation alone. Colocalization of both CAR and CoCAR is crucial for function and the LCK-binding domains present in the CoCAR contribute to functionality. The dual-CAR system is capable of being re-engineered to target BCMA, indicating modularity and the potential to be applied to other antigen targets. Furthermore, the system was able to tolerate different types of binding domains, working for both scFvs and nanobodies. While we were not able to re-engineer the CoCAR system to target CD19, we believe additional screening would identify a suitable pair of binders. Alternatively, we hypothesize that there are pairs of antigen that would work with the CoCAR system and that

targeting two different epitopes on the same antigen is not necessary. Evidence for dual-CARs interacting through their intracellular domains can be seen with the LINK CAR, binding both CD19 and HER2 and capable of heterodimerization [134].

The CoCAR's main strength lies in its potential to be applied to clinically-used, second-generation CARs. We believe the benefit of not having to undergo major re-engineering of current CAR constructs outweighs the screening needed for CoCAR implementation. Novel CAR designs, such as the εRKζ, BB$\varepsilon_{PRS+ITAM}\zeta$, and BBζlinkGRB2$_{SH2}$, have yet to be used in the clinical setting and their safety profiles and efficacies in human subjects is unknown. The CoCAR is not a full redesign of existing second-generation CARs, working to only enhance currently employed signaling pathways, and is incapable of inducing activation by itself. While the majority of the CoCAR's evaluation was done using split viruses, we provided evidence for bicistronic expression of both CAR and CoCAR which would reduce manufacturing costs associated with producing multiple GMP-grade viruses [135].

There are still functional and mechanistic questions that lie unanswered. Futher studies are needed to better assess the *in vivo* proliferation, phenotype, and persistence of CAR^+CoCAR^+ T cells. While we assessed the functionality of CoCAR-expressing cells across a range of antigen densities, it remains to be seen if the system's sensitivity approaches that of the TCR. While we have observed improved cytokine secretion and cytotoxicity with the CoCAR system, much of the mechanism needs closer examination. Specifically, experiments analyzing protein-protein interactions are needed to validate the binding of LCK to the CoCAR's cytoplasmic domain and phosphoproteomic analyses are needed to evaluate phosphorylation of CD3ζ ITAMs and ZAP-70.

While this proposal is most concerned with improving clinical efficacy of CAR constructs, the work accomplished through this study has increased the field's scientific knowledge regarding CAR design. It is the first study to simultaneously target two different epitopes of CD22. The CoCAR system contains distinct, co-expressed CAR molecules that interact with each other through cytoplasmic domains. Dual-CAR systems compose the minority of published designs and ones in which the cytoplasmic domains directly interact are incredibly rare. The iterative design process undertaken has generated a novel, useful CAR system and a better understanding of dual-CAR design and limitations.

REFERENCES

1. Matzinger, P. The danger model: a renewed sense of self. *Science* **296**, 301–305 (2002).

2. Lam, N., Lee, Y. & Farber, D. L. A guide to adaptive immune memory. *Nat Rev Immunol* 1–20 (2024).

3. Ackerman, A. L., Giodini, A. & Cresswell, P. A Role for the Endoplasmic Reticulum Protein Retrotranslocation Machinery during Crosspresentation by Dendritic Cells. *Immunity* **25**, 607–617 (2006).

4. Joffre, O. P., Segura, E., Savina, A. & Amigorena, S. Cross-presentation by dendritic cells. *Nat Rev Immunol* **12**, 557–569 (2012).

5. Pishesha, N., Harmand, T. J. & Ploegh, H. L. A guide to antigen processing and presentation. *Nat Rev Immunol* **22**, 751–764 (2022).

6. Serwold, T., Gonzalez, F., Kim, J., Jacob, R. & Shastri, N. ERAAP customizes peptides for MHC class I molecules in the endoplasmic reticulum. *Nature* **419**, 480–483 (2002).

7. Roche, P. A. & Furuta, K. The ins and outs of MHC class II-mediated antigen processing and presentation. *Nat Rev Immunol* **15**, 203–216 (2015).

8. Denzin, L. K. & Cresswell, P. HLA-DM induces CLIP dissociation from MHC class II alpha beta dimers and facilitates peptide loading. *Cell* **82**, 155–165 (1995).

9. Ridge, J. P., Di Rosa, F. & Matzinger, P. A conditioned dendritic cell can be a temporal bridge between a CD4+ T-helper and a T-killer cell. Nature 393, 474–478 (1998).

10. Castellino, F. *et al.* Chemokines enhance immunity by guiding naive CD8+ T cells to sites of CD4+ T cell–dendritic cell interaction. *Nature* **440**, 890–895 (2006).

11. Bassing, C. H., Swat, W. & Alt, F. W. The Mechanism and Regulation of Chromosomal V(D)J Recombination. *Cell* **109**, S45–S55 (2002).

12. Agrawal, A., Eastman, Q. M. & Schatz, D. G. Transposition mediated by RAG1 and RAG2 and its implications for the evolution of the immune system. *Nature* **394**, 744–751 (1998).

13. McDonald, B. D., Bunker, J. J., Erickson, S. A., Oh-Hora, M. & Bendelac, A. Crossreactive αβ T cell receptors are the predominant targets of thymocyte negative selection. *Immunity* **43**, 859–869 (2015).

14. Hogquist, K. A. *et al.* T cell receptor antagonist peptides induce positive selection. *Cell* **76**, 17–27 (1994).

15. Bonifaz, L. *et al.* Efficient Targeting of Protein Antigen to the Dendritic Cell Receptor DEC-205 in the Steady State Leads to Antigen Presentation on Major Histocompatibility Complex Class I Products and Peripheral CD8+ T Cell Tolerance. *Journal of Experimental Medicine* **196**, 1627–1638 (2002).

16. Anderson, M. S. *et al.* The Cellular Mechanism of Aire Control of T Cell Tolerance. *Immunity* **23**, 227–239 (2005).

17. Arstila, T. P. *et al.* A Direct Estimate of the Human αβ T Cell Receptor Diversity. *Science* **286**, 958–961 (1999).

18. Robins, H. S. *et al.* Comprehensive assessment of T-cell receptor β-chain diversity in αβ T cells. *Blood* **114**, 4099–4107 (2009).

19. Liu, B., Chen, W., Evavold, B. D. & Zhu, C. Accumulation of Dynamic Catch Bonds between TCR and Agonist Peptide-MHC Triggers T Cell Signaling. *Cell* **157**, 357–368 (2014).

20. Love, P. E. & Hayes, S. M. ITAM-mediated Signaling by the T-Cell Antigen Receptor. *Cold Spring Harb Perspect Biol* **2**, a002485 (2010).

21. Courtney, A. H., Lo, W.-L. & Weiss, A. TCR SIGNALING: MECHANISMS OF INITIATION AND PROPAGATION. Trends Biochem Sci 43, 108–123 (2018).

22. Marth, J. D., Peet, R., Krebs, E. G. & Perlmutter, R. M. A lymphocyte-specific protein-tyrosine kinase gene is rearranged and overexpressed in the murine T cell lymphoma LSTRA. *Cell* **43**, 393–404 (1985).

23. Chan, A. C., Irving, B. A., Fraser, J. D. & Weiss, A. The zeta chain is associated with a tyrosine kinase and upon T-cell antigen receptor stimulation associates with ZAP-70, a 70-kDa tyrosine phosphoprotein. Proc Natl Acad Sci U S A 88, 9166–9170 (1991).

24. Zhang, W., Sloan-Lancaster, J., Kitchen, J., Trible, R. P. & Samelson, L. E. LAT: The ZAP-70 Tyrosine Kinase Substrate that Links T Cell Receptor to Cellular Activation. *Cell* **92**, 83–92 (1998).

25. Putney, J. W. Capacitative calcium entry revisited: Review article. *Cell Calcium* **11**, 611–624 (1990).

26. Shaw, K. T. et al. Immunosuppressive drugs prevent a rapid dephosphorylation of transcription factor NFAT1 in stimulated immune cells. Proceedings of the National Academy of Sciences 92, 11205–11209 (1995).

27. Dienz, O. *et al.* Src Homology 2 Domain-Containing Leukocyte Phosphoprotein of 76 kDa and Phospholipase Cγ1 Are Required for NF-κB Activation and Lipid Raft Recruitment of

Protein Kinase Cθ Induced by T Cell Costimulation1. *The Journal of Immunology* **170**, 365–372 (2003).

28. Zhang, W. *et al.* Association of Grb2, Gads, and Phospholipase C-γ1 with Phosphorylated LAT Tyrosine Residues: EFFECT OF LAT TYROSINE MUTATIONS ON T CELL ANTIGEN RECEPTOR-MEDIATED SIGNALING *. *Journal of Biological Chemistry* **275**, 23355–23361 (2000).

29. Olivier, J. P. *et al.* A Drosophila SH2-SH3 adaptor protein implicated in coupling the sevenless tyrosine kinase to an activator of Ras guanine nucleotide exchange, Sos. *Cell* **73**, 179–191 (1993).

30. Lowenstein, E. J. et al. The SH2 and SH3 domain-containing protein GRB2 links receptor tyrosine kinases to ras signaling. *Cell* **70**, 431–442 (1992).

31. Clark, S. G., Stern, M. J. & Horvritz, H. R. C. elegans cell-signalling gene sem-5 encodes a protein with SH2 and SH3 domains. *Nature* **356**, 340–344 (1992).

32. Liu, S. K., Fang, N., Koretzky, G. A. & McGlade, C. J. The hematopoietic-specific adaptor protein Gads functions in T-cell signaling via interactions with the SLP-76 and LAT adaptors. *Current Biology* **9**, 67–75 (1999).

33. Tybulewicz, V. L. J., Ardouin, L., Prisco, A. & Reynolds, L. F. Vav1: a key signal transducer downstream of the TCR. *Immunological Reviews* **192**, 42–52 (2003).

34. Jackman, J. K. *et al.* Molecular Cloning of SLP-76, a 76-kDa Tyrosine Phosphoprotein Associated with Grb2 in T Cells (∗). *Journal of Biological Chemistry* **270**, 7029–7032 (1995).

35. June, C. H., Ledbetter, J. A., Gillespie, M. M., Lindsten, T. & Thompson, C. B. T-cell proliferation involving the CD28 pathway is associated with cyclosporine-resistant interleukin 2 gene expression. *Mol Cell Biol* **7**, 4472–4481 (1987).

36. Mueller, D. L., Jenkins, M. K. & Schwartz, R. H. Clonal Expansion Versus Functional Clonal Inactivation: A Costimulatory Signalling Pathway Determines the Outcome of T Cell Antigen Receptor Occupancy. *Annual Review of Immunology* **7**, 445–480 (1989).

37. Medzhitov, R. & Janeway, C. A. Decoding the Patterns of Self and Nonself by the Innate Immune System. *Science* **296**, 298–300 (2002).

38. Takahashi, C., Mittler, R. S. & Vella, A. T. Cutting Edge: 4-1BB Is a Bona Fide CD8 T Cell Survival Signal1. *The Journal of Immunology* **162**, 5037–5040 (1999).

39. Willoughby, J. E. *et al.* Differential Impact of CD27 and 4-1BB Costimulation on Effector and Memory CD8 T Cell Generation following Peptide Immunization. *The Journal of Immunology* **193**, 244–251 (2014).

40. Granja, C. B., Gozashti, C. S. & Dasgupta, J. D. CD4-independent signal transduction through the T-cell receptor (TCR/CD3). *Immunology* **83**, 414–419 (1994).

41. Boniface, J. J. *et al.* Initiation of Signal Transduction through the T Cell Receptor Requires the Multivalent Engagement of Peptide/MHC Ligands. *Immunity* **9**, 459–466 (1998).

42. Woods, M., Guy, R., Waldmann, H., Glennie, M. & Alexander, D. R. A Humanised Therapeutic CD4 mAb Inhibits TCR-Induced IL-2, IL-4, and IL-10 Secretion and Expression of CD25, CD40L, and CD69. *Cellular Immunology* **185**, 101–113 (1998).

43. Harding, S., Lipp, P. & Alexander, D. R. A Therapeutic CD4 Monoclonal Antibody Inhibits TCR-ζ Chain Phosphorylation, ζ-Associated Protein of 70-kDa Tyr319 Phosphorylation, and TCR Internalization in Primary Human T Cells. *The Journal of Immunology* **169**, 230–238 (2002).

44. Huppa, J. B. *et al.* TCR–peptide–MHC interactions in situ show accelerated kinetics and increased affinity. *Nature* **463**, 963–967 (2010).

45. Irvine, D. J., Purbhoo, M. A., Krogsgaard, M. & Davis, M. M. Direct observation of ligand recognition by T cells. *Nature* **419**, 845–849 (2002).

46. Purbhoo, M. A., Irvine, D. J., Huppa, J. B. & Davis, M. M. T cell killing does not require the formation of a stable mature immunological synapse. *Nat Immunol* **5**, 524–530 (2004).

47. Huang, J. *et al.* A single peptide-major histocompatibility complex ligand triggers digital cytokine secretion in CD4+ T cells. *Immunity* **39**, 10.1016/j.immuni.2013.08.036 (2013).

48. Artyomov, M. N., Lis, M., Devadas, S., Davis, M. M. & Chakraborty, A. K. CD4 and CD8 binding to MHC molecules primarily acts to enhance Lck delivery. *PNAS* **107**, 16916–16921 (2010).

49. Li, Q.-J. *et al.* CD4 enhances T cell sensitivity to antigen by coordinating Lck accumulation at the immunological synapse. *Nat Immunol* **5**, 791–799 (2004).

50. Wooldridge, L. *et al.* Anti-CD8 Antibodies Can Inhibit or Enhance Peptide-MHC Class I (pMHCI) Multimer Binding: This Is Paralleled by Their Effects on CTL Activation and Occurs in the Absence of an Interaction between pMHCI and CD8 on the Cell Surface. *The Journal of Immunology* **171**, 6650–6660 (2003).

51. Zareie, P. *et al.* Canonical T cell receptor docking on peptide–MHC is essential for T cell signaling. *Science* **372**, (2021).

52. Horkova, V. *et al.* Unique roles of co-receptor-bound LCK in helper and cytotoxic T cells. *Nat Immunol* **24**, 174–185 (2023).

53. Imai, C. *et al.* Chimeric receptors with 4-1BB signaling capacity provoke potent cytotoxicity against acute lymphoblastic leukemia. *Leukemia* **18**, 676–684 (2004).

54. Stopeck, A. T. *et al.* Loss of B7.2 (CD86) and intracellular adhesion molecule 1 (CD54) expression is associated with decreased tumor-infiltrating T lymphocytes in diffuse B-cell large-cell lymphoma. *Clin Cancer Res* **6**, 3904–3909 (2000).

55. Zhang, Q. *et al.* Molecular and Clinical Characterization of CD80 Expression via Large-Scale Analysis in Breast Cancer. *Front Pharmacol* **13**, 869877 (2022).

56. Cornel, A. M., Mimpen, I. L. & Nierkens, S. MHC Class I Downregulation in Cancer: Underlying Mechanisms and Potential Targets for Cancer Immunotherapy. *Cancers (Basel)* **12**, 1760 (2020).

57. Taylor, B. C. & Balko, J. M. Mechanisms of MHC-I Downregulation and Role in Immunotherapy Response. *Front Immunol* **13**, 844866 (2022).

58. Hazini, A., Fisher, K. & Seymour, L. Deregulation of HLA-I in cancer and its central importance for immunotherapy. *J Immunother Cancer* **9**, e002899 (2021).

59. Dhatchinamoorthy, K., Colbert, J. D. & Rock, K. L. Cancer Immune Evasion Through Loss of MHC Class I Antigen Presentation. *Front. Immunol.* **12**, (2021).

60. Kuwana, Y. *et al.* Expression of chimeric receptor composed of immunoglobulin-derived V resions and T-cell receptor-derived C regions. *Biochemical and Biophysical Research Communications* **149**, 960–968 (1987).

61. Gross, G., Waks, T. & Eshhar, Z. Expression of immunoglobulin-T-cell receptor chimeric molecules as functional receptors with antibody-type specificity. *Proceedings of the National Academy of Sciences* **86**, 10024–10028 (1989).

62. Eshhar, Z., Waks, T., Gross, G. & Schindler, D. G. Specific activation and targeting of cytotoxic lymphocytes through chimeric single chains consisting of antibody-binding domains and the gamma or zeta subunits of the immunoglobulin and T-cell receptors. *Proceedings of the National Academy of Sciences* **90**, 720–724 (1993).

63. Brentjens, R. *et al.* CD19-targeted T cells rapidly induce molecular remissions in adults with chemotherapy-refractory acute lymphoblastic leukemia. *Sci Transl Med* **5**, 177ra38 (2013).

64. Park, J. R. *et al.* Adoptive Transfer of Chimeric Antigen Receptor Re-directed Cytolytic T Lymphocyte Clones in Patients with Neuroblastoma. *Molecular Therapy* **15**, 825–833 (2007).

65. Till, B. G. *et al.* Adoptive immunotherapy for indolent non-Hodgkin lymphoma and mantle cell lymphoma using genetically modified autologous CD20-specific T cells. *Blood* **112**, 2261–2271 (2008).

66. Maher, J., Brentjens, R. J., Gunset, G., Rivière, I. & Sadelain, M. Human T-lymphocyte cytotoxicity and proliferation directed by a single chimeric TCRζ /CD28 receptor. *Nat Biotechnol* **20**, 70–75 (2002).

67. Milone, M. C. *et al.* Chimeric Receptors Containing CD137 Signal Transduction Domains Mediate Enhanced Survival of T Cells and Increased Antileukemic Efficacy In Vivo. *Mol Ther* **17**, 1453–1464 (2009).

68. Childhood and Adolescent Cancer. *American Cancer Society* https://cancerstatisticscenter.cancer.org/childhood-and-adolescent-cancer.

69. USCS Data Visualizations. https://gis.cdc.gov/grasp/USCS/DataViz.html.

70. Raponi, S. *et al.* Flow cytometric study of potential target antigens (CD19, CD20, CD22, CD33) for antibody-based immunotherapy in acute lymphoblastic leukemia: analysis of 552 cases. *Leuk Lymphoma* **52**, 1098–1107 (2011).

71. Dogan, A. *et al.* B-cell maturation antigen expression across hematologic cancers: a systematic literature review. *Blood Cancer J* **10**, 73 (2020).

72. Ayala Ceja, M., Khericha, M., Harris, C. M., Puig-Saus, C. & Chen, Y. Y. CAR-T cell manufacturing: Major process parameters and next-generation strategies. *J Exp Med* **221**, e20230903 (2024).

73. Maude, S. L. *et al.* Tisagenlecleucel in Children and Young Adults with B-Cell Lymphoblastic Leukemia. *N Engl J Med* **378**, 439–448 (2018).

74. Laetsch, T. W. *et al.* Three-Year Update of Tisagenlecleucel in Pediatric and Young Adult Patients With Relapsed/Refractory Acute Lymphoblastic Leukemia in the ELIANA Trial. *JCO* **41**, 1664–1669 (2023).

75. Novartis five-year Kymriah® data show durable remission and long-term survival maintained in children and young adults with advanced B-cell ALL. *Novartis* https://www.novartis.com/news/media-releases/novartis-five-year-kymriah-data-show-durable-remission-and-long-term-survival-maintained-children-and-young-adults-advanced-b-cell-all.

76. Rabian, F. *et al.* Efficacy and Tolerance of Brexucabtagene Autoleucel in Adults with Relapsed/Refractory B-Cell Precursor Acute Lymphoblastic Leukemia : A Graall Study from the Descar-T Registry. *Blood* **142**, 3498 (2023).

77. Bezerra, E. Real-World Outcomes of Brexucabtagene Autoleucel (brexu-cel) for Relapsed or Refractory (R/R) Adult B-Cell Acute Lymphoblastic Leukemia (B-cell ALL): Evidence from the CIBMTR Registry. in (ASH, 2023).

78. Roloff, G. Brexucabtagene Autoleucel in Adults with Relapsed/Refractory B-Cell ALL: Outcomes and Novel Insights from the Real-World Outcomes Collaborative of CAR T in Adult ALL (ROCCA). in (ASH, 2023).

79. Haso, W. *et al.* Anti-CD22–chimeric antigen receptors targeting B-cell precursor acute lymphoblastic leukemia. *Blood* **121**, 1165–1174 (2013).

80. Xiao, X., Ho, M., Zhu, Z., Pastan, I. & Dimitrov, D. S. Identification and characterization of fully human anti-CD22 monoclonal antibodies. *mAbs* **1**, 297–303 (2009).

81. Fry, T. J. *et al.* CD22-CAR T Cells Induce Remissions in CD19-CAR Naïve and Resistant B-ALL. *Nat Med* **24**, 20–28 (2018).

82. Shah, N. N. *et al.* CD4/CD8 T-Cell Selection Affects Chimeric Antigen Receptor (CAR) T-Cell Potency and Toxicity: Updated Results From a Phase I Anti-CD22 CAR T-Cell Trial. *JCO* **38**, 1938–1950 (2020).

83. Cohen, A. D. *et al.* B cell maturation antigen–specific CAR T cells are clinically active in multiple myeloma. *J Clin Invest* **129**, 2210–2221 (2019).

84. Munshi, N. C. *et al.* Idecabtagene Vicleucel in Relapsed and Refractory Multiple Myeloma. *New England Journal of Medicine* **384**, 705–716 (2021).

85. Brudno, J. N. *et al.* T Cells Genetically Modified to Express an Anti–B-Cell Maturation Antigen Chimeric Antigen Receptor Cause Remissions of Poor-Prognosis Relapsed Multiple Myeloma. *JCO* **36**, 2267–2280 (2018).

86. Maude, S. L. *et al.* Chimeric Antigen Receptor T Cells for Sustained Remissions in Leukemia. *N Engl J Med* **371**, 1507–1517 (2014).

87. Lee, D. W. *et al.* T cells expressing CD19 chimeric antigen receptors for acute lymphoblastic leukaemia in children and young adults: a phase 1 dose-escalation trial. *The Lancet* **385**, 517–528 (2015).

88. Baird, J. H. *et al.* CD22-directed CAR T-cell therapy induces complete remissions in CD19-directed CAR–refractory large B-cell lymphoma. *Blood* **137**, 2321–2325 (2021).

89. Gardner, R. A. *et al.* Intent-to-treat leukemia remission by CD19 CAR T cells of defined formulation and dose in children and young adults. *Blood* **129**, 3322–3331 (2017).

90. Davenport, A. J. *et al.* Chimeric antigen receptor T cells form nonclassical and potent immune synapses driving rapid cytotoxicity. *PNAS* **115**, E2068–E2076 (2018).

91. Dustin, M. L., Chakraborty, A. K. & Shaw, A. S. Understanding the Structure and Function of the Immunological Synapse. *Cold Spring Harb Perspect Biol* **2**, a002311 (2010).

92. Salter, A. I. *et al.* Comparative analysis of TCR and CAR signaling informs CAR designs with superior antigen sensitivity and in vivo function. *Sci. Signal.* **14**, (2021).

93. Gudipati, V. *et al.* Inefficient CAR-proximal signaling blunts antigen sensitivity. *Nature Immunology* **21**, 848–856 (2020).

94. Watanabe, K. *et al.* Target Antigen Density Governs the Efficacy of Anti–CD20-CD28-CD3 ζ Chimeric Antigen Receptor–Modified Effector CD8+ T Cells. *The Journal of Immunology* **194**, 911–920 (2015).

95. Salter, A. I. *et al.* Phosphoproteomic analysis of chimeric antigen receptor signaling reveals kinetic and quantitative differences that affect cell function. *Sci Signal* **11**, eaat6753 (2018).

96. Kawalekar, O. U. *et al.* Distinct Signaling of Coreceptors Regulates Specific Metabolism Pathways and Impacts Memory Development in CAR T Cells. *Immunity* **44**, 380–390 (2016).

97. Hofinger, E. & Sticht, H. Multiple Modes of Interaction between Lck and CD28. *The Journal of Immunology* **174**, 3839–3840 (2005).

98. Dobbins, J. *et al.* Binding of the cytoplasmic domain of CD28 to the plasma membrane inhibits Lck recruitment and signaling. *Science Signaling* **9**, ra75–ra75 (2016).

99. Sun, C. *et al.* THEMIS-SHP1 Recruitment by 4-1BB Tunes LCK-Mediated Priming of Chimeric Antigen Receptor-Redirected T Cells. *Cancer Cell* **37**, 216-225.e6 (2020).

100. Majzner, R. G. *et al.* Tuning the Antigen Density Requirement for CAR T-cell Activity. *Cancer Discovery* **10**, 702–723 (2020).

101. Xiao, Q. & Su, X. Imaging CAR-T synapse as a quality control for CAR engineering. *Methods Mol Biol* **2654**, 503–512 (2023).

102. Arcaro, A. *et al.* Essential Role of CD8 Palmitoylation in CD8 Coreceptor Function. *The Journal of Immunology* **165**, 2068–2076 (2000).

103. Nicholson, I. C. *et al.* Construction and characterisation of a functional CD19 specific single chain Fv fragment for immunotherapy of B lineage leukaemia and lymphoma. *Molecular Immunology* **34**, 1157–1165 (1997).

104. Cormack, B. P., Valdivia, R. H. & Falkow, S. FACS-optimized mutants of the green fluorescent protein (GFP). *Gene* **173**, 33–38 (1996).

105. Bang, S., Nagata, S., Onda, M., Kreitman, R. J. & Pastan, I. HA22 (R490A) Is a Recombinant Immunotoxin with Increased Antitumor Activity without an Increase in Animal Toxicity. *Clinical Cancer Research* **11**, 1545–1550 (2005).

106. Shemiakina, I. I. *et al.* A monomeric red fluorescent protein with low cytotoxicity. *Nat Commun* **3**, 1204 (2012).

107. Gasparrini, F. *et al.* Nanoscale organization and dynamics of the siglec CD22 cooperate with the cytoskeleton in restraining BCR signalling. *EMBO J* **35**, 258–280 (2016).

108. Doody, G. M. *et al.* A Role in B Cell Activation for CD22 and the Protein Tyrosine Phosphatase SHP. *Science* **269**, 242–244 (1995).

109. Depoil, D. *et al.* CD19 is essential for B cell activation by promoting B cell receptor–antigen microcluster formation in response to membrane-bound ligand. *Nat Immunol* **9**, 63–72 (2008).

110. Rossi, J. *et al.* Preinfusion polyfunctional anti-CD19 chimeric antigen receptor T cells are associated with clinical outcomes in NHL. *Blood* **132**, 804–814 (2018).

111. Porter, D. L. *et al.* Chimeric antigen receptor T cells persist and induce sustained remissions in relapsed refractory chronic lymphocytic leukemia. *Sci Transl Med* **7**, 303ra139 (2015).

112. Weber, E. W. *et al.* Transient rest restores functionality in exhausted CAR-T cells through epigenetic remodeling. *Science* **372**, eaba1786 (2021).

113. Liu, Z. *et al.* Systematic comparison of 2A peptides for cloning multi-genes in a polycistronic vector. *Sci Rep* **7**, 2193 (2017).

114. Sweeney, N. P. & Vink, C. A. The impact of lentiviral vector genome size and producer cell genomic to gag-pol mRNA ratios on packaging efficiency and titre. *Mol Ther Methods Clin Dev* **21**, 574–584 (2021).

115. Hopp, T. P. *et al.* A Short Polypeptide Marker Sequence Useful for Recombinant Protein Identification and Purification. *Nat Biotechnol* **6**, 1204–1210 (1988).

116. Evan, G. I., Lewis, G. K., Ramsay, G. & Bishop, J. M. Isolation of Monoclonal Antibodies Specific for Human c-myc Proto-Oncogene Product. *Molecular and Cellular Biology* **5**, 3610–3616 (1985).

117. Turner, J. M. *et al.* Interaction of the unique N-terminal region of tyrosine kinase p56lck with cytoplasmic domains of CD4 and CD8 is mediated by cysteine motifs. *Cell* **60**, 755–765 (1990).

118. Shaw, A. S. *et al.* Short related sequences in the cytoplasmic domains of CD4 and CD8 mediate binding to the amino-terminal domain of the p56lck tyrosine protein kinase. *Mol Cell Biol* **10**, 1853–1862 (1990).

119. Kim, P. W., Sun, Z.-Y. J., Blacklow, S. C., Wagner, G. & Eck, M. J. A Zinc Clasp Structure Tethers Lck to T Cell Coreceptors CD4 and CD8. *Science* **301**, 1725–1728 (2003).

120. Bosselut, R. *et al.* Association of the Adaptor Molecule Lat with Cd4 and Cd8 Coreceptors Identifies a New Coreceptor Function in T Cell Receptor Signal Transduction. *J Exp Med* **190**, 1517–1526 (1999).

121. Fan, X. (Frank) *et al.* Preclinical assessment of LCAR-B38M, a novel BCMA-targeting chimeric antigen receptor (CAR)-T cell therapy in relapsed/refractory multiple myeloma. *Clinical Lymphoma, Myeloma and Leukemia* **19**, e160 (2019).

122. Martin, T. *et al.* Ciltacabtagene Autoleucel, an Anti–B-cell Maturation Antigen Chimeric Antigen Receptor T-Cell Therapy, for Relapsed/Refractory Multiple Myeloma: CARTITUDE-1 2-Year Follow-Up. *JCO* **41**, 1265–1274 (2023).

123. Zhang, Y. *et al.* Safety and efficacy of a novel anti-CD19 chimeric antigen receptor T cell product targeting a membrane-proximal domain of CD19 with fast on- and off-rates against non-Hodgkin lymphoma: a first-in-human study. *Mol Cancer* **22**, 200 (2023).

124. Holland, E. M. *et al.* Chimeric Antigen Receptor T Cells as Salvage Therapy for Post-Chimeric Antigen Receptor T Cell Failure. *Transplantation and Cellular Therapy, Official Publication of the American Society for Transplantation and Cellular Therapy* **29**, 574.e1-574.e10 (2023).

125. Dai, H. *et al.* Bispecific CAR-T cells targeting both CD19 and CD22 for therapy of adults with relapsed or refractory B cell acute lymphoblastic leukemia. *Journal of Hematology & Oncology* **13**, 30 (2020).

126. Hu, Y. *et al.* CRISPR/Cas9-Engineered Universal CD19/CD22 Dual-Targeted CAR-T Cell Therapy for Relapsed/Refractory B-cell Acute Lymphoblastic Leukemia. *Clinical Cancer Research* **27**, 2764–2772 (2021).

127. Shalabi, H. *et al.* Abstract CT051: Safety and efficacy of CD19/CD22 CAR T cells in children and young adults with relapsed/refractory ALL. *Cancer Research* **80**, CT051 (2020).

128. Spiegel, J. Y. *et al.* CAR T cells with dual targeting of CD19 and CD22 in adult patients with recurrent or refractory B cell malignancies: a phase 1 trial. *Nat Med* **27**, 1419–1431 (2021).

129. Flugel, C. L. *et al.* Overcoming on-target, off-tumour toxicity of CAR T cell therapy for solid tumours. *Nat Rev Clin Oncol* **20**, 49–62 (2023).

130. Hartl, F. A. *et al.* Noncanonical binding of Lck to CD3ε promotes TCR signaling and CAR function. *Nature Immunology* **21**, 902–913 (2020).

131. Liu, Y. *et al.* Chimeric STAR receptors using TCR machinery mediate robust responses against solid tumors. *Science Translational Medicine* **13**, eabb5191 (2021).

132. Mansilla-Soto, J. *et al.* HLA-independent T cell receptors for targeting tumors with low antigen density. *Nat Med* **28**, 345–352 (2022).

133. Dobrin, A. *et al.* Synthetic dual co-stimulation increases the potency of HIT and TCR-targeted cell therapies. *Nat Cancer* **5**, 760–773 (2024).

134. Tousley, A. M. *et al.* Co-opting signalling molecules enables logic-gated control of CAR T cells. *Nature* 1–10 (2023).

135. Levine, B. L., Miskin, J., Wonnacott, K. & Keir, C. Global Manufacturing of CAR T Cell Therapy. *Mol Ther Methods Clin Dev* **4**, 92–101 (2016).